

Models on CO_2 abatement under uncertainty

Inaugural-Dissertation zur Erlangung des akademischen Grades eines Doktors der
Wirtschafts- und Sozialwissenschaften der Wirtschafts- und
Sozialwissenschaftlichen Fakultät der Christian-Albrechts-Universität zu Kiel

vorgelegt von

Thomas S. Lontzek, M.Sc.
aus Schwientochlowitz, geb. 29.09.1978

Kiel, Oktober 2009

Gedruckt mit Genehmigung der Wirtschafts- und Sozialwissenschaftlichen
Fakultät der Christian-Albrechts-Universität zu Kiel

Dekan: Professor Dr. Thomas Lux
Erstberichterstattender: Professor Dr. Till Requate
Zweitberichterstattender: Professor Dr. Martin Quaas

Tag der Abgabe der Arbeit: 23. Oktober 2009

Tag der mündlichen Prüfung: 17. Dezember 2009

Contents

1	General Introduction	1
1.1	Research Motivation	1
1.2	Research Goals and Main Results	3
2	The Effects of Carbon Capture & Storage on Carbon Cycle Dynamics	6
2.1	Introduction	6
2.2	An Economic Model of the Global Carbon Cycle	10
2.2.1	The Carbon System Diagram	12
2.2.2	The optimal control problem	16
2.2.3	Steady-State Analysis	19
2.2.4	The Decentralized Economy	22
2.2.5	Possible Carbon Tax Paths	23
2.3	Simulation of Optimal Paths	27
2.3.1	Simulation of the Model	32
2.3.2	Sequestration vs. no sequestration	33
2.3.3	The impact of discounting	34
2.3.4	Optimal Carbon Tax Paths	35
2.4	The basic model with uncertainty	38
2.5	Concluding Remarks	49

3	The Effect of Damage Uncertainty on Climate Change Mitigation: A Numerical Approach of Stochastic Control	51
3.1	Introduction	51
3.2	The Model	55
3.3	Numerical Solution of the Model	58
3.4	Results and Discussion	59
3.5	Concluding Remarks	67
4	Transition from Polluting to Clean Technology: A Differentiated Capital Approach	69
4.1	Introduction	69
4.2	The Model	73
4.2.1	Capital installation and utilization	73
4.2.2	Adjustment costs of investment	75
4.2.3	Social optimum	76
4.2.4	Steady state conditions	80
4.3	Comparative statics of the steady state	84
4.4	Simulation of the model.	87
4.4.1	Nonnegativity Constraint on Investment	91
4.4.2	Different initial values	92
4.4.3	Sensitivity analysis for different Parameter Values	93
4.5	Stock Pollution & Uncertainty about Damage	95
4.6	Concluding Remarks	104
5	General Conclusion	106
6	Appendix	115
6.1	Appendix A1	115
6.2	Appendix A2	116

6.3 Appendix A3	122
Eidesstattliche Erklärung (Certificate of Authorship/Originality)	124

Chapter 1

General Introduction

1.1 Research Motivation

The discussion on climate change has clearly intensified over the last few years. While there exists strong agreement about the actual happening of climate change, there is a wide-spread range of different opinions on how the world will be affected by climatic changes and which measures could and should be taken in order to mitigate it. These measures include the conceptualization of a policy framework which goes far beyond setting up a global price on carbon and includes other topics, e.g. the diffusion of energy saving technologies. It also requires the design of a legal framework for the private sector which e.g. enhances the development of cleaner technologies on one hand and creates incentives for retrofitting existing power plants, on the other hand.

For the public acceptance of energy policy it requires rising public awareness of the climate change problem and consequently public support. The latter one is in particular relevant for nuclear energy but also for carbon capture and storage technologies. Populism on possible leakage of carbon from storage sites can create an adverse public attitude towards carbon capture and storage, and consequently

jeopardize its application due to public opposition.

While it seems inevitable that the so called "green technologies" are the future technologies for energy generation, a major question is how one can achieve a smooth transition towards its on scale application, taking into account (i) the ever growing global demand for energy (ii) the limited economic availability of the green technologies and (iii) the irreversibility of climate change.

In order to answer these questions, economists and climate scientists face the task to develop meaningful models for the analysis of the interplay of climate and the economy. This requires interdisciplinary work in order to asses the climate change problem properly. To the same extent as many climate models lack the representation of the economy, economist in the past have only managed sporadically to include an adequate formulation of climate change in theory models.

What has been neglected in economic models of climate change is the role of carbon sinks other than the atmosphere. This simplification heavily weakens the analysis of the reciprocity between climate and economy since the role of e.g. the ocean, by far the largest carbon reservoir is not accounted for.

Another aspect of the climate change debate which has traditionally been not accounted for in climate-economy models is the heterogeneity of capital. New technologies most likely need to be matched by new capital investments. Assuming homogenous capital may oversimplify the easiness of a technology switch and as a consequence, provide distorted signals for policy makers.

Finally, since the set of possible technologies to mitigate climate change has broadened over the last years, one has to include these modern technologies in climate-economy models. Carbon capture and storage has recently been established as a promising technology which might facilitate the switch towards renewables over the next decades. It is a compromise between mitigating emissions on one hand and the ability of using fossil fuels on the other hand.

In order to assess properly the mutual impact of climate change and the economy one has to account for the intrinsic uncertainty that is inherent to the real world. Thus, the role of uncertainty in the economic analysis of climate change should not be neglected. Uncertainty appears in different forms, e.g.: uncertainty about economic parameters, e.g.: consumers' preferences, production and investment costs or R&D outcomes. Furthermore, uncertainty exists about natural parameters related to e.g.: leakage rates, carbon cycle dynamics or changes of global mean temperature levels and the resulting damage to the economy.

Modern, climate-economic models hardly account for uncertainty. This is mainly due to the methodological complexity of the topic. From an economic point of view we have to develop more detailed models of ecological-economic interaction which include uncertainty. From a computational point of view, we have to develop and implement efficient algorithms that allow us to solve these stochastic, nonlinear multidimensional dynamic programs.

An explicit treatment of uncertainty is indispensable if we want to analyze how rational economic agents form their decisions in an uncertain environment.

1.2 Research Goals and Main Results

The major goal of this thesis is to contribute answering the question how changes in economic actions affect the climate and at the same time, how do changes in the climate affect the economy.

This thesis consists of three parts. In the first part (Chapter 2) we stress the role of the oceans as a sink for atmospheric carbon by developing a dynamic global carbon cycle model with two reservoirs containing atmosphere and two ocean layers. We consider a special form of carbon capture and storage: The capture of carbon and its sequestration into the deep ocean reservoir. Adding a non-renewable

resource stock we study the socially optimal extraction and carbon capture and storage decision rules. We show that carbon capture and storage accelerates the slow natural flux within the carbon cycle, and because of its temporary abatement character it dampens the overshooting of the atmospheric reservoir. After studying the decentralized economy we show that the optimal carbon tax has an inverted u-shape. Depending on the initial sizes of the reservoirs and the speed of carbon fluxes between the reservoirs carbon taxes can also be increasing, decreasing or u-shaped. Our model is the first of its kind which can generate this result. Furthermore, we conclude that the level of the carbon tax should be positively adjusted to account for (i) damage uncertainty and (ii) the declining ability of the deep ocean to absorb atmospheric carbon.

In the second part of the thesis (Chapter 3) we apply standardized numerical techniques of stochastic optimization to the climate change issue. We ask the question how the optimal mitigation of climate change evolves if intrinsic uncertainty about damage is inherent to the model. In particular, we are interested in how the effect of uncertainty on climate change mitigation changes with different levels of risk aversion.

A major finding is that the effects of stochasticity differ even in sign as to emission control with varying parameters: introduction of stochasticity may increase or decrease emission control depending on the specific parameter setting. Our analysis covers a large range of the parameter space, in particular the degree of risk aversion and the level of uncertainty. We identify regions of the state space for which higher levels of uncertainty or risk aversion result in different policy rules for emission control. Similarly, given a certain state of the world we conclude that the effect of uncertainty on emission control changes (in level and sign) with the degree of risk aversion. In other words, uncertainties in climatic trends may induce people's precautionary emission reduction but also may drive away money from

abatement.

In the third part of the thesis (Chapter 4) we are interested in how a capital stock which is linked to a polluting technology is maintained, accumulated and utilized optimally. In order to analyze the inter- and intra-sectoral tradeoffs between capacity building and capacity using which guide the economy's transition process towards a balanced growth equilibrium we develop a model with two production sectors that generate a homogenous consumption good. The production processes in these two sectors differ with respect to the technology which is used. While in one sector the process is clean, generating output in the other sector also creates environmental damage. The technologies are completely embedded in the corresponding stock of physical capital. Hence, the application of one technology can only be intensified by investing more in the associated capital stock or utilizing it more intensively.

Our findings show that the combination of heterogeneous capital, endogenous depreciation and capital intensity is essential for extracting qualitative and quantitative implications for policy makers about the easiness of a technology switch. If the economic environment requires a change in the energy portfolio, an economy driven by our model structure can not react without severe time lags, due to the ex post clay nature of investment. Installation of the desired capital stock simply takes time if we do not want to abstain from smooth consumption patterns. In a next step we introduce a stock of carbon which is subject to uncertainty. With this modification we can investigate how uncertainty about damage resulting from climate change influences the optimal interplay between capacity building and capacity utilization in a more realistic environment. We conclude that increasing uncertainty intensifies the need for a rapid build-up of the clean capital stock. It also reduces the demand for effective capital services associated with the polluting technology.

Chapter 2

The Effects of Carbon Capture and Storage on Carbon Cycle Dynamics

2.1 Introduction

For a long time, scarcity of resources, such as fossil fuels has been considered as the major obstacle to sustainability. Meanwhile it has become clear that the external cost of CO_2 emissions is the true limiting factor of using fossil fuels. Regulatory instruments, such as the EU emission trading system and carbon taxes aim at internalizing these external costs. Designing the optimal path of the carbon tax has been a major goal in the theoretical literature on optimal resource extraction.

One major component of the global carbon cycle which has traditionally been neglected in this part of literature is the role of the deep ocean in absorbing anthropogenic carbon. The ocean itself is by far the largest reservoir of carbon and possesses a large uptake capacity. However, on long time scales the CO_2 uptake

capacity becomes exhausted with rising CO_2 concentrations because each unit of carbon emitted will remain in the carbon cycle. A reduction of carbon concentrations in the atmosphere can be enhanced by switching from conventional energy resources to ecologically friendly renewables. But, drastic reductions are not viable yet because the use of renewables on a large scale is both, economically and technologically not feasible.

Carbon capture and storage (CCS) is considered to have potential of facilitating the transition phase towards an on-scale usage of renewables. The most standard approach is to capture carbon directly from the power plants. This however, requires building of new, CCS-ready power plants or retrofitting old ones. Regarding the storage of carbon, the most prominent kind of storage is underground storage, e.g. in oil and (depleted) gas fields, coal beds or saline aquifers. Through CCS technologies, carbon is effectively removed from the carbon cycle, provided leakage rates are low. Ocean sequestration via deep sea injection is different. It has the unique characteristic that carbon removed from the atmosphere remains in the carbon cycle. Ocean sequestration alters the relative distribution of carbon between its reservoirs (e.g. ocean and atmosphere) because the natural transfer of carbon from the atmosphere to the ocean is accelerated.

The purpose of this paper is (i) to study the optimal carbon path by explicitly including the ocean as an additional carbon reservoir and (ii) to analyze the potential of carbon capture and ocean sequestration as an additional control in managing the global carbon cycle.

In order to model the global carbon cycle we introduce two reservoirs: a lower reservoir containing the deep ocean and an upper reservoir containing the atmosphere and the upper ocean layer. We show that starting at the pre-industrial levels

of both reservoirs, the optimal extraction rates are initially high and decreasing. As a consequence, the upper reservoir overshoots its long run equilibrium level while the carbon content in the lower reservoir is monotonically increasing.

Because of its delayed damage effect, ocean sequestration proves to be an effective instrument to dampen the overshooting of the upper reservoir. Using the CCS technology results in lower steady state atmospheric carbon concentrations and, at the same time, higher total resource extraction. But it also reduces the natural uptake ability of the deep ocean.

The externality in this model consists of two parts, (1) the negative effect of rising carbon concentration levels and (2), the positive effect of removing carbon from the atmosphere via CCS. The latter in fact constitutes an abatement option which is only temporary since the carbon which is removed from the atmosphere and injected into the deep sea will eventually be transferred back to the atmosphere as the carbon reservoirs keep on mixing. Studying the decentralized economy, the first-best solution can be obtained with a carbon tax and a subsidy on the CCS technology.

We show that the optimal path of the carbon tax can be decreasing, increasing, u-shaped or inverted u-shaped. Its shape depends on the initial values of the stock variables and the speed of the flux between the carbon reservoirs. Its level is heavily linked to the ability of the deep ocean to absorb additional atmospheric carbon. Since we observe a decreasing potential of the deep ocean to serve as a carbon sink, we conclude that the level of the carbon tax should be adjusted for this effect.

So far, theoretical models of multiple carbon stocks are found in the literature on nonconstant pollution decay, e.g. Tahvonen and Withagen (1996), and Toman

and Withagen (2000). In contrast to the standard resource extraction problem in which carbon simply vanishes from the carbon cycle, this strand of literature takes account of the fact that the uptake potential of anthropogenic carbon by other reservoirs is limited. In addition, the mostly numerical literature on Integrated Assessment Models (IAM), e.g. Nordhaus (1994b) and Nordhaus and Boyer (2000) has been dealing with several stocks of carbon. However CCS has not been included into these models. CCS has so far mainly been analyzed using complex integrated assessment models (e.g., Akimoto et al. (2004), McFarland et al. (2003), McFarland and Herzog (2006) or Edmonds et al. (2004)). Ocean sequestration via deep see injection has been suggested by IPCC (2005) and is analyzed by Herzog et al. (2003). However, Herzog et al. (2003) do not put ocean sequestration into an optimization framework. Besides deep-see injection there are other ways of applying CCS, e.g. injection into geological formations, such as alkaline mineral strata or into natural off-shore storage facilities like oil and gas fields such as in the North Sea. Lackner (2003) provides an excellent survey of sequestration from an economic, ecological as well as technological point of view.

Ulph and Ulph (1994) show that the optimal carbon tax is increasing if the stock of CO_2 is below its steady state. We can show that including the deep ocean as an additional carbon reservoir the carbon tax could also be U-shaped in that case if e.g. carbon is absorbed very quickly by the deep ocean. To the best of our knowledge Farzin and Tahvonen (1996) is the only study in which four qualitatively different paths of the carbon tax can occur (monotonically increasing, decreasing, U-shaped, or inversely U-shaped). The resulting path depends on the initial conditions of their two atmosphere stocks and the factors that determine the allocation of total emissions between these two stocks. If in addition, no resource

constraint is included, steady states with positive pollution and decay rates can emerge. We are able to obtain this result even with a resource constraint because in our model the total carbon content of the global carbon cycle cannot be reduced at any time.

In a next step we build a stochastic version of the model in which we assume uncertainty about damage. We conclude that damage uncertainty in general leads to lower extraction of the non-renewable resource but it also calls for higher levels of carbon capture and storage. Furthermore we infer that the level of the carbon tax rises with damage uncertainty.

This chapter is structured as follows: In the next section we present the modeling framework and analyze the system dynamics. In section 2.3 we parameterize the model and discuss the model results. Section 2.4 presents the stochastic version of the basic model and its results. Section 2.5 concludes.

2.2 An Economic Model of the Global Carbon Cycle

In our set-up of the global carbon cycle we incorporate both, a natural exchange of carbon between the two reservoirs and an anthropogenic influence on the reservoirs' size via burning fossil fuels and sequestering. The stocks of the upper reservoir S (atmosphere and upper ocean layer) and the lower reservoir W (deep ocean) are driven by the following differential equations:

$$\dot{S} = q - a - \gamma(\sigma S - \omega W) \tag{2.1}$$

$$\dot{W} = a + \gamma(\sigma S - \omega W) \tag{2.2}$$

By $q \geq 0$ we denote the amount of CO_2 emissions. Extraction of q shifts carbon from a fossil resource to the atmosphere. Furthermore, $a \geq 0$ denotes the amount of carbon which is captured from the air and injected into the deep ocean (i.e. removed from the upper reservoir). We interpret both, q and a as anthropogenic components of the global carbon cycle. By contrast, the term $\gamma(\sigma S - \omega W)$ represents the natural flow between the carbon stocks. It describes the natural force of the carbon system to equilibrate and to neutralize the difference in partial pressure of its components. Whereas the term $\sigma S - \omega W$ describes the difference of the carbon content in the two reservoirs, the parameter¹ γ is an indicator for the pace of the net flux between the two reservoirs.

By R we denote the stock of a non-renewable resource stock with carbon content. It is extracted at the rate q .

$$\dot{R} = -q \tag{2.3}$$

Figure 1 illustrates the functioning of our model economy. With this formulation the net flux of CO_2 into the system can be negative because carbon can be extracted from the air and sequestered into the deep see even if the resource stock is economically/physically depleted.

¹Alternatively, one could think of treating γ as a variable, e.g. $\gamma(S)$ with $\gamma_S < 0$ and $\gamma_{SS} > 0$. This specification would explicitly take into account the weakening of the ocean's uptake capability due to increasing carbon concentrations in the atmosphere.

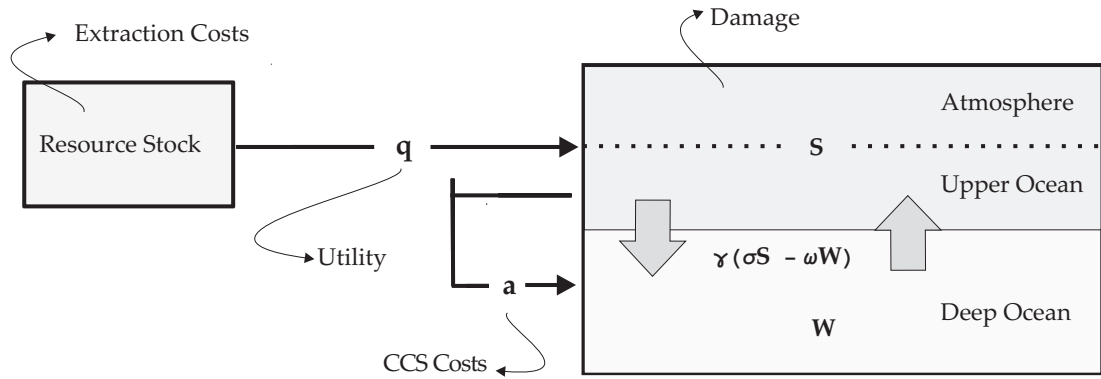


Figure 2.1: CCS & the Global Carbon Cycle

2.2.1 The Carbon System Diagram

Before analyzing the dynamic optimization problem we introduce the carbon system diagram which should simplify the understanding of the climate module within our model.

We observe that equations (2.1)-(2.3) imply a balanced carbon content system from which carbon cannot vanish. Each unit of carbon extracted from the stock of the non-renewable resource must flow either to the upper reservoir or (partly) to the lower reservoir. This feature stands in contrast to that part of the literature which assumes a constant decay rate. In the latter case carbon may simply vanish from the carbon cycle². This feature is at the core of our model and can be illustrated in a diagram. Figure 2.1 shows the carbon balance diagram which illustrates the dynamics of the simplified carbon cycle. The upper reservoir's carbon content S is displayed along the horizontal axis, and W , the carbon content of the lower

²For simplicity, we neglect other carbon deposition such as seabed sedimentary deposition of carbon or carbon content of plants.

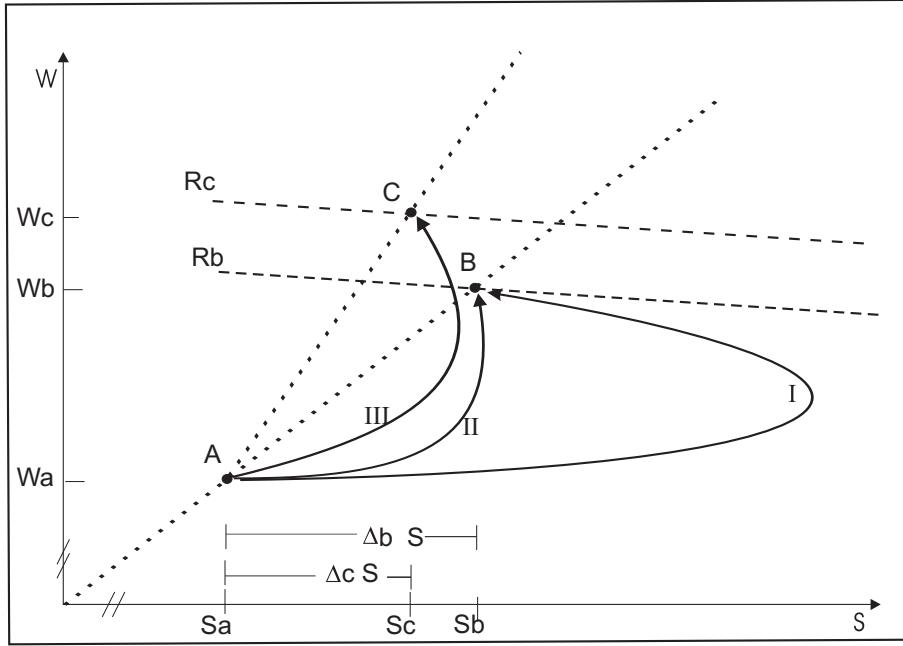


Figure 2.2: The Carbon System Diagram

reservoir is displayed along the vertical axis. Let A denote an initial steady state (e.g. the preindustrial state) of the system (2.1)-(2.3) which is characterized by $a = q = 0$, $R = R_0$ and $Wa = \frac{\sigma}{\omega} Sa$. Recall from Equation (2.2) and (2.3) that, since the dotted line passing through points A and B (\overline{AB}) has the slope $\frac{\sigma}{\omega}$, we observe no carbon transfer via the natural component of the carbon cycle at A . In the following, we want to demonstrate how carbon capture and ocean sequestration affect the global carbon cycle. We investigate three possible paths³ of the carbon cycle, each being subject to different scenarios on the anthropogenic disturbance of the carbon system. These scenarios are: (I) sequestration not possible. In this scenario the only control option is the extraction of the non-renewable resource

³Note that these paths are just examples of how optimal paths may look like.

stock. (II) sequestration possible with $(0 \leq a \leq q)$. The second scenario does not allow for negative emissions. It mimics the effects of CCS on the global carbon cycle when a carbon capture technology is installed directly at a power plant. Scenario (III) on the other hand assumes that sequestration is also possible with $a \geq q$.

Path I sequestration not possible:

Since sequestration is not possible, the only control is the extraction of the non-renewable resource. Along the initial part of Path *I* anthropogenic release of carbon into the upper reservoir is higher than natural transfer to the lower reservoir. As a consequence, the upper carbon stocks overshoots its steady-state level. Beyond its maximum, S decreases for two reasons. First, the extraction of the carbon stock is reduced constantly and second, the natural transfer is high because we observe a large difference in partial pressure. The new steady state is at B with $q = 0$ and equalization of the partial pressure, i.e. $Wb = \frac{p}{\omega} Sb$.

Definition 1. *Consider the $\{S, W\}$ space of the system (2.1)-(2.3) and its steady state (S^*, W^*) . A carbon iso-content line is the combination of all (S, W) with the same total carbon content.*

By Definition 1, Rb is the carbon iso-content line corresponding to the steady-state carbon content at point B ⁴.

Path II, sequestration possible and $0 \leq a \leq q$:

⁴Notice that all paths starting at A and ending at B may never leave the area bounded by Sa from the left, Wa from below and Rb from above. This is due to the fact that carbon cannot vanish from the carbon cycle since we assume a balanced carbon content

In this scenario we assume that ocean sequestration is possible but limit it to be less than emissions.⁵ Recall, that the unique characteristic of deep sea injection of carbon is, that it accelerates the natural, but slow mixing of the two carbon reservoirs. As a consequence, the overshooting of the steady state level of the upper reservoir is significantly reduced. For path *II* the steady state is also at *B*, implying that the total amount of carbon which has been extracted from the non-renewable resource is the same (same carbon iso-content line). Notice also, that since at *B* extraction q is zero, ocean sequestration does no longer take place, because we impose the constraint $0 \leq a \leq q$.

Path III, sequestration possible and $a \geq 0$:

For path *III* we allow carbon capture and sequestration to be positive even in the absence of extraction⁶. This automatically implies that in a new steady state the natural component of the carbon cycle does not need to be in equilibrium. This is reflected in Figure 2.3 by point *C* which is not on the line passing through \overline{AB} with a slope $= \frac{\sigma}{\omega}$. Since *C* is above \overline{AB} the lower reservoir is supersaturated and hence, a net source of carbon release. As a consequence, the steady state level of carbon in the upper reservoir has been reduced ($S_c < S_b$) even though more of the non-renewable resource has been extracted. The latter fact is indicated by the higher carbon iso-content line Rc corresponding to *C*.

⁵From a technical point of view this scenario assumes end-of-pipe capture

⁶From a technical point of view this scenario assumes the use of an air capture technology. Air capture requires the installation of specific devices which act as artificial trees. These devices have sorbents which can capture carbon dioxide from the air (see Zeman and Lackner (2004), Keith and Minh (2003) and Keith et al. (2005)). Air capture has been applied successfully on a very low scale so far. Its major advantage over other carbon capture technologies is that an air capture device can be installed in any location, preferably ones very close to sequestration sites.

In the following we analyze the model from a social planner's perspective.

2.2.2 The optimal control problem

In the previous section we were using fictitious paths to illustrate the behavior of the carbon cycle. This section derives the socially optimal paths.

Equations (2.1)-(2.3) reveal one fundamental characteristic about the carbon cycle used in this model: The total carbon content of all reservoirs (the upper reservoir, the lower reservoir and the resource stock) must be constant at each point in time. This constant is determined by the initial contents of the carbon stocks.

$$R_t + W_t + S_t = \text{constant} = R_0 + W_0 + S_0 \quad \forall t \quad (2.4)$$

Dropping the time index for convenience we can use the carbon balance equation to reduce the dimension of the dynamic system, as implied by (2.1)-(2.3). We solve (2.4) for W to obtain⁷ :

$$W = R_0 + W_0 + S_0 - R - S \quad (2.5)$$

Inserting (2.5) into (2.1) we can reformulate the dynamic equation for the upper reservoir.

$$\dot{S} = q - a - \gamma(\sigma S - \omega(R_0 + W_0 + S_0 - R - S)) \quad (2.6)$$

⁷Note that, due to the carbon balance equation the upper and lower reservoir have an implicit upper bound which is given respectively by $\bar{S} = \frac{\omega}{\sigma+\omega}(R_0+S_0+W_0)$ and $\bar{W} = \frac{\sigma}{\sigma+\omega}(R_0+S_0+W_0)$.

Consumption of the fossil fuel q generates utility $U(q)$ with $U_q(q) > 0$ and $U_{qq}(q) < 0$. The cost of extraction are stock dependent and given by

$$c(q, R) = qC(R) \quad (2.7)$$

with $C_R < 0$, $C_{RR} \geq 0$. By $A(a)$ we denote the costs of sequestration with $A_a > 0$ and $A_{aa} > 0$ ⁸. $D(S)$ is the social damage that is caused by the stock of carbon in the atmosphere. We assume $D_S > 0$ and $D_{SS} > 0$. The social planner solves the following dynamic optimization problem:

$$\max_{q,a} \int_0^{\infty} e^{-\rho t} (U(q) - A(a) - qC(R) - D(S)) dt \quad (2.8)$$

subject to (2.3), (2.6) and

$$S(0) = S_0 > 0, \quad R(0) = R_0 > 0, \quad W(0) = W_0 > 0.$$

We formulate the current value Hamiltonian⁹ as:

$$\begin{aligned} H &= U(q) - A(a) - qC(R) - D(S) \\ &- \lambda_S(q - a - \gamma(S - \omega(R_0 + W_0 + S_0 - R_t - S_t))) \\ &+ \lambda_R \cdot (-q) \end{aligned} \quad (2.9)$$

⁸For the rest of this paper we use the term sequestration to describe air capture and ocean sequestration for convenience.

⁹Note, that we have changed the sign of λ_S to facilitate interpreting it as the carbon tax in later sections. We have also normalized $\sigma = 1$

The shadow value of the exhaustible resource, λ_R can be interpreted as the resource rent, λ_S as a carbon tax. Applying the maximum principle yields the following first-order conditions:

$$U_q(q) = C(R) + \lambda_R + \lambda_S \quad (2.10)$$

$$A_a(a) = \lambda_S \quad (2.11)$$

$$\dot{\lambda}_S - \rho\lambda_S = \lambda_S\gamma(1 + \omega) - D_S(S) \quad (2.12)$$

$$\dot{\lambda}_R - \rho\lambda_R = qC_R(R) - \gamma\omega\lambda_S \quad (2.13)$$

The transversality conditions are given by

$$\lim_{t \rightarrow \infty} \lambda_S \cdot e^{-\rho t} \geq 0, \quad \lim_{t \rightarrow \infty} R \cdot \lambda_R \cdot e^{-\rho t} \geq 0 \quad (2.14)$$

The static efficiency condition (2.10) relates marginal utility from extracting and consuming q units of the resource to the marginal costs of extraction, the resource rent and the carbon tax. From (2.11) we deduct that it is optimal to sequester the extracted carbon up to the amount where the marginal sequestration costs are equal to the shadow price of the upper carbon reservoir. Equation (2.12) is the dynamic efficiency condition for the carbon rent. It has basically the same form as the standard model of resource extraction, except for the term $-\gamma\omega\lambda_S$ which results from the carbon balance equation. It reflects the fact that part of the emissions into the atmosphere is transferred to the lower reservoir and therefore, does not contribute to damage. We analyze the dynamic properties of the carbon tax as given by (2.12) in section 2.2.5.

2.2.3 Steady-State Analysis

In a next step we analyze general properties of the steady state. For this purpose we establish the modified Hamiltonian dynamic system (MHDS). From equation (2.10) we can write q as $q(R, \lambda_S, \lambda_R)$, with $q_R > 0$, $q_{\lambda_S} < 0$ and $q_{\lambda_R} < 0$. Similarly, equation (2.11) defines $a = a(\lambda_S)$ with $a_{\lambda_S} > 0$. Using these specifications together with (2.3), (2.6), (2.12) and (2.13) we obtain the MHDS:

$$\dot{S} = q(R, \lambda_S, \lambda_R) - \gamma(S - \omega(R_0 + S_0 + W_0 - R - S)) - a(\lambda_S) \quad (2.15)$$

$$\dot{R} = -q(R, \lambda_S, \lambda_R) \quad (2.16)$$

$$\dot{\lambda}_S = \lambda_S(\gamma(1 + \omega) + \rho) - D_S(S) \quad (2.17)$$

$$\dot{\lambda}_R = \rho\lambda_R - \gamma\omega\lambda_S + q(R, \lambda_S, \lambda_R)C_R(R) \quad (2.18)$$

Applying the steady-state conditions $\dot{S} = \dot{R} = \dot{\lambda}_S = \dot{\lambda}_R = 0$ to (2.15)-(2.18) we obtain.

$$a(\lambda_S) = -\gamma(S - \omega(R_0 + S_0 + W_0 - R - S)) \quad (2.19)$$

$$q(R, \lambda_S, \lambda_R) = 0 \quad (2.20)$$

$$\lambda_S = \frac{D_S(S)}{\gamma(1 + \omega) + \rho} \quad (2.21)$$

$$\lambda_R = \frac{\gamma\omega\lambda_S}{\rho} \quad (2.22)$$

Since $q(R, \lambda_R, \lambda_S) = 0$, the LHS of equation (2.19) can be interpreted as the net anthropogenic transfer of carbon from the upper reservoir to the lower reservoir. According to (2.19) this net anthropogenic transfer must be equal to the net natural transfer of carbon from the lower reservoir to the upper reservoir. Thus, the steady

state corresponds qualitatively to point C in figure 2.2. Equation (2.21) states that in the steady state the carbon tax must be equal to the marginal damage weighted by the discount rate and the parameters describing the lagged adjustment effect of the natural component of the carbon cycle. Since $S > 0$ in a steady state, $D_S(S) > 0$ and the carbon tax must be positive. Finally, equation (2.22) implies a steady state resource rent being linearly proportional to the carbon tax. Hence, the resource rent must be strictly positive as well. At first glance, this seems counterintuitive, since in the basic resource extraction model, the steady state resource rent is zero. However, note that because we have substituted W from (2.5) into (2.2), the resource stock now explicitly occurs in the equation of motion of the upper reservoir (equation 2.6). The economic intuition is as follows: For a given level of the upper reservoir, a higher level of the resource stock implies a lower carbon content of the lower reservoir (following equation 2.5). As a consequence, the difference in the partial pressure between the reservoirs is increased and the net natural carbon transfer to the lower reservoir is positive. In a next step we derive saddle point properties of the MHDS.

Proposition 1. *The steady state of the MHDS system (2.15)-(2.18) is saddle point stable.*

Proof. The Jacobian of the MHDS evaluated at the steady state is given by ¹⁰:

$$\begin{aligned}
J &= \begin{bmatrix} \frac{\partial \dot{S}}{\partial S} & \frac{\partial \dot{S}}{\partial R} & \frac{\partial \dot{S}}{\partial \lambda_S} & \frac{\partial \dot{S}}{\partial \lambda_R} \\ \frac{\partial \dot{R}}{\partial S} & \frac{\partial \dot{R}}{\partial R} & \frac{\partial \dot{R}}{\partial \lambda_S} & \frac{\partial \dot{R}}{\partial \lambda_R} \\ \frac{\partial \dot{\lambda}_S}{\partial S} & \frac{\partial \dot{\lambda}_S}{\partial R} & \frac{\partial \dot{\lambda}_S}{\partial \lambda_S} & \frac{\partial \dot{\lambda}_S}{\partial \lambda_R} \\ \frac{\partial \dot{\lambda}_R}{\partial S} & \frac{\partial \dot{\lambda}_R}{\partial R} & \frac{\partial \dot{\lambda}_R}{\partial \lambda_S} & \frac{\partial \dot{\lambda}_R}{\partial \lambda_R} \end{bmatrix} \\
&= \begin{bmatrix} -\gamma(1 + \omega) & -\gamma\omega + q_R & -a_{\lambda_S} + q_{\lambda_S} & q_{\lambda_R} \\ 0 & -q_R & -q_{\lambda_S} & -q_{\lambda_R} \\ -D_{SS} & 0 & \gamma + \rho + \gamma\omega & 0 \\ 0 & C_R q_R & -\gamma\omega C_R q_{\lambda_S} & \rho + C_R q_{\lambda_R} \end{bmatrix} \quad (2.23)
\end{aligned}$$

For this system of four linear first-order differential equations the four characteristic roots can be obtained by using (Dockner, 1985), Theorem 1, p.10:

$$p_{1,2,3,4} = \frac{\rho}{2} \pm \left[\left(\frac{\rho}{2} \right)^2 - \frac{1}{2} \Omega \pm \frac{1}{2} (\Omega^2 - 4 * \Delta)^{0.5} \right]^{0.5}, \quad (2.24)$$

where Δ is the determinant of the Jacobian of (2.23) being:

$$\Delta = -\gamma\omega D_{SS}(\gamma\omega q_{\lambda_R} + \rho q_{\lambda_S}) + \rho(\gamma(1 + \omega)(\gamma + \rho + \gamma\omega) + a_{\lambda_S} D_{SS}) q_R > 0$$

and

$$\Omega = -\gamma(1 + \omega)(\gamma + \rho + \gamma\omega) + D_{SS}(q_{\lambda_S} - a_{\lambda_S}) - \rho q_R < 0 \quad (2.25)$$

¹⁰For space reasons we omit denoting functions in terms of the state and co-state variables when necessary)

Given that $\Delta > 0$ and $\Omega < 0$ the system has saddle point properties. In addition, by showing that $\Omega^2 - 4\Delta > 0$ we show that the roots are real.

$$\begin{aligned} \Omega^2 - 4\Delta &= \underbrace{-4(-\gamma(1+\omega)(\gamma + \rho + \gamma\omega) + D_{SS}(q_{\lambda_S} - a_{\lambda_S}) - \rho q_R)}_{>0} & (2.26) \\ &+ \underbrace{(\gamma\omega D_{SS}(\gamma\omega q_{\lambda_R} + \rho q_{\lambda_S}) - \rho(\gamma(1+\omega)(\omega + \rho + \gamma\omega) + a_{\lambda_S} D_{SS})q_R)^2}_{>0} \end{aligned}$$

□

2.2.4 The Decentralized Economy

The externality in this model consists of two parts, (1) the negative effect of rising carbon concentration levels and (2), the positive effect of removing carbon from the atmosphere via CCS. Note that, since the latter effect is only temporary and carbon added into the carbon cycle is not removed, the overall effect is negative. In this section we consider the decentralized economy and study how the externality should be internalized. Consider two representative firms. Firm 1 has access to the non-renewable resource and serves the output market for the resource product. The profit maximization problem of firm 1 reads:

$$\max_{q>0} \int_0^{\infty} e^{-\rho t} (pq - \tau q - qC(R)) dt \quad (2.27)$$

subject to

$$\dot{R} = -q \quad (2.28)$$

where τ denotes the tax on carbon dioxide and p is the market price. Firm 2 owns the CCS technology. We introduce a subsidy on sequestration which we denote by θ . The profit maximization problem of firm 2 reads:

$$\max_{a>0} \int_0^{\infty} e^{-\rho t} (\theta a - A(a)) dt \quad (2.29)$$

The Euler equations for firm 1 and firm 2 are given by

$$0 = p - \tau - C(R) \quad (2.30)$$

$$0 = \theta - A_a(a) \quad (2.31)$$

Utility maximization of consumers implies $U_q = p$. Using this, we can compare (10)-(11) to (30)-(31) and obtain the optimal decentralized policy $\lambda_S = \tau = \theta$ which generates the first best solution. Thus, the optimal carbon tax is equal to marginal damage which is also the optimal subsidy rate. For the rest of this paper we will use the term carbon tax for λ_S , the shadow price of the upper reservoir.

2.2.5 Possible Carbon Tax Paths

From the dynamic efficiency condition (2.17) we can extract some information about the optimal paths of the carbon tax. We restate (2.17) as:

$$\dot{\lambda}_S = \lambda_S \cdot \theta - D_S(S) \quad (2.32)$$

with $\theta = \rho + \gamma(1 + \omega)$. Consequently λ_S grows at the rate θ and decreases with higher levels of the marginal damage. Notice that we can express the isocline of

λ_S by

$$\lambda_S(S)|_{\dot{\lambda}_S=0} = \frac{D_S(S)}{\theta} = z(S) \quad (2.33)$$

where $z_S(S) > 0$. Using equation (2.33) we want to illustrate the possible shapes of the optimal carbon tax paths. These are: increasing, decreasing, u-shaped and inversely u-shaped. Figure 2.3 illustrates the implications of equation (2.32).

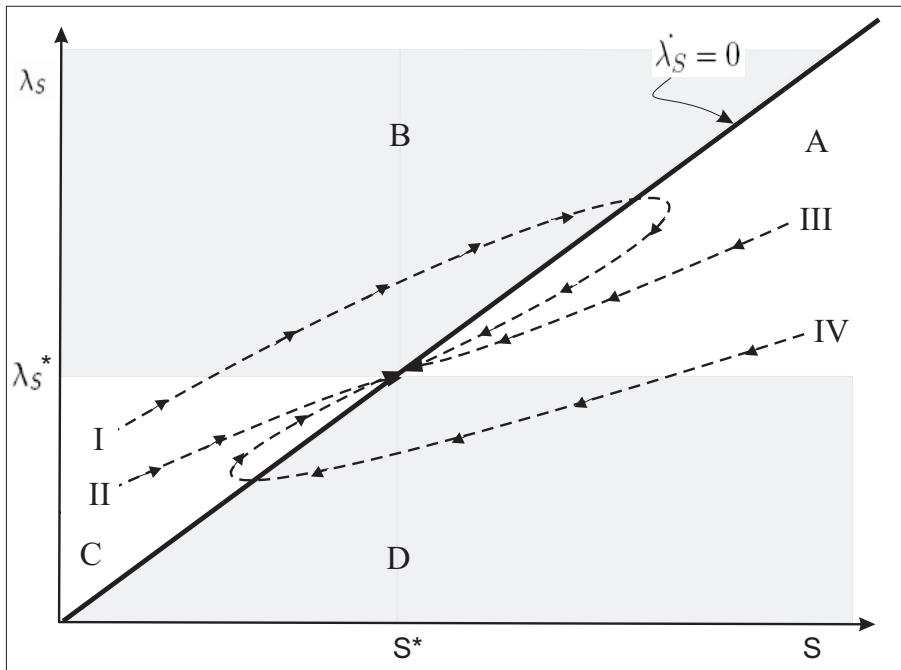


Figure 2.3: non-monotonic carbon tax paths

Proposition 2. Consider the isocline $\lambda_S = z(S)$ from (2.33) in the $S - \lambda_S$ space with the steady state (λ_S^*, S^*) . Define the set B as $B = \{\lambda > \lambda_S^*\} \cap \{\lambda > z(S)\}$. Let $P(t)$ be a trajectory resulting from the optimization problem. If there is some $\bar{t} \in [0, \infty]$ such that $P(\bar{t}) \in B$ then λ_S is inversely U-shaped.

Proof. We argue that the carbon tax has to be initially increasing and decreasing afterwards. By construction of $z(S)$ (equation 2.33), any trajectory crossing B implies an increasing carbon tax. Because of the properties of $z(S)$, λ_S must cross the $z(S)$ isocline at some \tilde{t} with $\lambda_S(\tilde{t}) > \lambda_S^*$ at which $\dot{\lambda}_S(\tilde{t}) = 0$. For all $t > \tilde{t}$, $\dot{\lambda}_S(t) < 0$ and λ_S is decreasing. \square

Notice, that at the maximum of an inversely u-shaped carbon tax, the upper reservoir must be increasing. This can be seen by differentiating (2.32) w.r.t. time.

$$\ddot{\lambda}_S = \theta \dot{\lambda}_S - D_{SS} \dot{S} \quad (2.34)$$

Since $\dot{\lambda}_S = 0$ at a maximum and $D_{SS} > 0$ it follows that $\ddot{\lambda}_S < 0$ if $\dot{S} > 0$. In a next step we show the possibility of a U-shaped carbon tax.

Proposition 3. *Consider the isocline $\lambda_S = z(S)$ in the $S - \lambda_S$ space with the steady state (λ_S^*, S^*) . Define the set D as $D = \{\lambda < \lambda_S^*\} \cap \{\lambda < z(S)\}$. Let $P(t)$ be a trajectory resulting from the optimization problem. If there is some $\bar{t} \in [0, \infty]$ such that $P(\bar{t}) \in D$ then λ_S is U-shaped.*

Proof. This proof is similar to the one of Proposition 2. We argue that the carbon tax has to be initially decreasing and increasing afterwards. By construction of $z(S)$ (equation 2.33), any trajectory crossing D implies a decreasing carbon tax. Because of the properties of $z(S)$, λ_S must cross the $z(S)$ isocline at some \tilde{t} with $\lambda_S(\tilde{t}) < \lambda_S^*$ at which $\dot{\lambda}_S(\tilde{t}) = 0$. For all $t > \tilde{t}$, $\dot{\lambda}_S(t) > 0$ and λ_S is increasing. \square

Proposition 3 implies that at a minimum of the carbon tax, the upper reservoir must be decreasing, since now $\ddot{\lambda}_S > 0$ if $\dot{S} < 0$.

While paths crossing B or D must be non-monotonic, the converse is not necessarily true. Optimal trajectory which pass through A or C are not necessarily monotonic. The natural transfer rate γ plays an important role for the monotonicity of the optimal trajectories. Consider e.g. a situation in which the carbon stock in the upper reservoir at $t = 0$ is extremely high. Whether λ_S is high or low (i.e. paths originating in A or D) depends among other model parameters on the natural transfer rate. If the transfer rate is very high as well, this implies that the flux from the upper reservoir to the lower reservoir is very high (lower λ_S initially) and the possibility of undershooting the steady state carbon content in S is more likely. As a consequence we obtain a U-shaped carbon tax (e.g. path IV). By contrast, a low transfer rate implies a weaker flux from the upper reservoir to the lower reservoir (higher λ_S initially). As a consequence we obtain a monotonically decreasing carbon tax (e.g. path III). By similar reasoning we cannot rule out paths originating in C to be non-monotonic. For low initial levels of S and a high transfer rate there need not be an overshooting of the upper reservoir, implying a monotonically increasing carbon tax (e.g. Path II). However, a low natural transfer rate of carbon combined with high emission levels can result in an overshooting of the upper reservoir which in turn leads to a inversely U-shaped carbon tax (Path I).

2.3 Simulation of Optimal Paths

We impose the following functional forms with $a_1, u_1, u_2, s_3, c_1, c_2, s_1 > 0$

$$U(q) = u_1q - u_2q^2 \quad (2.35)$$

$$A(a) = a_1a^2 \quad (2.36)$$

$$C(R) = c_1 - c_2R \quad (2.37)$$

$$D(S) = s_3(s_1S - s_2)^2 \quad (2.38)$$

Since S is the stock of carbon in the upper box containing the atmosphere and the upper ocean layer, we introduce the parameter s_1 , the percentage of the carbon stock in the upper box which is situated in the atmosphere. Using the FOC's (2.10) and (2.11) we can solve for q and a :

$$q = \frac{-c_1 + c_2R + u_1 - \lambda_R - \lambda_S}{2u_2} \quad (2.39)$$

$$a = \frac{\lambda_S}{2a_1} \quad (2.40)$$

Using the specific functional forms and the two previous equations we can rewrite the MHDS in canonical form:

$$\begin{pmatrix} \dot{S} \\ \dot{R} \\ \dot{\lambda}_S \\ \dot{\lambda}_R \end{pmatrix} = \begin{pmatrix} -\gamma(1+\omega) & -\gamma\omega + \frac{c_2}{2u_2} & \frac{-a_1 - u_2}{2u_2 a_2} & \frac{-1}{2u_2} \\ 0 & \frac{-c_2}{2u_2} & \frac{1}{2u_2} & \frac{1}{2u_2} \\ -s_1^2 s_3 & 0 & \gamma\omega + \gamma + \rho & 0 \\ 0 & \frac{-c_2}{2u_2} & -\gamma\omega + \frac{c_2}{2u_2} & \rho + \frac{c_2}{2u_2} \end{pmatrix} \cdot \begin{pmatrix} S \\ R \\ \lambda_S \\ \lambda_R \end{pmatrix} + \begin{pmatrix} k_1 \\ k_2 \\ k_3 \\ k_4 \end{pmatrix}$$

with

$$\begin{aligned}
k_1 &= \omega\gamma(R_0 + S_0 + W_0) - \frac{c_1 - u_1}{2u_2} \\
k_2 &= \frac{c_1 - u_1}{2u_2} \\
k_3 &= 2s_1s_3s_2 \\
k_4 &= \frac{c_2(c_1 - u_1)}{2u_2}
\end{aligned}$$

We can solve for the steady-state values of λ_S , λ_R , S and R which are obtained by setting $\dot{\lambda}_S = \dot{\lambda}_R = \dot{S} = \dot{W} = \dot{R} = 0$. The steady-state values for the canonical system when $t \rightarrow \infty$ are:

$$\tilde{S} = \frac{1}{k_5} \cdot \left[-a_2(c_1 - c_2k_6)\gamma\rho\omega(\gamma + \rho + \gamma\omega) \right. \quad (2.41)$$

$$\left. + s_2s_1s_3(c_2\rho + 2a_2\gamma\omega(\rho + \gamma\omega)) + a_2\gamma\rho\omega(\gamma + \rho + \gamma\omega)u_1 \right]$$

$$\tilde{R} = \frac{1}{k_5} \cdot \left[2a_2s_1s_3\gamma(\rho + \gamma\omega)(s_1k_6\omega - s_2(1 + \omega)) \right. \quad (2.42)$$

$$\left. + c_1\rho(s^2v + a_2\gamma(1 + \omega)(\gamma + \rho + \gamma\omega)) \right.$$

$$\left. - \rho(s^2v + a_2\gamma(1 + \omega)(\gamma + \rho + \gamma\omega))u_1 \right]$$

$$\tilde{\lambda}_S = \frac{1}{k_5} \cdot \left[2a_2s_1s_3\gamma\rho(s_1(-c_1 + c_2k_6)\omega - s_2c_2(1 + \omega) + s\omega u_1) \right] \quad (2.43)$$

$$\tilde{\lambda}_R = \frac{1}{k_5} \cdot \left[2a_2s_1s_3\gamma^2\omega(s_1(-c_1 + c_2k_6)\omega - s_2c_2(1 + \omega) + s\omega u_1) \right] \quad (2.44)$$

with

$$k_5 = 2a_2s_1^2v\gamma\omega(\rho + \gamma\omega) + c_2\rho(s_1^2s_3 + a_2\gamma(1 + \omega)(\gamma + \rho + \gamma\omega))$$

$$k_6 = R_0 + S_0 + W_0$$

In order to analyze the optimal paths of the model variables in detail we parameterize the model. Concerning the parameter space, there are some nature-given parameters which we have obtained from current estimates. The remaining (economic) parameters were chosen to match current carbon fluxes damage and cost estimates.¹¹ We assume that the pre-industrial ocean was in steady-state, i.e. there

Nature-given Parameter	Value	Economic Parameter	Value
γ	.005	ρ	.01
σ	1	a_2	2
ω	.1	u_1	50
W_0	20,000	u_2	.5
R_0	10,000	c_1	50
S_0	2,000	c_2	.004
s_2	600	s_1	.3
		s_3	.001

Table 2.1: Parameter Values: Base run

was a balance between carbon sources and sinks in the ocean. Since the onset of the industrial revolution (mid 19th century), this balance has been disturbed by release of CO_2 into the atmosphere, of which concentration of CO_2 has increased dramatically. About 36,100 Pg-C are currently stored in the deep ocean, compared to 910 Pg-C in the surface ocean and 820 Pg-C (about 385 ppm) in the atmosphere.¹² We have calculated these numbers by assuming that the average deep dissolved inorganic carbon (DIC) concentration is about $2.290 \cdot 10^6 \frac{mol}{km^3}$ and the volume of the deep ocean reservoir is about $1.3138 \cdot 10^9 km^3$. We divide the upper

¹¹Note that we measure W_0 , S_0 and R_0 in Pg-C. The parameters γ and ρ have dimension t^{-1} while the remaining variables are dimensionless.

¹²We measure these stocks in mass-units of carbon (i.e. Pg-C), as it appears in different chemical forms within the reservoirs.

ocean layer and the deep ocean layer at about 100 meters depth. While it takes several centuries for the deep ocean to mix with the atmosphere, the exchange between the atmosphere and the upper ocean layer takes place at a much lower time scale. It takes about one year for the upper reservoir to mix. Therefore, we assume instant equilibration between the surface ocean and the atmosphere which is justified in this context. For the upper ocean we assume an average DIC concentration of $2.100 \cdot 10^6 \frac{\text{mol}}{\text{km}^3}$ and a volume of $36.1 \cdot 10^6 \text{km}^3$. For the initial levels of the reservoirs we have chosen: 20,000 Pg-C for the deep see reservoir W_0 ¹³, 600 Pg-C for the atmosphere and 1,200 Pg-C for the upper ocean layer. The values for γ , the dynamic adjustment parameter and ω , the factor of proportionality of the two reservoirs have been chosen such as to represent observed fluxes

According to the German Federal Office for Geoscience and Natural Resources (BGR) current non-renewable reserves are estimated to be at an order of 1,350 Pg-C equivalent [BGR, 2006]. Non-renewable carbon resources on the other hand are estimated between 5,000 Pg-C (Lackner, 2003) and 12,000 Pg-C [BGR, 2006]. We have chosen R_0 , i.e. the pre-industrial stock of R_0 to be at 10,000 Pg-C. We can parameterize our model such that the resource stock will not be used entirely in finite time.

In order to obtain an expression for the optimal paths, we consider the Jacobian

¹³The pre-industrial level of W , the deep-sea reservoir is difficult to calculate, with estimates ranging from 20,000 - 40,000 Pg-C

of the MHDS applying the functional forms (2.35)-(2.38).

$$J = \begin{bmatrix} \gamma + \rho + \gamma\omega & 0 & -2s_1^2v & 0 \\ -\gamma\omega + \frac{c_2}{2u_2} & \rho + \frac{c_2}{2u_2} & 0 & -\frac{c_2^2}{2u_2} \\ -\frac{a_2+u_2}{2a_2u_2} & -\frac{1}{2u_2} & -\gamma(1+\omega) & -\gamma\omega + \frac{c_2}{2u_2} \\ \frac{1}{2u_2} & \frac{1}{2u_2} & 0 & -\frac{c_2}{2u_2} \end{bmatrix} \quad (2.45)$$

Using the parameter values above we can then calculate the eigenvalues associated with this Jacobian. They are: $r_1 = 0.012$, $r_2 = -0.002$, $r_3 = 0.024$, $r_4 = -0.014$. Thus, the system has two negative eigenvalues, as we have shown in Proposition 1. Therefore, the steady state is saddle-point stable. The steady state values are: $\tilde{S} = 2503.66$, $\tilde{R} = 1535.34$, $\tilde{\lambda}_S = 5.85$, $\tilde{\lambda}_R = .29$ and additionally, $\tilde{a} = 1.46$, $\tilde{q} = 0$. Furthermore, from the carbon balance equation we obtain $\tilde{W} = 27961.01$. Given the information above, we can formulate the optimal paths for $S(t)$, $R(t)$, $\lambda_S(t)$ and $\lambda_R(t)$ (where we denote optimal paths by an asterisk).

$$X_t^* = \tilde{X} + e^{r_1 t} \cdot \Theta_1 \cdot \Upsilon_{r_1, X} + e^{r_2 t} \cdot \Theta_2 \cdot \Upsilon_{r_2, X} \quad \text{for } X = S, R, \lambda_S, \lambda_R \quad (2.46)$$

where r_1 and r_2 are the negative eigenvalues of the Jacobian above, $\Upsilon_{r_i, X}$ is the eigenvector of X related to the eigenvalue i and Θ_1 and Θ_2 are constants which are obtained by solving

$$X_0^* = X_0 \quad \text{for } X = S, R \quad (2.47)$$

The optimal paths of W , q and a are obtained using equations (2.5), (2.35) and (2.36) respectively.

2.3.1 Simulation of the Model

Figure 2.4 depicts the results of the model. The abscissae denote time t . Recall that

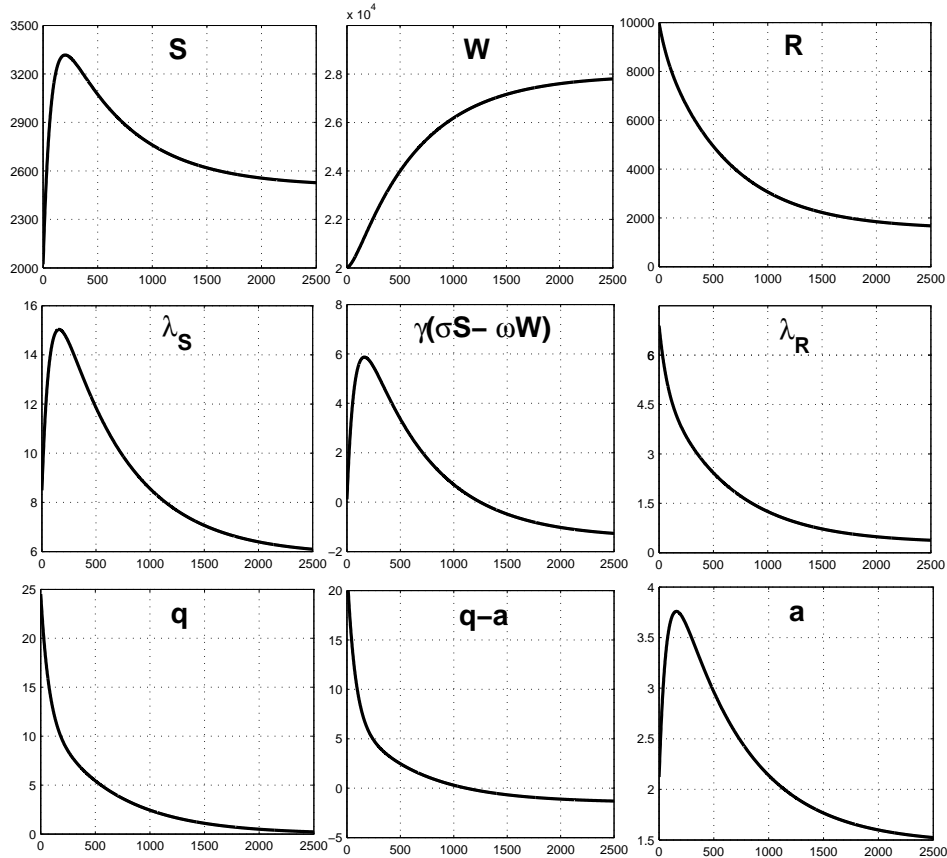


Figure 2.4: The basic model

$S_0 = 2,000$, $R_0 = 10,000$ and $W_0 = 20,000$. Extraction is high at the beginning and decreases monotonically to zero. The resource stock R is only economically depleted and not fully used. Extraction and emission of the non-renewable resource has an instant damage effect. Sequestration of carbon into the deep ocean has a delayed damage effect. Thus, it is optimal to extract the resource rapidly and sequester larger amounts at initial stages of the time horizon. As a consequence of higher extraction rates, the carbon concentration in the upper reservoir and in

turn, the carbon tax rises. The upper reservoir overshoots its steady state level. This is because the natural transfer of carbon to the deep ocean is not fast enough to absorb the carbon added to the upper reservoir. The lower reservoir is a net sink of carbon and its content increases monotonically. The resource scarcity rent is monotonically declining. In the new steady state the natural transfer of carbon to the lower reservoir is negative and the net anthropogenic transfer of carbon to the lower reservoir is positive. This implies for the new steady state that lower reservoir is supersaturated and we obtain an emitting ocean.

2.3.2 Sequestration vs. no sequestration

In this section we compare the basic model with the case in which the CCS technology is not available. The upper plot in figure 2.5 depicts the carbon content diagram. The solid line represents the basic model while the dashed line depicts the case without the CCS technology. Note that, without sequestration, the new steady state is characterized by equal partial pressure in both reservoirs since now sequestration and extraction are both zero. Without the CCS technology the overshooting of the upper reservoir is much stronger and the steady state carbon content in the atmosphere is much larger when compared to the basic model. In addition, less of the resource stock has been extracted as can be seen by the lower iso carbon content line R_1 . We obtain this result because sequestering carbon at a constant rate in the steady state allows for a larger equilibrium share of carbon in the lower reservoir. The lower graph in figure 2.5 shows the carbon tax. Without sequestration, the carbon tax path is shifted upwards, thus at any point in time the carbon tax is higher. The reason for this is the larger overshooting of the upper carbon reservoir which results in a higher damage.

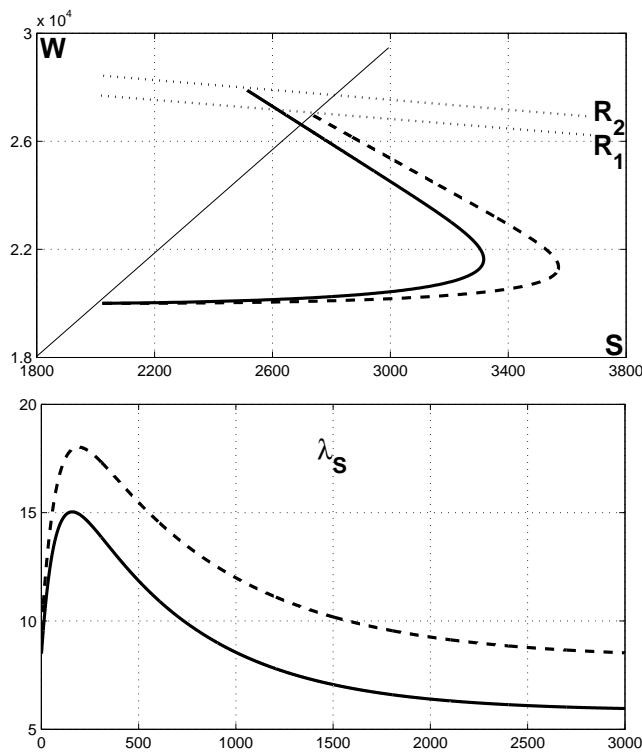


Figure 2.5: Sequestration vs. No sequestration

2.3.3 The impact of discounting

In a next step we investigate how the optimal solution changes if we decrease the discount rate. The solid lines in figure 2.6 depict the base run case again where the discount rate is 1%. There is an ongoing debate about the proper discount rate in presence of global warming. Stern (2006) suggests a discount rate close to zero. The dotted line in figure 6 represents the optimal solution where we have lowered the discount rate to 0.1%. Since a high discount rate means that we value the future less, ocean sequestration will be used more intensively because of its lagged damage effect. On the other hand, placing more weight on the future damages leads to fewer total extraction as implied by the lower carbon isocontent line in

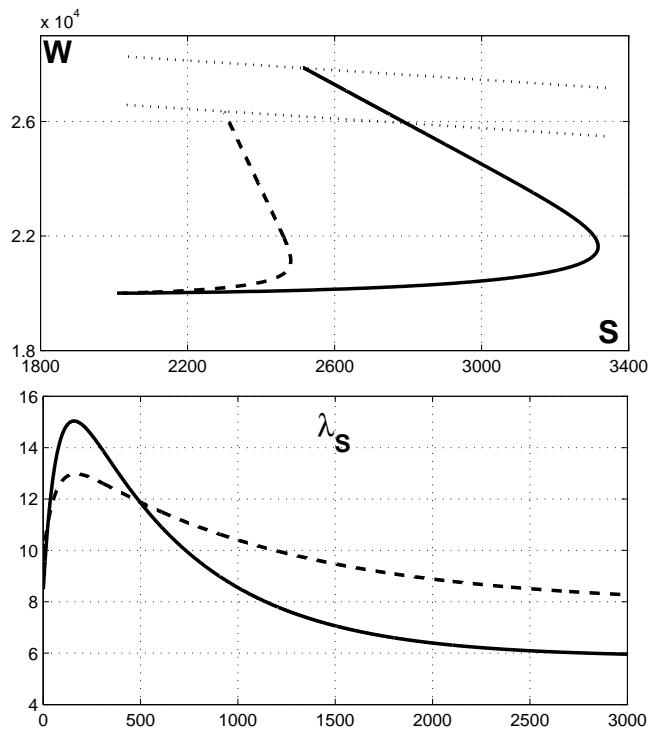


Figure 2.6: 1% vs. 0.1% discounting

Figure 6. In that case, future and current damages are perceived more equally.

2.3.4 Optimal Carbon Tax Paths

In the basic model the carbon tax is hump-shaped. This is because the path of S is hump-shaped. In general, the path of the carbon tax will be similar to the one of the upper reservoir. It is therefore possible to obtain different shapes of the carbon tax. Figure 2.7 displays four possible paths of the carbon tax within our modeling framework. These plots differ from each other w.r.t. the initial carbon stock size and the natural transfer speed of carbon between the two reservoirs. The base run simulation scenario (low γ , low S_0) is depicted in the upper left plot. It

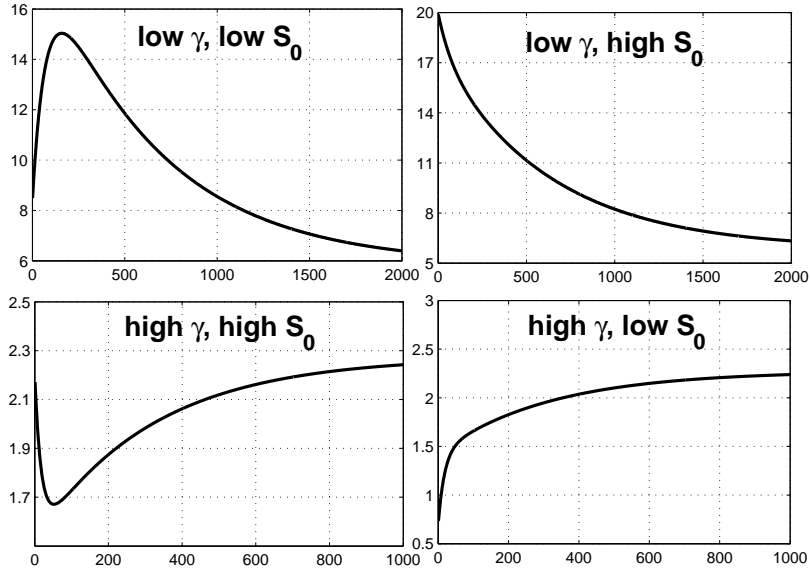


Figure 2.7: Possible paths of the carbon tax

shows the same inverted u-shaped pattern as seen earlier. By contrast, the upper right plot shows the optimal carbon tax resulting from increasing the initial stock of carbon in the upper reservoir (low γ , high S_0). As a result, the carbon tax is monotonically decreasing to the same steady state as in the upper left scenario. The decrease occurs for two reasons. (1) A high initial S_0 induces much higher rates of sequestration (equation 2.12) and (2.2), since the carbon balance equation must hold at any point in time, increasing S_0 automatically implies a lower W_0 . As a consequence, there is a high difference in the partial pressure between the two reservoirs and the natural transfer is very strong.

The two lower plots in Figure 2.7 illustrate scenarios for which γ , the natural transfer speed is significantly increased¹⁴. As a consequence, carbon moves much

¹⁴Note that time scale for the lower two plots has 1000 periods while the upper plots have

faster between the two reservoirs and a steady state is reached earlier. In the lower right plot in particular (low γ , high S_0), the optimal carbon tax is monotonically increasing. The only difference to the base run scenario is a higher transfer speed of carbon. As a consequence the overshooting of the upper reservoir does no longer occur since now carbon is absorbed by the deep ocean much faster. This absorption effect is at its highest in the lower left plot. Here, the scenario (low γ , low S_0) implies that because (i) the transfer speed is very high and (ii) the difference in the partial pressure of the two reservoirs is very high as well, we obtain an undershooting of the upper carbon reservoir and consequently, a U-shaped carbon tax.

As a general remark, note that the level of the carbon tax is much higher in the upper plots. The natural transfer speed is the major determinant of the carbon tax level. Because it determines for "how long" the emitted carbon will remain in the atmosphere and hence, contribute to the damage resulting from higher carbon concentration levels in the atmosphere. Figure 2.8 is analogous to figure 2.2. We depict the four possible carbon tax paths in the $S - \lambda_S$ space. Notice that the subplots differ w.r.t the initial level of S while within the subplots only γ has been changed. In the upper plot we observe the base run case where we start with a carbon tax above its steady state level, but the carbon tax must increase first before it can monotonically fall towards its steady state.

In the lower plot of Figure 2.8 we observe that the carbon tax increases even if resource extraction goes to zero. The way we model the carbon cycle accounts for the fact that each unit of carbon is persistent and has a instant or lagged damage

2000 periods.

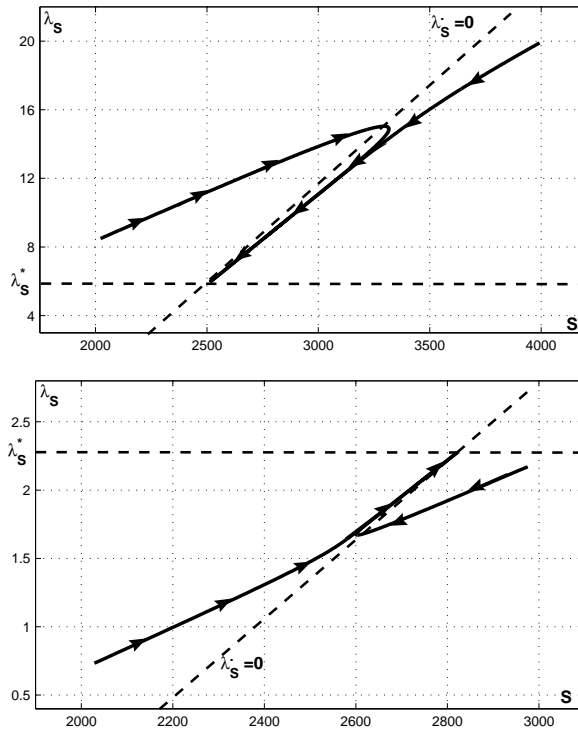


Figure 2.8: Carbon tax paths

effect, with the latter being due to sequestration.

2.4 The basic model with uncertainty

The previous analysis has shown that γ , the speed of natural transfer of carbon plays a crucial role for the shape of the optimal carbon tax path. From the model formulation we notice that the natural transfer of carbon and the anthropogenic transfer of carbon via ocean sequestration are substitutes in their impact on the carbon cycle dynamics. In this section we analyze the dependency of the model results on different rates of the speed of natural transfer of carbon. We conduct this analysis within a stochastic version of the basic model laid out in the previous

sections. In particular, we impose uncertainty about the damage which occurs due to the atmospheric carbon stock.

In this context we study the optimal extraction and sequestration policies given this uncertainty. As mentioned earlier, we extend this analysis to cover a grater range of γ , the speed of natural transfer of carbon.

Since we assume that the damage arising from carbon in the atmosphere is subject to uncertainty, we redefine the damage equation in (2.38) by $D(S, \eta) = \eta \cdot s_3(s_1 S - s_2)^2$. In the following we define the behavior of η over time as

$$d\eta = \theta \cdot (\bar{\eta} - \eta)dt + \sigma\eta dB \quad (2.48)$$

i.e, η follows an Ornstein-Uhlenbeck process, the continuous time equivalent of a mean-reverting AR(1) process. The mean of η is denoted by $\bar{\eta}$ and θ is the strength of mean reversion. For the diffusion, we assume a geometric brownian motion with $B \sim N(0, \sigma^2)$.

We formulate the stochastic optimization problem from the social planner's perspective. Given the uncertainty over η , the social planner maximizes the expected present value welfare.

$$\max_{q_t > 0, 0 \leq a_t} E \int_0^\infty e^{-\rho t} [U(q_t) - A(a_t) - C(R_t)q_t - D(S_t, \eta_t)] dt \quad (2.49)$$

subject to (2.3), (2.6), (2.49), $S(0) = S_0$, $W(0) = K_0$, $R(0) = R_0$ and $\eta(0) = \eta_0$. To solve (2.49) we perform stochastic control, the continuous time version of stochastic programming. Applying Ito's Lemma, the corresponding Hamilton-Jacobi-Bellman (HJB) equation is

$$\begin{aligned}
0 = \max_{c>0, 0 \leq m \leq 1} \{ & U(q) - A(a) - C(R)q - D(S, \eta) \\
& + V_S(S, R, \eta)(q - a - \gamma(\sigma S - \omega(R_0 + W_0 + S_0 - R - S))) \\
& + V_R(S, R, \eta)(-q) \\
& + V_\eta(S, R, \eta)(\theta \cdot (\bar{\eta} - \eta)) \\
& + \frac{1}{2}\sigma^2\eta^2 V_{\eta\eta}(S, R, \eta) - \rho V(S, R, \eta)\} \tag{2.50}
\end{aligned}$$

where $V(S, R, \eta)$ is the value function. A solution to (2.50) requires finding a value function and policy functions $q(S, R, \eta)$ and $a(S, R, \eta)$ which constitute explicit control rules. The first-order conditions for q and a are

$$U_q = C(R) - V_S(S, R, \eta) + V_R(S, R, \eta) \tag{2.51}$$

$$A_a = -V_S(S, R, \eta) \tag{2.52}$$

Equations (2.51) and (2.52) are similar to the first-order conditions of the deterministic case and explained in section 2.2.2. In the following we determine numerically the value function and the policy functions.

From the first-order conditions (2.51) and (2.52) we can obtain explicit solutions for the optimal stochastic control of q and a as functions of the state variables.

$$\tilde{q} = \Gamma_U^{-1}(C(R) - V_S(S, R, \eta) + V_R(S, R, \eta)) \tag{2.53}$$

$$\tilde{a} = \Gamma_A^{-1}(-V_S(S, R, \eta)) \tag{2.54}$$

Inserting (2.53) and (2.54) into (2.50) we obtain the concentrated HJB equation in terms of the value function and its derivatives with respect to the states. Thus,

the concentrated HJB equation is three-dimensional in S , R and η and reads

$$\begin{aligned}
0 = & U(q) - A(\Gamma_A^{-1}(-V_S(S, R, \eta))) - C(R)(\Gamma_U^{-1}(C(R) - V_S(S, R, \eta) + V_R(S, R, \eta))) \\
& + V_S(S, R, \eta)(\Gamma_U^{-1}(C(R) - V_S(S, R, \eta) + V_R(S, R, \eta))) - D(S, \eta) \\
& + V_S(S, R, \eta)(-\Gamma_A^{-1}(-V_S(S, R, \eta))) - \gamma(\sigma S - \omega(R_0 + W_0 + S_0 - R - S)) \\
& + V_R(S, R, \eta)(-\Gamma_U^{-1}(C(R) - V_S(S, R, \eta) + V_R(S, R, \eta))) \\
& + V_\eta(S, R, \eta)(\theta \cdot (\bar{\eta} - \eta)) \\
& + \frac{1}{2}\sigma^2\eta^2V_{\eta\eta}(S, R, \eta) - \rho V(S, R, \eta)
\end{aligned} \tag{2.55}$$

Equation (2.55) constitutes a nonlinear second-order partial differential equation which can be solved numerically using projection methods (Judd (1992), (1998)). Projection methods work very well with continuous-time, continuous-state problems (Judd (1998)). We estimate the value function with the Chebyshev collocation method using Matlab's CompEcon toolbox (Miranda and Fackler (2002)). Making use of the Weierstrass theorem, the collocation method approximates the solution to (2.55) with a linear combination of basis functions with coefficients approximately solving (2.55) at specific collocation nodes by value function iteration with Newton's method until a convergence rule is satisfied. The approximated value function is given by

$$\tilde{V}(S, R, \eta) = \sum_{i=1}^{n_i} \sum_{j=1}^{n_j} \sum_{k=1}^{n_k} g_{ijk} T_i(x_S) T_j(x_R) T_k(x_\eta)$$

$T_i(x_S)$, $T_j(x_R)$ and $T_k(x_\eta)$ are n_i, n_j, n_k -degree Chebyshev polynomials which are evaluated at the states with x_S, x_R, x_η being the mapping $[S_{\min}, S_{\max}] \times [R_{\min}, R_{\max}] \times [\eta_{\min}, \eta_{\max}] \mapsto [-1, 1] \times [-1, 1] \times [-1, 1]$. The collocation coeffi-

icients g_{ijk} are then estimated in order to deliver a good approximation of (2.55).

The functional forms and parameter values used for the numerical analysis are taken from section 2.3. We define $\eta = 1$ in the deterministic case. Given these values we set up the projection grid by discretizing the spate space. We choose $S \in [2000, 3500]$, $R \in [0, 10000]$ and $\eta \in [0, 4]$. The Chebyshev polynomials are of degree 5 in all states i.e.: $n_i, n_j, n_k = 5$. Figure 2.9 displays contour plots

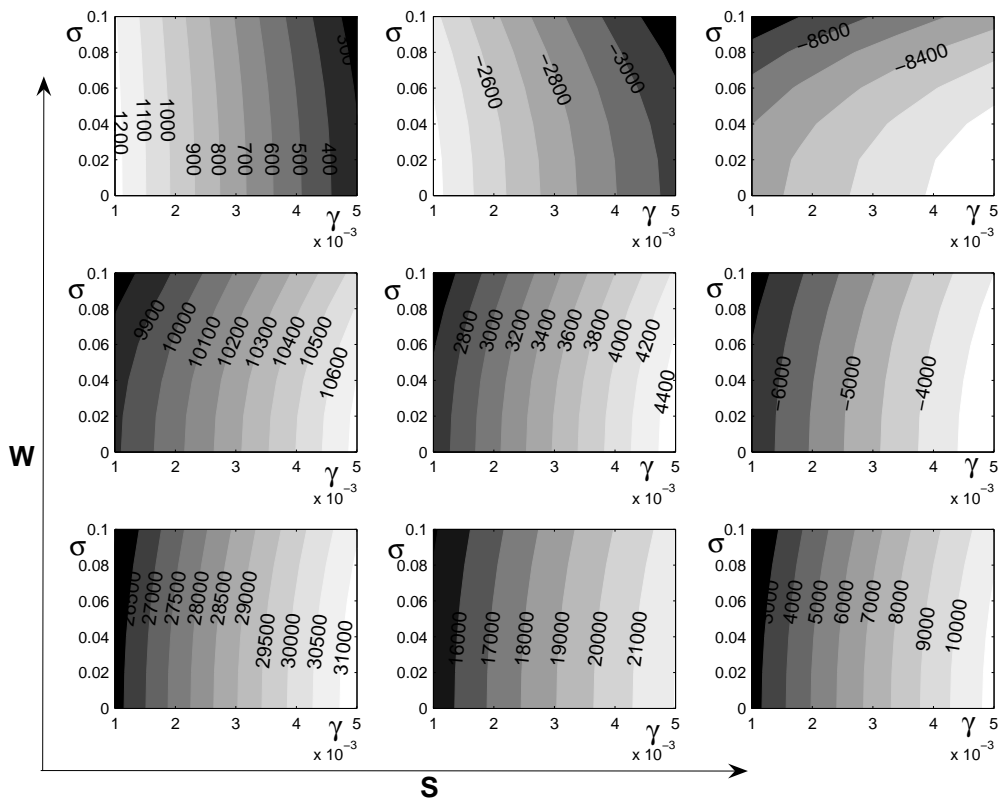


Figure 2.9: Value function - Contour plots in the $\gamma - \sigma$ space for combinations of S and W . $S \in \{2000, 2550, 3100\}$ and $W \in \{20000, 23750, 27500\}$, with $(S, W) = (2000, 20000)$ in the lower left subplot.

of the value function in the $\gamma - \sigma$ space for different combinations of S and W . In particular, we choose $S \in \{2000, 2550, 3100\}$ and $W \in \{20000, 23750, 27500\}$.

The damage coefficient η is equal to one. From Figure 2.9 we deduce that the value function decreases with higher levels of carbon in both, the upper and lower reservoirs. Furthermore, we observe that for any $S - W$ combination and any level of γ uncertainty about damage reduces the value function. A higher speed of the natural transfer of carbon, γ has a positive effect on the value function if the upper reservoir is supersaturated, while its effect is negative if the lower reservoir is supersaturated with carbon. This is an intuitive result since supersaturation implies a net outflow of carbon from the supersaturated reservoir. Using the

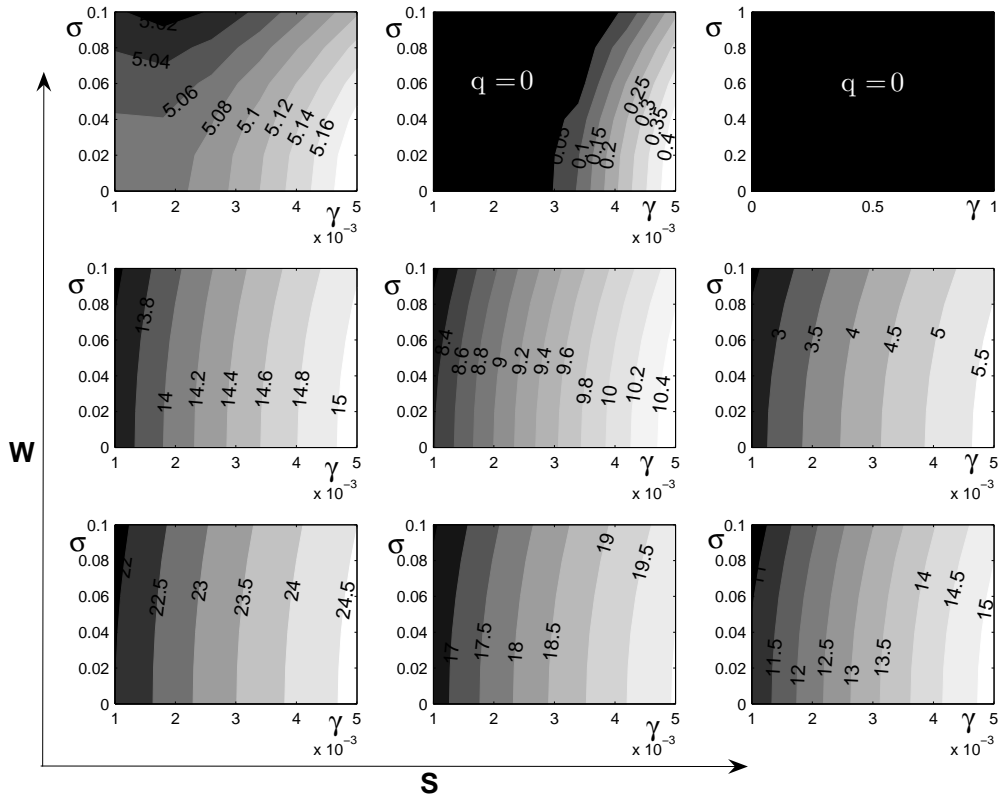


Figure 2.10: Optimal Extraction policy - Contour plots in the $\eta - \sigma$ space for combinations of S and W . $S \in \{2000, 2550, 3100\}$ and $W \in \{20000, 23750, 27500\}$, with $(S, W) = (2000, 20000)$ in the lower left subplot.

same state and parameter space as in the previous figure, Figure 2.10 displays the optimal extraction rates of the resource stock.

Three major characteristics of the optimal extraction policy can be deduced from Figure 2.10. (1) The general tendency is that both a high level of atmospheric and oceanic carbon yields low extraction of the resource. (2) For any combination in the $S - W$ space, optimal resource extraction increases with higher values of γ , the speed of natural transfer of carbon, an intuitive result. (3) Uncertainty about damage resulting from the atmospheric carbon stock implies lower resource extraction volumes for any level of γ . While we have fixed the damage coefficient ($\eta = 1$)

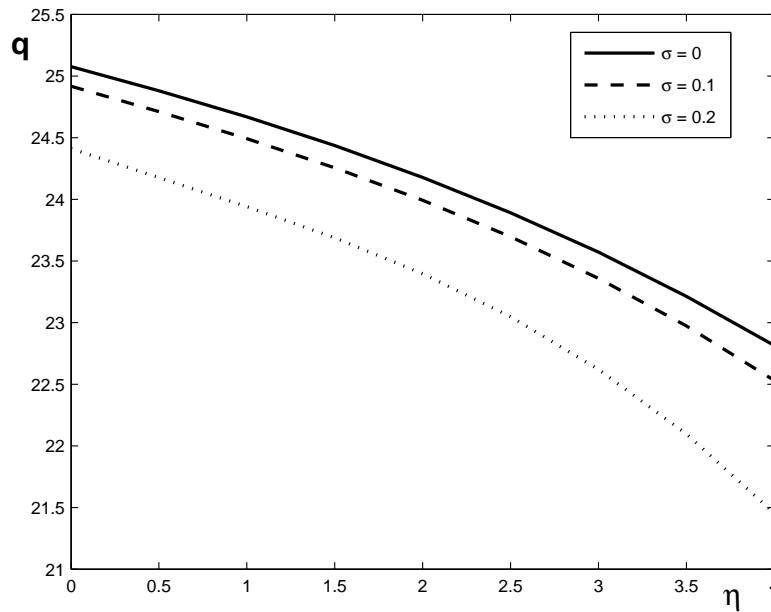


Figure 2.11: Optimal extraction as a function of the stochastic damage coefficient for $S = 2,000$, $W=20,000$ (for different degrees of uncertainty)

in Figure 2.10, Figure 2.11 analyzes the relationship between different levels of the stochastic damage parameter and optimal extraction. This time however, we assume fixed levels of the two reservoirs. Figure 2.11 displays $q(\eta)$ for different

degrees of uncertainty. We observe that optimal extraction decreases with higher levels of the damage coefficient (i.e. $q_\eta < 0$). Thus, it is optimal to reduce extraction if higher damage levels are observed. This reduction occurs at an increasing rate (i.e. $q_{\eta\eta} < 0$). Furthermore, an increase in the degree of uncertainty (higher σ) shifts $q(\eta)$ downwards. We can conclude that for any level of the stochastic damage parameter, higher uncertainty about damage leads to lower extraction and consequently, lower emissions. This relationship confirms our findings from Figure 2.10. In Figure 2.12 we display the optimal sequestration policy, again in

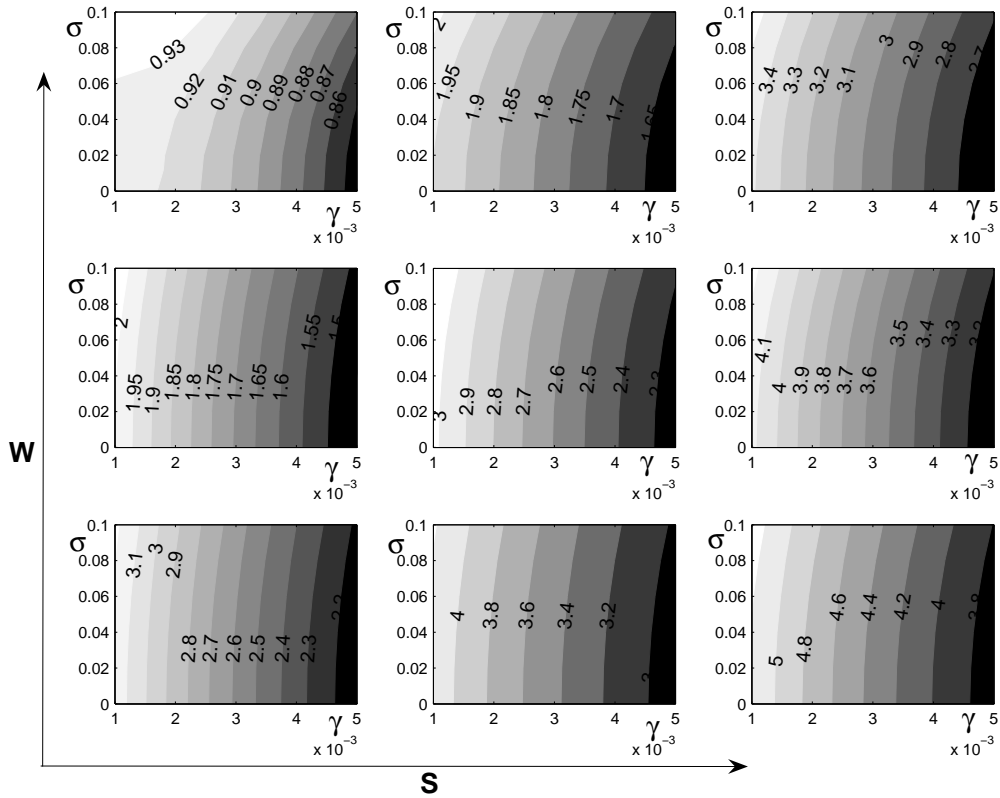


Figure 2.12: Optimal Sequestration policy - Contour plots in the $\eta - \sigma$ space for combinations of S and W . $S \in [2000, 2550, 3100]$ and $W \in [20000, 23750, 27500]$, with $(S,W)=(2000, 20000)$ in the lower left subplot.

the $S - W$ state space and the $\gamma - \sigma$ parameter space. It can be observed that optimal sequestration increases with rising concentrations of carbon in the upper reservoir while it is reduced for rising carbon concentrations in the lower reservoir. As mentioned earlier, ocean sequestration is the anthropogenic substitute for the natural carbon transfer. For this reason we observe optimal sequestration to fall with higher values of γ . Finally, Figure 2.12 reveals that uncertainty about the damage induces larger volumes of carbon to be sequestered. Analogous to

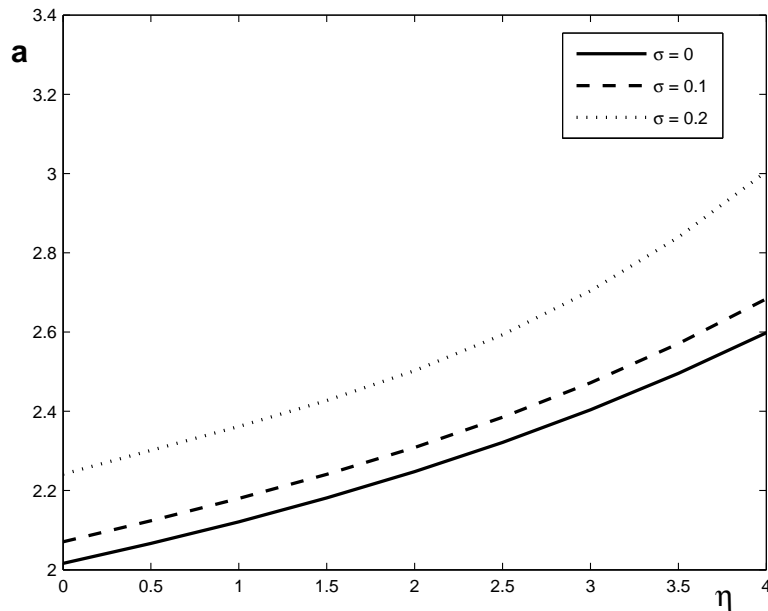


Figure 2.13: Optimal sequestration as a function of the stochastic damage coefficient for $S = 2,000$, $W=20,000$ (for different degrees of uncertainty)

Figure 2.11, Figure 2.13 depicts the optimal sequestration policy as a function of the stochastic damage coefficient for three different degrees of uncertainty. We find that higher levels of the observed damage coefficient intensify sequestration activities (i.e. $a_\eta > 0$) at an increasing rate ($a_{\eta\eta} > 0$). Furthermore, as already deducted from Figure 2.12, we notice that rising uncertainty about damage causes

higher sequestration, which is expressed in an upward shift of $a(\eta)$.

Next, Figure 2.14 displays the optimal carbon tax, again in the $S - W - \gamma - \sigma$ space. Quite naturally, the optimal carbon tax level rises with increasing

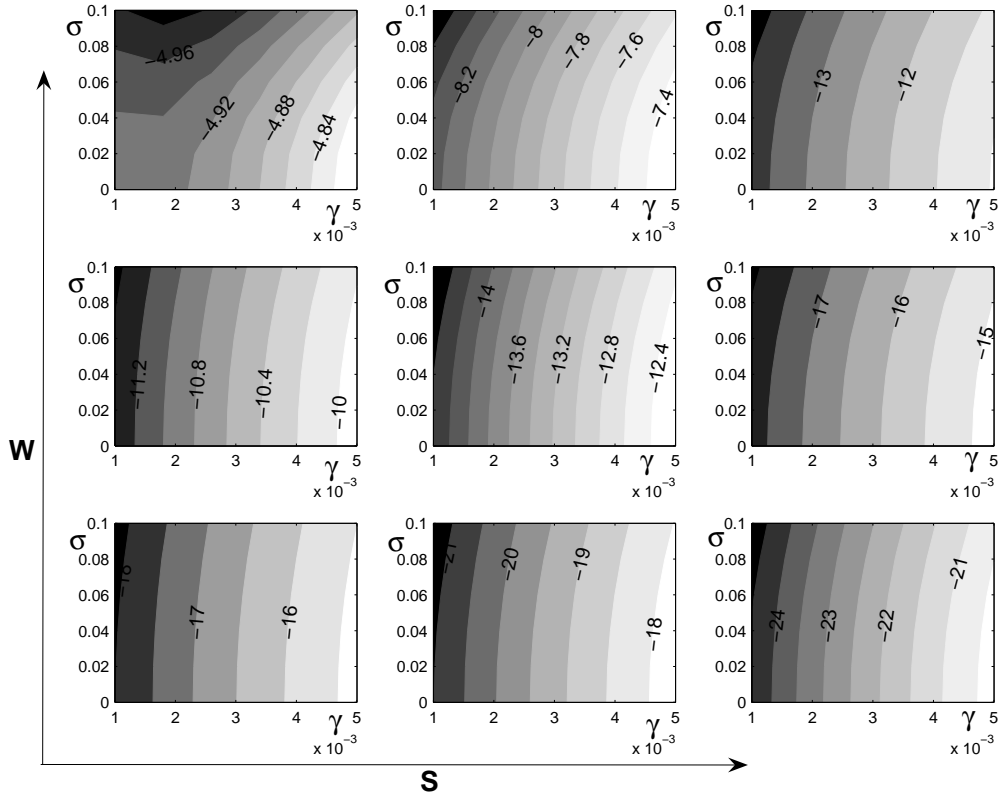


Figure 2.14: Optimal Carbon Tax - Contour plots in the $\eta - \sigma$ space for combinations of S and W . $S \in [2000, 2550, 3100]$ and $W \in [20000, 23750, 27500]$, with $(S, W) = (2000, 20000)$ in the lower left subplot.

atmospheric carbon concentrations. However, higher carbon concentrations in the lower reservoir imply lower carbon tax levels. The intuition behind this result is the following: Given a certain level of atmospheric carbon, a higher carbon content of the lower reservoir implies that more of the resource stock has been extracted (carbon balance equation 2.4 always holds) and since optimal paths may never

cross, the overshooting of the atmospheric carbon reservoir is reduced. This in turn reduces the damage and consequently the carbon tax. Furthermore, Figure 2.14 shows that higher levels of speed of the natural transfer of carbon reduce the carbon tax since the lagged damage effect of the atmospheric supersaturation of carbon is enhanced. Finally, for any level of γ in the entire state space we observe that uncertainty about damages increases significantly the carbon tax. The effect of different levels of the stochastic damage parameter on the carbon tax

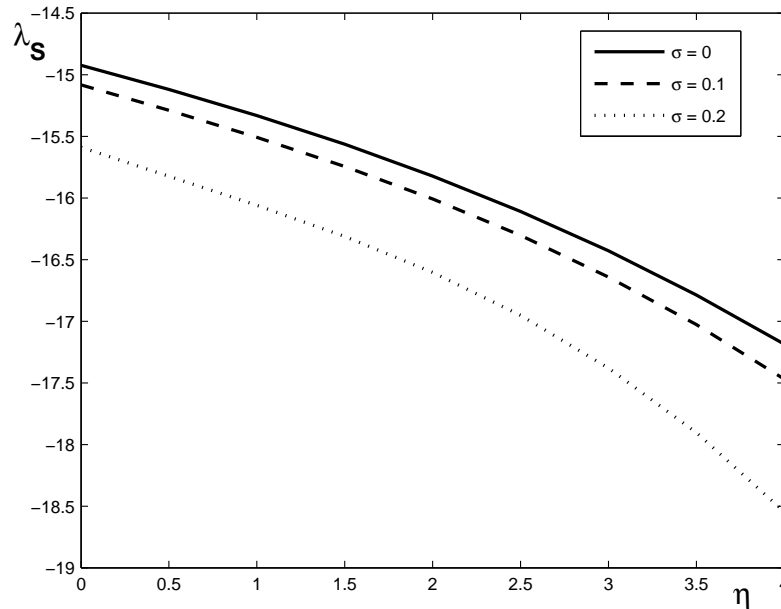


Figure 2.15: Optimal carbon tax as a function of the stochastic damage coefficient for $S = 2,000$, $W=20,000$ (for different degrees of uncertainty)

is depicted in Figure 2.15. We observe that the optimal carbon tax increases with higher levels of the damage coefficient. This increase occurs at an increasing rate. Furthermore, an increase in the degree of uncertainty (higher σ) calls for higher levels of the carbon tax. Again, this relationship confirms our findings from Figure 2.14.

2.5 Concluding Remarks

In order to assess the problem of the appropriate path and level of the carbon tax one has to take into account the lagged and persistent effect of emitting carbon on the ocean's capacity to absorb carbon from the atmosphere. However, the role of the oceans has not received much attention in theoretical models of optimal resource extraction. Especially, when analyzing global warming, not only the stock of carbon in the atmosphere is important, but also the functioning of the deep ocean as a carbon sink.

We take account of the latter effect by assuming two carbon reservoirs: The upper reservoir and the lower reservoir. The upper reservoir consists of the stock of carbon in the atmosphere and the upper ocean layer. The lower reservoir comprises the carbon stock in the deep ocean. The natural flux of carbon is driven by the relative size of the carbon reservoirs. The relatively "carbon-abundant" reservoir will therefore be a natural source of carbon outflow. This is the natural component of the global carbon cycle. We have added an anthropogenic component to this by introducing an exhaustible resource with carbon content.

The economic extraction of the fossil resource releases carbon that is added to the global carbon cycle. Without CCS, the whole amount of carbon released will be captured by the atmosphere and only slowly transferred into the deep ocean. In order to accelerate the slow natural mix of the deep ocean with the atmosphere and upper ocean layer we focus on the possibility of carbon capture and storage via deep sea injection.

Overall, our results show that the CCS technology accelerates the free, but slow natural flux within the carbon cycle. The results of our analysis are consistent for

a broad range of parameters measuring the natural pace of transfer of carbon between the carbon reservoirs. Thus, the usage of carbon capture and storage may help achieving stricter stabilization targets in the coming decades without relying to much on the expensive and subsidy intensive renewables. Policy makers are well advised to consider investments into modern and efficient coal fired power plants while at the same time to support R&D of CCS technologies which have a huge potential to ensure a smooth transition towards the usage of renewables in the long run.

For the optimal carbon tax our findings suggest that it is inverted u-shaped and its level should be adjusted with the uptake capacity of other carbon sinks, such as the oceans.

The analysis of a stochastic version of this model has shown that when the damage which results from higher atmospheric carbon stock levels is subject to uncertainty, extraction volumes of a resource with carbon content should be reduced. Also, the usage of carbon capture and storage, the anthropogenic mechanism of carbon transfer is enhanced. Regarding the carbon tax, our results suggest that the optimal level of the carbon tax should be positively adjusted for the risk of larger damages to the economy.

Chapter 3

The Effect of Damage

Uncertainty on Climate Change

Mitigation: A Numerical

Approach of Stochastic Control

3.1 Introduction

Uncertainty has been regarded as a key issue in the economics of climate change (for reviews, see Heal and Kriström (2002), Peterson (2006) and Pindyck (2007)). While the entire range of research on climate change and uncertainty goes well beyond the realm of economics, a question with a particular economic implication regarding this topic is the decision making under uncertainty which outcome is not reversible. The concept of quasi-option value (Arrow and Fisher (1974) and Henry (1974)) clarifies that the combination of irreversibility and uncertainty, which is

the case for climate change being caused by irreversible accumulation of carbon dioxide in the atmosphere, would justify precautionary actions against the worst possible outcome, in other words, stronger mitigation under uncertainty relative to a deterministic case.

There are a number of studies that examine the validity and applicability of this thesis. They are broadly categorized into two groups. The first group, whose works draw on Epstein's seminal paper (Epstein (1980)), is analytical models with simple settings (often limited to two time periods) to clarify the conditions in which uncertainty leads to precautionary actions. A major insight obtained by this set of literature is that the effect of uncertainty becomes ambiguous if two sorts of irreversibility coexist, namely the irreversibility of atmospheric carbon dioxide concentrations and of investment in mitigation that is sunk (Kolstad (1996a), Kolstad (1996b), Pindyck (2000), Fisher and Narain (2003)). If a part of investment costs in mitigation is not recoverable, a wait-and-see approach to delay actions may rather be preferred because of a possibility that climate change proves to cause smaller damage than expected. Other papers in this group (e.g. Ulph and Ulph (1997), Gollier et al. (2000)) look into some other mathematical features leading to the result, such as sufficiency of conditions, the effects of functional shape, and informational structures.

The second group of studies addressing the above question is of integrated assessment models incorporating uncertainty, e.g. Peck and Teisberg (1993), Nordhaus (1994a), Nordhaus (2008), and Pizer (1999). They use comprehensive economic-climate models calibrated with empirical data on key parameters (e.g., TFP, climate sensitivity to carbon dioxide increase, discount rate) showing a variance of estimates. Here, the effects of uncertainties are examined essentially

through a large number of runs with parameters being set at different levels. This group of studies generally show that uncertainty leads to stronger mitigation, although apparently what matters most in their models is not the uncertainty of climate system but of growth and technology parameters such as TFP.

While the two groups of works shed light on the question in a considerable way, there is still an unfilled gap between them. On the one hand, analytical models are only solvable with parsimonious assumptions, and a number of parameters commonly considered in modeling climate change are omitted. On the other hand, the second group of studies, integrated assessment models, does not directly conduct stochastic optimization due to computational difficulties. This means that they do not take account of the effect that uncertainty influences optimal decisions through agents' risk aversion. Furthermore, this limitation frames constraints on uncertainties they investigate; they mostly focus on uncertainties of parameters (e.g., energy intensity) with pre-defined probability distributions, not randomness of state or control variables themselves (e.g., atmospheric temperatures). This feature makes the models less suitable for examining the question of uncertainty and irreversibility about climate, because a part of climatic patterns could only be explained by highly non-linear, possibly inherently unpredictable, mechanisms of the climate system, which evidence includes paleoclimatic records of abrupt temperature changes (e.g., NRC (2002)). Accordingly, studies of integrated assessment models have not explicitly examined this question.

This paper is an attempt to fill the current gap between the two sets of scholarship described above. We directly perform stochastic optimization with variable randomness represented as a Brownian motion. A numerical approach allows us much greater latitude for parameter choice than analytical model studies would

do. Stochastic dynamic optimization has an established body of analytical model studies (in the field of environmental and resource economics, e.g., Arrow and Chang (1982), Tsur and Zemel (1998)), but has been generally considered difficult in finding numerical solutions. Recently, however, standardized techniques are developed (e.g. Judd (1998)), and some simple models are now able to be solved readily. Our approach is to apply these techniques to the climate change issue with representations that are simple but could still have direct relevance to the actual climatic-economic interactions. Though not the focus of this paper, this approach would leave us a scope to link the quasi-option value literature and the economic studies on abrupt climate change (e.g. Azar and Lindgren (1992), Keller et al. (2004), Lempert et al. (2006), McInerney and Keller (2008) and Weitzman (2009)). In this model we investigate the effect of climatic uncertainty on the optimal mitigation policy. Our analysis covers a large range of parameters, in particular the degree of risk aversion and the level of uncertainty. We identify regions of the state space for which higher levels of uncertainty or risk aversion result in different policy rules for emission control. Furthermore, we conclude that the effect of uncertainty on emission control crucially depends on the degree of risk aversion.

We proceed as follows: In section 3.2 we describe the model framework. In section 3.3 we briefly describe the Chebyshev collocation method, the computational technique which we use for solving our stochastic control problem in continuous time. Section 3.4 presents the main results of our model and provides a discussion. Section 5 concludes.

3.2 The Model

Consider an economy where total output Y is a function of the capital stock K , with $Y_K > 0$ and $Y_{KK} < 0$. The production process generates emissions $\epsilon \cdot Y$, where ϵ denotes the emissions coefficient of output. With additional expenditure, the amount of emissions is reduced; m represents the fraction of carbon emissions which is under control, i.e. not emitted in the atmosphere. Consequently, the atmospheric stock of carbon S evolves with

$$dS = (\epsilon \cdot Y(K) \cdot (1 - m) - \beta \cdot S)dt \quad (3.1)$$

where β is the constant removal rate of atmospheric carbon into the ocean. At this point we assume that the atmospheric stock of carbon causes a rise in the level of global mean temperature. Let $T(S)$ be the increase of global mean temperature from the pre-industrial level with $T_S > 0$ and $T_{SS} \geq 0$. We assume that rising levels of global mean temperature cause damage to output and the damage is subject to randomness. Denote the damage by $D(T, \eta)$ with η being a scaling factor of the temperature's impact on damage: we assume $D_T, D_\eta > 0$, $D_{TT}, D_{\eta\eta} > 0$, $D_{T,\eta} > 0$ and $D(T, 0) = D(0, \eta) = 1$. For the rest of the paper we assume that η is stochastic with

$$d\eta = (\theta \cdot (\bar{\eta} - \eta))dt + \sigma dB \quad (3.2)$$

i.e, the damage coefficient follows an Ornstein-Uhlenbeck process, the continuous time equivalent of a mean-reverting AR(1) process. The mean of η is denoted by $\bar{\eta}$ and θ is the strength of mean reversion. For the diffusion, we assume $B \sim (0, \sigma^2)$.

Furthermore, the output balance condition reads

$$\frac{Y(K)}{D(T(S), \eta)} = I + c + M(m, Y(K)) \quad (3.3)$$

The left-hand side of (3.3) is the net output inclusive of damage. The net output is in balance with the sum of the following: (i) consumption c which yields utility $U(c)$ with $U_c > 0$ and $U_{cc} < 0$; (ii) $M(m, Y(K))$, the emission control costs with $M_m > 0$, $M_{mm} > 0$, $M_Y > 0$, $M_{mY} > 0$ and $M_{YY} = 0$; (iii) capital accumulation via investment I . The stock of capital K evolves according to

$$dK = (I - \delta \cdot K)dt \quad (3.4)$$

where δ is the capital depreciation rate. Our purpose is to investigate the dynamically optimal choice of consumption, emissions control and capital investment given uncertainty about the temperature's impact on damage to gross output. To this end, we formulate the problem from the social planner's perspective. Given the uncertainty over η , the social planner maximizes the expected present value welfare.

$$\max_{c_t > 0, 0 \leq m_t \leq 1} E \int_0^{\infty} e^{-\rho t} [U(c_t)] dt \quad (3.5)$$

subject to (3.1)-(3.4) and $S(0) = S_0$, $K(0) = K_0$ and $\eta(0) = \eta_0$. To solve (3.5) we perform stochastic control, the continuous time version of stochastic programming.

The corresponding Hamilton-Jacobi-Bellman (HJB) equation is ¹

$$\begin{aligned}
0 = \max_{c>0, 0 \leq m \leq 1} \{ & U(c) + V_S(S, K, \eta)(\epsilon \cdot Y(K) \cdot (1 - m) - \beta \cdot S) \\
& + V_K(S, K, \eta)\left(\frac{Y(K)}{D(\eta, S)} - c - M(m, K) - \delta \cdot K\right) \\
& + V_\eta(S, K, \eta)(\theta \cdot (\bar{\eta} - \eta)) \\
& + \frac{1}{2}\sigma^2 V_{\eta\eta}(S, K, \eta) - \rho V(S, K, \eta)\} \tag{3.6}
\end{aligned}$$

where $V(S, K, \eta)$ is the value function. A solution to (3.6) requires finding a value function and policy functions $c(S, K, \eta)$ and $m(S, K, \eta)$ which constitute explicit control rules. The first-order conditions for c and m are

$$U_c = V_K(S, K, \eta) \tag{3.7}$$

$$M_m = -\frac{V_S(S, K, \eta) \cdot \epsilon \cdot Y(K)}{V_K(S, K, \eta)} \tag{3.8}$$

Equation (3.7) states that the marginal utility from consumption should be equal to the derivative of the value function with respect to capital, i.e. the shadow price of capital. From (3.8) it can be easily seen that $V_S \geq 0$. The optimal choice of m , the emissions control rate, thus positively depends on the shadow price of atmospheric carbon (in absolute terms) and instant emissions. It negatively depends on the shadow price of capital.

¹Notice that by setting up the maximization problem as in (3.6), we do not restrict capital investments I to be non-negative. In fact, for some areas of the state and parameter space optimal investment is negative.

A closed form solution to (6)-(8) could be obtained by applying specific function forms to Y, D, M, T and U and using an intelligent guess for the value function $V(S, K, \eta)$. However, due to the dimension of the state space and the nonlinearities of the functional forms we are not able to derive a closed form solution. Instead, we determine the value function and the policy functions numerically.

3.3 Numerical Solution of the Model

From the first-order conditions (3.7) and (3.8) we can obtain explicit solutions for the optimal stochastic control of c and m as functions of the state variables.

$$\tilde{c} = \Gamma_U^{-1}(V_K(S, K, \eta)) \quad (3.9)$$

$$\tilde{m} = \Gamma_M^{-1}\left(-\frac{V_S(S, K, \eta) \cdot \epsilon \cdot Y(K)}{V_K(S, K, \eta)}\right) \quad (3.10)$$

Inserting (3.9) and (3.10) into (3.6) we obtain the concentrated HJB equation in terms of the value function and its derivatives with respect to the states. Thus, the concentrated HJB equation is three-dimensional in S, K and η and reads

$$\begin{aligned} 0 = & V_S(S, K, \eta)(\epsilon \cdot Y(K) \cdot \left(1 - \Gamma_M^{-1}\left(-\frac{V_S(S, K, \eta) \cdot \epsilon \cdot Y(K)}{V_K(S, K, \eta)}\right)\right) - \beta \cdot S) \\ & + V_K(S, K, \eta)\left(1 + \frac{Y(K)}{D(\eta, S)} - \Gamma_U^{-1}(V_K(S, K, \eta)) + \frac{V_S(S, K, \eta) \cdot \epsilon \cdot Y(K)}{V_K(S, K, \eta)} - \delta \cdot K\right) \\ & + V_\eta(S, K, \eta)(\theta \cdot (\bar{\eta} - \eta)) + \frac{1}{2}\sigma^2 V_{\eta\eta}(S, K, \eta) - \rho V(S, K, \eta) \end{aligned} \quad (3.11)$$

Equation (3.11) constitutes a nonlinear second-order partial differential equation which, similar to the model in the previous chapter can be solved numerically using

projection methods. For that purpose, we estimate the value function with the Chebyshev collocation method which approximates the solution to (3.11) with a linear combination of basis functions. The approximated value function is given by

$$\tilde{V}(S, K, \eta) = \sum_{i=1}^{n_i} \sum_{j=1}^{n_j} \sum_{k=1}^{n_k} g_{ijk} T_i(x_S) T_j(x_K) T_k(x_\eta)$$

$T_i(x_S), T_j(x_K)$ and $T_k(x_\eta)$ are n_i, n_j, n_k -degree Chebyshev polynomials which are evaluated at the states with x_S, x_K, x_η being the mapping $[S_{\min}, S_{\max}] \times [K_{\min}, K_{\max}] \times [\eta_{\min}, \eta_{\max}] \mapsto [-1, 1] \times [-1, 1] \times [-1, 1]$. The collocation coefficients g_{ijk} are then estimated in order to deliver a good approximation of (3.11).

3.4 Results and Discussion

The functional forms and parameter values used for the numerical analysis are reported in Appendix A1. With these parameter values we numerically compute the deterministic steady state and obtain $\tilde{S} = 1546.6$, $\tilde{K} = 1180.2$. Furthermore, we define $\eta = 1$ in the deterministic case. Given these values we set up the projection grid by discretizing the spate space around the steady state. We choose $S \in [800, 3500]$, $K \in [500, 3000]$ and $\eta \in [0, 2]$. The Chebyshev polynomials are of degree 10 in all states i.e.: $n_i, n_j, n_k = 10$. Figure 3.1 illustrates the value function for the stochastic case in the $S - K$ grid ². The value function is concave and smooth. It increases with larger volumes of the capital stock and decreases with

²For the graphical presentation of the results we choose $\eta = 1$ unless stated otherwise

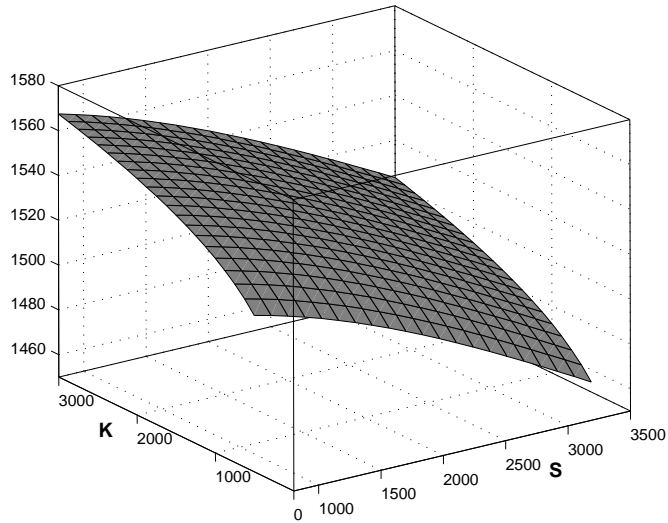


Figure 3.1: Value function

rising atmospheric carbon concentrations³. The relative value function residual is at around $\times 10^{-8}$ over the entire state grid. Figure 3.2 displays the shadow values of the atmospheric carbon stock (V_S) and the capital stock (V_K). Notice that V_S is negative over the entire state space - an intuitive result, since rising temperature levels are proportional to the atmospheric carbon stock. This fact also explains why V_S decreases with rising levels of the carbon stock while it is rather invariant to changes in capital. An analogous picture is obtained for V_K , the shadow value of the capital stock (right plot in Figure 3.3). It is positive over the entire state

³Notice that low levels of the capital stock imply low levels of gross output. This in turn results in low emissions. On the other hand, lower output volumes are available for consumption, investment and emission control. Furthermore, for any level of capital a higher S invokes more damage and consequently less net output while the level of gross output is unchanged.

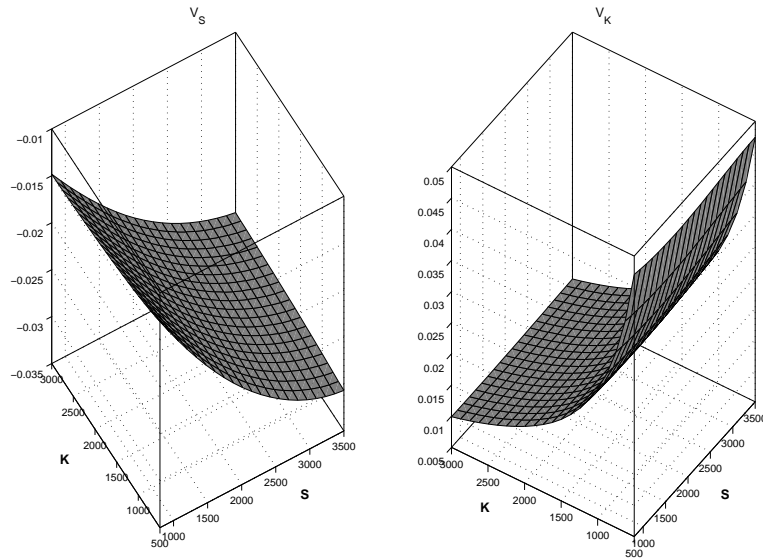


Figure 3.2: Shadow prices of atmospheric carbon stock (λ_S) and capital stock (λ_K)

space and decreases with rising levels of the capital stock. Figure 3.3 maps the policy functions for consumption c , emissions control m and investment I into the $K - S$ space, again for the stochastic case. The optimal consumption policy rule follows the Euler equation which sets equal marginal utility to the shadow price of capital. Consumption thus increases with the level of capital.

The emissions control policy generally replicates the tendency that most integrated assessment models exhibit, i.e., both carbon stock and capital accumulation increase enhances mitigation (e.g., Nordhaus, 1994). Notice that for a constant level of K , a higher atmospheric carbon concentration generates more damage to output, and that less output is available to be divided between consumption, emission control and investment. Also, for any level of K optimal emissions control increases with higher values of S . Since consumption is constant, capital invest-

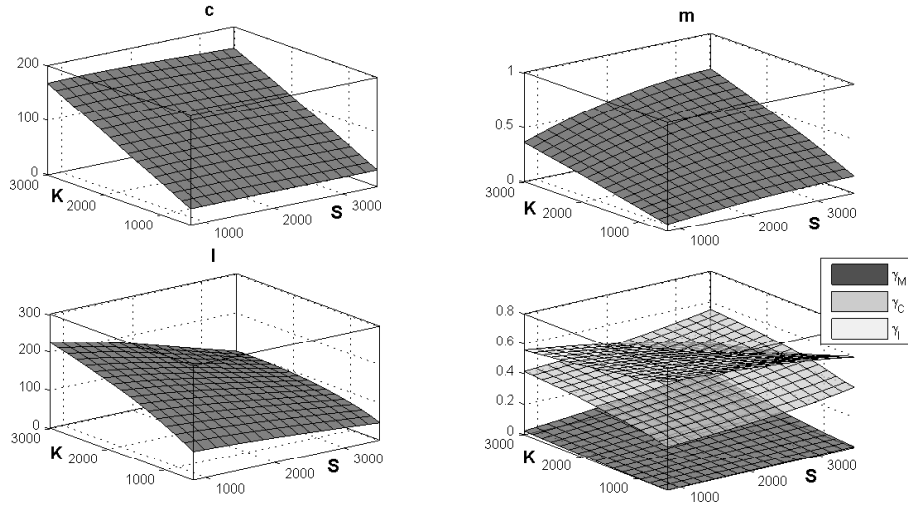


Figure 3.3: Policy functions for consumption (c), emission control (m), investment (I) and shares of net output spent on c , m and I

ments must decrease in order to balance the economy's budget (Equation 3.3). This behavior is shown in the lower left plot of Figure 3.3. On the other hand, higher levels of the capital stock invoke more investment. The lower right plot in Figure 3 displays the shares of net output⁴ spent on consumption, emissions control and investment which we define as $\gamma_M = \frac{M(m)}{Y^{net}}$, $\gamma_C = \frac{C}{Y^{net}}$ and $\gamma_I = \frac{I}{Y^{net}}$ respectively⁵. We observe that γ_C and γ_M both follow the same pattern. They increase with higher levels of capital and atmospheric carbon stock. However, while the share of net output spent on consumption ranges from 25% (low K , low S) to 60% (high K , high S), a lower fraction of net output is used for emission control. Its share ranges from 5% (low K , low S) to 20% (high K , high S). On the contrary,

⁴Net output is defined as $Y^{net} = \frac{Y}{D}$

⁵Consumption, emission control and investment are defined in units of output. It holds that: $\gamma_M + \gamma_C + \gamma_I = 1$

the policy function for investment implies lower investment values for rising levels of capital and atmospheric carbon stock.

In order to shed more light on the effect of uncertainty on the distribution of net output over consumption, emission control and investment Figure 3.4 displays the absolute change in γ_C , γ_M and γ_I when including uncertainty. We define

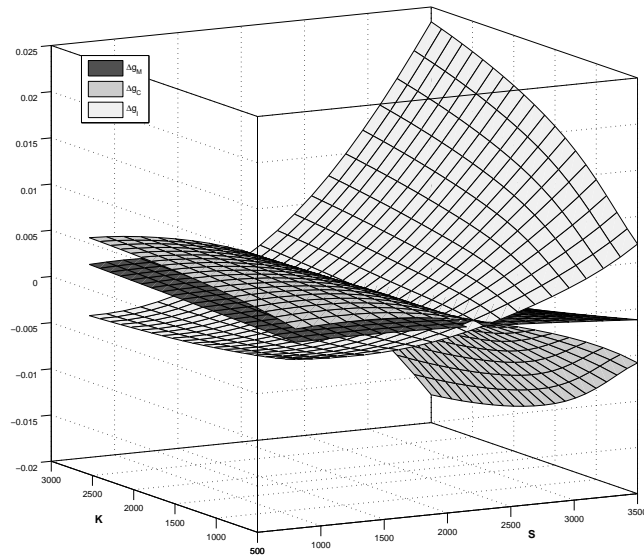


Figure 3.4: Difference in the shares of net output spent on emission control, investment, and consumption ($\Delta g_M, \Delta g_I, \Delta g_C$) when uncertainty is included.

$\Delta g_M = \gamma_M(\sigma = 0.05) - \gamma_M(\sigma = 0)$, $\Delta g_C = \gamma_C(\sigma = 0.05) - \gamma_C(\sigma = 0)$ and $\Delta g_I = \gamma_I(\sigma = 0.05) - \gamma_I(\sigma = 0)$ Three important points can be made: 1) For low values of the atmospheric carbon stock, uncertainty leads to higher emission control and consumption while it lowers capital accumulation. 2) The previous effect is reversed for high values of the atmospheric carbon stock. When uncertainty is included, a larger share of net output is spent on capital accumulation while a lower share of net output is used for consumption and emission control. 3) The

impact of uncertainty on reallocating net output optimally among c , m and I decreases (lower amplitude) with smaller levels of the capital stock. The latter effect mirrors the fact that a low value of the capital stock limits the freedom of action to adapt to stochasticity.

From Figure 3.4 it becomes clear that if the carbon content in the atmosphere is large, uncertainty about damage to output induces a reallocation of net output towards capital services. A perhaps striking feature of this model is also that in the latter case emission control is reduced. To obtain more insights on the effect of stochasticity on emission control, we examine the optimal levels of emission control with varying levels of risk aversion and uncertainty (Figure 3.5). We show nine contour plots in the $\alpha - \sigma$ space for different levels of S and K . They exhibit three major patterns. (1) The general tendency is that both, a high capital and a high carbon stock result in higher emission control. A large carbon stock corresponds to a large emission reduction, while a large capital stock is linked to a low capital return and thus a diversion of resource from investment to emission control. (2) The risk aversion is a very influential parameter on the level of emission control. Interestingly however, the risk aversion exerts different effects on the control level depending on the level of capital. For moderate or high levels of capital, more risk aversion leads to more abatement. The emission control decreases with higher levels of risk aversion when the capital level is low. This is because a risk averse agent prefers capital investment over emission control when the return to capital is relatively high (i.e., for low levels of capital), In other words, capital investment facilitates inter-temporal income smoothing more effectively than emission control does. (3) The effect of stochasticity on the emission control crucially depends on the size of the carbon stock. Higher uncertainty leads to higher emission control

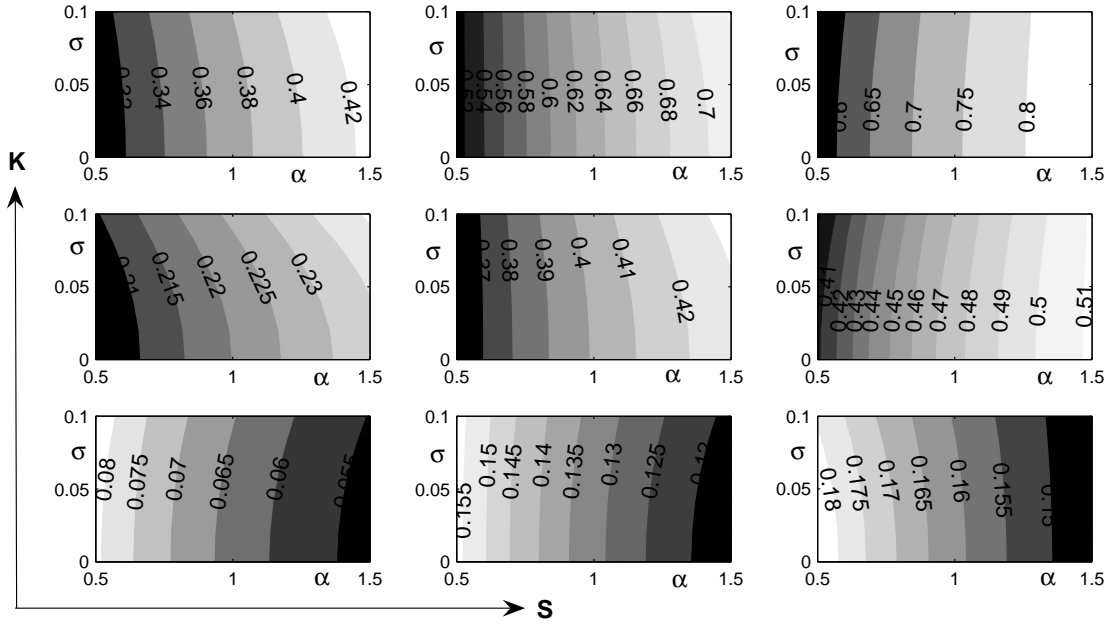


Figure 3.5: Optimal Emission control - Contour plots in the $\alpha - \sigma$ space for combinations of S and K . $S \in 800, 2150, 3500$ and $K \in 500, 1750, 3000$, with $(S,K)=(800,500)$ in the lower left subplot.

with a low S but lower emission reduction with a high S . In other words, a risk conscious agent rather prefers consumption over emission control when climate mitigation needs considerable effort and in turn the effect of actions is highly uncertain in absolute terms.

Among the above findings, the ambiguity regarding the effect of uncertainty on optimal emission control levels addresses a feature that is not adequately discussed in previous studies in the economics of climate change. In fact, this ambiguity is a persistent feature of our model, and we can present it even in a more illustrative way. Figure 3.6 is a contour plot for low K and high S when the climate change

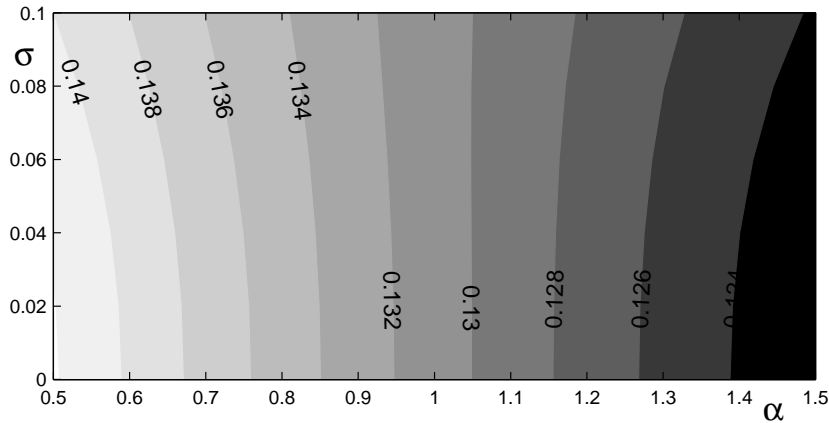


Figure 3.6: Optimal Emission control - Contour plot in the $\alpha - \sigma$ space for high S and low K, i.e. $(S,K)=(3500,500)$.

damage coefficient is set low ($\eta = 0.5$). It clearly shows that the effect of uncertainty on the sign of change in emission control even depends on the level of risk aversion. With a low risk aversion, uncertainty decreases emission reduction, whereas it increases emission reduction with a high risk aversion.

A particularly interesting point regarding these patterns is that uncertainty may in fact reduce the optimal level of emission control. It is straightforward to interpret this feature. Previous studies already clarified that if investment in abatement involves sunk costs, uncertainty in stock pollution can either enhance or decrease abatement, dependent on the parameter choice (e.g., Pindyck (2000)). This is because both the installation of abatement equipment and the pollution stock have irreversibility. Our model does not have an explicit representation of sunk investment on abatement, but there is a similar, though indirect, mechanism at work. Abatement costs (flow) are subtracted from the output, and thus reduce either consumption, capital investment, or both, if the output is unchanged. Capi-

tal produces a continuous flow of income from the time of investment onwards, and foregone capital investment due to excessive abatement therefore sets irreversibility in the other direction. This argument could be paraphrased as follows: The presence of uncertainty leads to increasing abatement of stock pollution because one cannot reduce the pollution stock later in case the pollution damage is greater than expected. Since the risk goes in both directions, a similar argument holds for the other direction. If we overspend our resource on abatement, capital investment could be decreased. Lower investment leads to lower capital accumulation. By the time we realize the overspending on abatement, the accumulated abatement cannot be converted into capital, and one cannot recover the income flow that capital would bring about if our resource was allocated in investment, not abatement. The relative significance between capital returns on one hand and climate damage on the other hand determines the dynamics to either of the two directions.

3.5 Concluding Remarks

We carried out a numerical stochastic optimization in the context of climate change. We applied standardized numerical techniques of stochastic optimization recently developed by Judd (1998) to the climate change issue with uncertainty about the climate system. The novelty of this study is that we directly performed stochastic dynamic optimization, rather than reproducing randomness by conducting a large number of simulation runs, to see changes of key determinants of climate policy. An advantage of our stochastic optimization approach over previous climate-economy simulation studies is that the model internalizes agents preference about risk in optimization. Our analysis covers a large range of the pa-

parameter space, in particular the degree of risk aversion and the level of uncertainty. We identify regions of the state space for which higher levels of uncertainty or risk aversion result in different optimality rules for emission control.

The results show that the effects of uncertainty are indeed different with different levels of agents risk aversion. A main finding is that the effects of stochasticity on emission control differ even in sign with varying parameters: Uncertainty may increase or decrease emission control depending on parameter settings, in other words, uncertainties of climatic trends may induce people's precautionary emission reduction but also draw away money from abatement. This paper's conclusions would set a call for a more precise conceptualization about the meaning of uncertainties in the decision making on climate change. This aspect would have a particular importance in the context of policy discussions, where uncertainty is often used as a justification for policy actions. Yet, uncertainty tends to be vaguely framed, notably as phrased in the United Nations Framework Convention on Climate Change's objective to "prevent dangerous anthropogenic interference with the climate system." Finally, while our model highlights some important features of uncertainties and climate change, the simulations are admittedly simplistic for explaining the complex phenomena of climate change. A more comprehensive numerical stochastic model, perhaps with uncertainties in technological change and global business cycle in addition to climate indicators, would allow us to conduct a complete sensitivity analysis of parameters. Impacts of uncertainties about large discrete shocks, a feature that could be represented with a jump process, should also be a future research question.

Chapter 4

Transition from Polluting to Clean Technology: A Differentiated Capital Approach

4.1 Introduction

Energy is the driving force of economic growth. Currently about 85 percent of the world's energy use comes from fossil fuels. However, generating energy from burning fossil fuels also causes CO_2 , which is the most important greenhouse gas and thus is called responsible for global warming (see forth IPCC assessment report). While the earlier literature on sustainability was concerned about depletion of finite resources such as fossil fuels, and thus about its increasing scarcity, it has meanwhile become clear that the external cost of CO_2 emissions is the limiting factor of using fossil fuels. Several authors analyze the transitional dynamics from using conventional technologies towards employing backstop technologies (see e.g.

Dasgupta and Heal (1979), Pezzey (1998) and Tahvonen and Salo (2001)). Most of these models, however, tend to neglect the fact that non-renewable and renewable resources are associated with their own, hardly shiftable capital stock. As a consequence, policy implications extracted from these models are based on a too optimistic picture about how easy the transitional dynamics from exhaustible and polluting resources towards renewable and less polluting technologies can be accomplished. If we assume that installed capital is fully embodied in an existing technology, the average productivity characteristics and environmental impact of the total capital stock will change only slowly, as new installed capital fills the gaps left by the physical decay of the capital stock in place.

Therefore this paper takes a different approach. We develop a growth model with two production sectors that generate a homogeneous consumption good. Output in each sector is generated solely by using physical capital. We assume that both sectors are associated with different technologies, a conventional one generating emissions and thus contributing to pollution, which in turn causes environmental damage, on the one hand, and an advanced technology producing free of emissions, on the other. The technologies are completely embedded in the corresponding stocks of physical capital. Hence, the extent to which either of both technologies is employed can only be altered by increasing or depreciating the size of the associated capital stocks. If it turned out that the environmental damage generated from the conventional technology were prohibitively high, it may be optimal to leave some idle capacity of the conventional capital stock, giving rise to corner solutions, thus making the model little tractable. We therefore follow a more elegant path by endogenizing the depreciation rate: a higher (lower) rate of capacity utilization causes the capital stock to depreciate faster (more slowly).

Thus, each sector faces the trade-off between the benefits of producing more output from a given capital stock and the costs of over-utilizing it. Moreover we introduce adjustment costs of investment in order to smooth out investment paths. Since output in a given period does not only depend on the capital stock in place but also on the intensity of utilization and thus the flow of capital services extracted from it, the control over capital utilization enables firms to adjust faster to exogenous shocks or to other changes in the economic environment. There are only a few models so far which have analyzed optimal investment with several stocks of physical capital, e.g.: Pitchford (1977). The author deals with the optimal investment into two regions of an economy. In a dynamic growth model with two heterogeneous capital stocks, the author investigates the optimal investment decisions and their change towards the steady state. Chatterjee (2005) analyzes the relationship between depreciation and capital utilization in the context of convergence between countries. The author concludes that assuming a constant depreciation rate and full capital utilization, standard growth models may be overstating the magnitude of the steady state equilibrium. Rumbos and Auernheimer (2001) conduct a similar analysis. The authors find that implementing adjustment costs of investment and capacity utilization into a modified Ramsey-type growth model significantly slows the rate of convergence towards the steady state. These findings can be directly translated to the case of heterogeneous capital stocks, one of them being polluting, the other one clean.

Applying methods of dynamic programming we, first, determine the socially optimal use and transition paths of the capital stocks and, hence, the socially optimal mix of the technologies involved. In particular, we are interested in the inter- and intra-sectoral trade-offs between capacity building and capacity using which

guide the economy's transition process towards a balanced growth equilibrium.

We derive analytical results accompanied by numerical simulations. First, we find that it is always optimal to use some of the conventional, i.e. polluting technology. Second, the optimal path of capacity utilization, investment, and de-investment heavily depends on both the initial allocation of capital stocks of both technologies and the damage from pollution. In particular, starting with a low initial level of the "clean" capital stock calls for its fast accumulation initially, slowing down as the steady state is approached. Its utilization is initially high but decreases sharply due to the high maintenance cost of rising levels of the installed and operating capital stock. For the "polluting" capital stock we observe the opposite pattern. If its stock is initially above the optimal steady state level, gross investment will be (close to) zero approaching its steady state level slowly during the adjustment process. Thus, net investment is negative and the size of the capital stock is mainly driven by depreciation. In addition, the "polluting" capital stock becomes less utilized as the clean capital is built up steadily.

The main message from our study is that if shocks concerning environmental damage (which can also be induced by "shocks" in knowledge about the impact of certain pollutants) call for development and employment of new technologies, a change of the technology mix cannot be accomplished without time lags due to the ex post "clay" nature of investment and capital. Thus not the aggregate stock of capital is what matters, as suggested by the earlier literature on sustainability in the presence of exhaustible resources, but rather the quality of capital and the right allocation of differentiated capital is crucial.

The paper is organized as follows. The next section outlines the model and stresses some important features of the transitional dynamics. Section 3 then,

presents the results of some simulations which have been carried out. Section 4 concludes.

4.2 The Model

Similar to Pitchford (1977) there are two output sectors in the economy producing one homogenous consumption good. Capital in its broad notion is the only factor of production in both output sectors. The output sectors differ with respect to the production process of the consumption good. While sector 1 is assumed to apply a clean technology, the production process in sector 2 generates pollution. In order to keep things as simple as possible, we assume that these technologies enter the production structure of a firm via the firm's capital stock. By introducing capacity utilization and allowing for negative investment volumes, the model economy has more options to adjust its mix of capital services. However, this adjustment is limited by (i) adjustment costs of investment and (ii) an endogenous depreciation rate.

4.2.1 Capital installation and utilization

We denote effective capital in sector i by the product of the installed capital stock K_i and κ_i , the intensity with which the capital stock is utilized.¹ Thus, K_i^e

¹Alternatively, we could model capacity utilization as a fraction/part of the existing capital stock in use as in Fisher et al. (2004). Our approach is similar to Chatterjee (2005) and while being technically equivalent to Fisher et al. (2004), it does not necessitate imposing upper-bound constraints on the capacity utilization rates.

represents the flow of capital services in sector i .

$$K_1^e = \kappa_1 \cdot K_1 \quad (4.1)$$

$$K_2^e = \kappa_2 \cdot K_2 \quad (4.2)$$

Let $\delta_i(\kappa_i)$, with $\delta_i' > 0$ and $\delta_i'' > 0$ be the rate of depreciation as a function of κ_i , the intensity of capital stock utilization. Let I_i denote the gross volume of investment in sector i . Then, the instantaneous change in the capital stocks over time in both sectors is given by

$$\dot{K}_1 = I_1 - \delta_1(\kappa_1) \cdot K_1 \quad (4.3)$$

$$\dot{K}_2 = I_2 - \delta_2(\kappa_2) \cdot K_2 \quad (4.4)$$

Output in each sector is a twice differentiable function of effective capital. Total output of the economy (and hence, total production of the homogenous good) is the sum of the sector-specific output levels

$$Y(K_1^e, K_2^e) = Y_1(K_1^e) + Y_2(K_2^e) \quad (4.5)$$

with its derivatives satisfying $Y_i' > 0$ and $Y_i'' < 0$, $\forall i \in \{1, 2\}$. Furthermore, we assume that the Inada-Uzawa conditions hold, i.e.:

$$\lim_{K_i^e \rightarrow \infty} Y_i' = 0, \quad \lim_{K_i^e \rightarrow 0} Y_i' = \infty, \quad Y_i(0) = 0, \quad Y_i(\infty) = \infty \quad (4.6)$$

4.2.2 Adjustment costs of investment

As in Fisher et al. (2004) we assume the installment of additional capital to be costly. Within our two-sector model we therefore account for imperfect capital mobility. Contrary to Fisher et al. (2004), in our model the adjustment costs of capital are not measured in labor units but rather in forgone consumption. We assume that investment costs only depend on the level of gross investment (see e.g.: Karp and Zhang (2002)). We denote by $A_i(I_i)$ the instantaneous adjustment costs which occur from installing additional capacity I_i in sector i .² We assume $A_i(I_i)$ has the following properties:

$$A_i(0) = 0, A_i(I_i) \geq 0, A'_i \begin{cases} > 0, & I_i > 0 \\ = 0, & I_i = 0 \\ < 0, & I_i < 0 \end{cases}$$

$$A''_i > 0, \lim_{I_i \rightarrow \infty} A'_i = \infty, \lim_{I_i \rightarrow -\infty} A'_i = -\infty. \quad (4.7)$$

We explicitly allow for negative gross investment levels in both sectors of the economy simply because we are interested in the optimal management of both capital stocks over the entire (K_1, K_2) state space. Negative gross investment implies that the stock of unproductive or idle capital can be reduced faster than

²An alternative representation of investments costs would be $A_i(I_i, K_i)$ (see e.g. Bovenberg (1988) where A_i is typically a strictly concave and increasing function in the ratio of investment to the actual capital stock. This formulation was first introduced by Uzawa (1969) and implies large (small) installation costs at low (high) levels of the capital stock. We do not adopt this formulation since we are rather interested in the volume of investment and not the size of the capital stock as the main component of the adjustment costs of investment.

by physical depreciation ³. The released investment volumes can be either used to build up the alternative capital stock or to increase consumption. Consumption C is then given by

$$C = Y(\kappa_1, K_1, \kappa_2, K_2) - I_1 - I_2 - A_1(I_1) - A_2(I_2) \quad (4.8)$$

Note, that installing I_i units of capital in sector i requires $I_i + A_i(I_i)$ units of the consumption good. Consumption of the produced commodity generates utility $U(C)$ with

$$U(C) \geq 0, U(0) = 0, U_C > 0, U_{CC} < 0. \quad (4.9)$$

We assume that the capital stock in sector 2 causes pollution. We therefore use $D(\kappa_2, K_2)$ to denote the damage generated by using the environmental bad. We assume that $D(K_2^e)$ has the following properties:

$$D(K_2^e) \geq 0, D(0) = 0, D'(K_2^e) > 0, D''(K_2^e) > 0 \quad (4.10)$$

4.2.3 Social optimum

Welfare at time t is the difference between the utility derived from consumption of the homogeneous commodity and the damage caused by the flow of pollution.⁴

³In a later section we will study how a nonnegativity constraint on investment (i.e. fully sector-specific capital) affects the dynamics of the socially optimal policy.

⁴In this section we model pollution as a stock variable to focus explicitly on inter- and intra-sectoral tradeoffs between capacity building and capacity using which guide the transition process towards the steady state. In a later section we will introduce the more appropriate stock pollution assumption to investigate the history effect of investment on the polluting capital stock.

The objective function is given by

$$\max_{I_1, I_2, \kappa_1, \kappa_2} \int_{t=0}^{\infty} e^{-\rho \cdot t} \cdot [U(C) - D(\kappa_2, K_2)] dt \quad (4.11)$$

subject to the following constraints

$$\dot{K}_1 = I_1 - \delta_1(\kappa_1) \cdot K_1 \quad (4.12)$$

$$\dot{K}_2 = I_2 - \delta_2(\kappa_2) \cdot K_2 \quad (4.13)$$

$$C = Y(\kappa_1, \kappa_2, K_1, K_2) - I_1 - I_2 - A_1(I_1) - A_2(I_2) \quad (4.14)$$

$$\kappa_1 \geq 0 \quad (4.15)$$

$$\kappa_2 \geq 0 \quad (4.16)$$

The current value Hamiltonian is then given by

$$\begin{aligned} H &= U(Y(\kappa_1, \kappa_2, K_1, K_2) - I_1 - I_2 - A_1(I_1) - A_2(I_2)) \\ &\quad - D(\kappa_2, K_2) + \lambda_1 \cdot [I_1 - \delta_1(\kappa_1) \cdot K_1] + \lambda_2 \cdot [I_2 - \delta_2(\kappa_2) \cdot K_2] \end{aligned} \quad (4.17)$$

where λ_1 and λ_2 are the costate variables. The corresponding Lagrangian is

$$L = H + \mu_1 \cdot \kappa_1 + \mu_2 \cdot \kappa_2 \quad (4.18)$$

μ_1 and μ_2 are the Kuhn-Tucker multipliers. Applying the maximum principle yields the following F.O.C.

$$\frac{\partial L}{\partial I_1} = 0 \Rightarrow U_C \cdot (1 + A'_1) = \lambda_1 \quad (4.19)$$

$$\frac{\partial L}{\partial I_2} = 0 \Rightarrow U_C \cdot (1 + A'_2) = \lambda_2 \quad (4.20)$$

$$\frac{\partial L}{\partial \kappa_1} = 0 \Rightarrow U_C \cdot Y_{\kappa_1} - \lambda_1 \cdot \delta'_1 \cdot K_1 + \mu_1 = 0 \quad (4.21)$$

$$\frac{\partial L}{\partial \kappa_2} = 0 \Rightarrow U_C \cdot Y_{\kappa_2} - D_{\kappa_2} - \lambda_2 \cdot \delta'_2 \cdot K_2 + \mu_2 = 0 \quad (4.22)$$

$$\frac{\partial L}{\partial K_1} = \lambda_1 \cdot \rho - \dot{\lambda}_1 \Rightarrow U_C \cdot Y_{K_1} - \lambda_1 \cdot \delta_1 = \lambda_1 \cdot \rho - \dot{\lambda}_1 \quad (4.23)$$

$$\frac{\partial L}{\partial K_2} = \lambda_2 \cdot \rho - \dot{\lambda}_2 \Rightarrow U_C \cdot Y_{K_2} - D_{K_2} - \lambda_2 \cdot \delta_2 = \lambda_2 \cdot \rho - \dot{\lambda}_2 \quad (4.24)$$

The necessary Kuhn Tucker conditions are

$$\kappa_1 \geq 0, \quad \mu_1 \geq 0, \quad \kappa_1 \cdot \mu = 0 \quad (4.25)$$

$$\kappa_2 \geq 0, \quad \mu_2 \geq 0, \quad \kappa_2 \cdot \mu = 0 \quad (4.26)$$

In order to calculate the optimal converging paths, we need the initial conditions, $K_1(t=0) = K_1^0$, $K_2(t=0) = K_2^0$ and

$$\lim_{t \rightarrow \infty} e^{-\rho \cdot t} \cdot \lambda_i \cdot K_i = 0 \quad \forall x \in \{1, 2\} \quad (4.27)$$

Before we turn to the interpretation of the FOCs we show that the complementary slackness conditions in (4.26) and (4.27) are non-active, i.e. μ_1 and μ_2 are both zero.

Proposition 4. *The system described by (4.20)-(4.27) implies $\kappa_i > 0$.*

Proof. We show that $\forall t \in \{0, \infty\}$ $\mu_i = 0$ and hence, $\kappa_i > 0$. First, consider κ_1 . We have to show that if starting from $\kappa_1 = 0$, welfare at time t can be increased by setting $\kappa_i > 0$. From (4.21) we have $\frac{\partial L}{\partial \kappa_1} = U_C \cdot Y_{\kappa_1} - \lambda_1 \cdot \delta'_1 \cdot K_1 + \mu_1$. Since by equations (4.6), (4.25) and the properties of $\delta_i(\kappa_i)$, $\lim_{\kappa_1 \rightarrow 0} Y_{\kappa_1} = \infty$, $\lim_{\kappa_1 \rightarrow 0} \delta'_1 = 0$, and $\mu_1 \geq 0$ it follows that $\lim_{\kappa_1 \rightarrow 0} \frac{\partial L}{\partial \kappa_1} = \infty$. We can apply the same approach to κ_2 . From (4.22) we have $\frac{\partial L}{\partial \kappa_2} = U_C \cdot Y_{\kappa_2} - \lambda_2 \cdot \delta'_2 \cdot K_2 - D_{\kappa_2} + \mu_2$. Since by equations (4.6), (4.10), (4.25) and the properties of $\delta_i(\kappa_i)$ $\lim_{\kappa_2 \rightarrow 0} Y_{\kappa_2} = \infty$, $\lim_{\kappa_2 \rightarrow 0} \delta'_2 = 0$, $\lim_{\kappa_2 \rightarrow 0} D_{\kappa_2} = 0$ and $\mu_2 \geq 0$ it follows that $\lim_{\kappa_2 \rightarrow 0} \frac{\partial L}{\partial \kappa_2} = \infty$ \square

Proposition 1 states that it always pays off to employ capital because the marginal welfare gains for the first unit of capital intensity are infinite. This line of reasoning holds even for the case with a polluting capital stock because the marginal pollution of the first unit of capital is nil.

Within each sector of our model economy there exists the tradeoff between capital usage and capital build-up, which translates into the optimal choice of κ_i and I_i . Let us first consider sector 1. From the static efficiency conditions (4.19), (4.21) and Proposition 1 we can derive an optimal rule for the trade-off between the two control variables κ_1 and I_1 in sector 1. It is given by:

$$Y_{\kappa_1} = (1 + A'_1) \cdot \delta'_1 \cdot K_1 \quad (4.28)$$

The LHS of equation (4.28) is the marginal product of capacity intensity. The RHS of (4.28) describes the marginal costs of expanding capacity by one extra unit, i.e. the marginal depreciation weighted by the marginal investment costs to maintain a certain level of capital. Notice, that from (4.28) we can establish a condition for negativity of I_1 . Using the assumptions in (4.7) it can be easily verified that

$I_1 < 0$ iff $\delta'_1 \cdot K_1 > Y_{\kappa_1}$. This is intuitive, since it implies that for a given level of installed capital stock, gross investment will be negative if the marginal product of capital utilization is less than the marginal capital depreciation.

We can conduct a similar analysis for sector 2. From the optimality conditions (4.20), (4.22) and proposition 1 we obtain

$$Y_{\kappa_2} - \frac{D_{\kappa_2}}{U_C} = (1 + A'_2) \cdot \delta'_2 \cdot K_2 \quad (4.29)$$

The only difference to sector 1 is the LHS of (4.29). Because of the disutility from pollution due to the capital usage, the marginal product of capacity intensity is larger than its marginal social product which is the LHS of (4.29). It is equated to the marginal costs of expanding capacity by one extra unit. If e.g. the marginal disutility from pollution rises, the LHS term becomes smaller. To keep equation (4.29) in balance, this effect will induce a reduction in the flow of capital services and consequently a lower investment level. The nonnegativity condition on investment now reads: $I_2 < 0$ iff $\delta'_2 \cdot K_2 > Y_{\kappa_2} - \frac{D_{\kappa_2}}{U_C}$. The difference to sector 1 is the D_{κ_2} term on the RHS which contributes to the damage accounted marginal social product of capacity utilization.

4.2.4 Steady state conditions

Differentiating (4.19) with respect to time and using (4.19) and (4.23) we can solve for the change in consumption to obtain $\dot{C} = -\frac{U'}{U''} \cdot [\frac{Y_{K_1}}{1+A'_1} - \rho - \delta_1 - \frac{A''_1 \cdot \dot{I}_1}{1+A'_1}]$. For the special case with $A'_1 = 0$, $A''_1 = 0$ and $\delta_1 = \delta$ we can reproduce the standard Ramsey type equation for the time path of consumption. Similarly, we can differentiate (4.20) with respect to time and use (4.20) and (4.24) to obtain

$\dot{C} = -\frac{U'}{U''} \cdot \left[\frac{Y_{K_2}}{1+A'_2} - \rho - \delta_2 - \frac{A''_2 \cdot \dot{I}_2}{1+A'_2} - \frac{D'_{K_2}}{U' \cdot (1+A'_2)} \right]$ which for $A'_2 = 0$, $A''_2 = 0$ and $\delta_2 = \delta$ reproduces the standard result of a neoclassical model with pollution. For the dynamic analysis we are rather interested in the optimal paths of investments and capacity utilization. This is why we obtain the equations of motion for the two stock variables and the four control variables to form the dynamic system. For this purpose we have to eliminate the co-state variables from equations (4.19)-(4.24). let us define \dot{X} as the vector of the equations of motion. \dot{X} is given by

$$\dot{X} = \left(\dot{I}_1, \dot{I}_2, \dot{\kappa}_1, \dot{\kappa}_2, \dot{K}_1, \dot{K}_2, \right)^T \quad (4.30)$$

(See Appendix A2 for a derivation of (4.30).) Next, we define the balanced growth equilibrium as a path along which all control and stock variables have a zero growth rate. We derive steady-state conditions by setting $\dot{X} = 0$ and solving for the steady-state values of the four control and two state variables which we denote by $\tilde{I}_1, \tilde{I}_2, \tilde{\kappa}_1, \tilde{\kappa}_2, \tilde{K}_1, \tilde{K}_2$. Since we do not apply specific functional forms at this moment, we establish conditions that need to hold in the steady state. Let us first consider sector 1. From (4.30), setting $\dot{I}_1 = 0$ we obtain the following condition:

$$0 = \frac{U_C((1 + A'_1)(\rho + \delta_1) - Y_{K_1})}{\underbrace{(A'_1)^2 U_{CC}}_{<0} - \underbrace{A''_1 U_C}_{>0}} \quad (4.31)$$

Convexity of $A_1(I_1)$ and concavity of $U(C)$ implies $(A'_1)^2 U_{CC} - A''_1 U_C < 0$. Thus, we deduct from equation (4.31) that in the steady state it must hold that:

$$Y_{K_1} = (1 + A'_1)(\rho + \delta_1) \quad (4.32)$$

The interpretation is straightforward. The marginal social product of capital in sector 1 must be equal to the marginal social costs of capital, i.e.: the sum of the discount rate and the depreciation multiplied with the marginal costs of investment. This result is similar to the standard Ramsey model with two exceptions. First, in the Ramsey model $A_1(I_1) = 0$ and hence, $A_{I_1} = 0$ and second, δ_1 in this model is a function of κ_1 , whereas in the Ramsey model it is just a constant. Let us now consider κ_1 . Setting $\dot{\kappa}_1 = 0$ in 4.30 we obtain the following condition:

$$0 = \frac{Y_{\kappa_1}(\rho + \delta_1) - Y_{K_1}\delta'_1 K_1}{\underbrace{U_{CC}Y_{\kappa_1}^2\delta'_1}_{<0} + \underbrace{U_C(Y_{\kappa_1\kappa_1}\delta'_1 - Y_{\kappa_1}\delta''_1)}_{<0}} \quad (4.33)$$

which we can solve for the marginal social product of κ_1 . We obtain:

$$Y_{\kappa_1} = Y_{K_1} \frac{\delta'_1 K_1}{\rho + \delta_1} \quad (4.34)$$

This relationship implies that in the steady state the marginal social product of capacity utilization must be equal to the marginal social product of capital times a weighting factor, which itself depends on the levels of K_1 and κ_1 .

Finally, by setting $\dot{K}_1 = 0$, we obtain the third steady-state condition in sector 1.

$$I_1 = \delta_1 K_1 \quad (4.35)$$

which is also standard and implies that the steady-state volume of investment in sector 1 has to match the depreciated volume of the existing capital stock. Turning now to sector 2 we can apply the same procedure to analyze the steady-state in

the polluting sector. Setting $\dot{I}_2 = 0$ we obtain the following condition:

$$0 = \frac{D_{K_2} + U_C((1 + A'_2)(\rho + \delta_2) - Y_{K_2})}{\underbrace{(A'_2)^2 U_{CC}}_{<0} - \underbrace{A''_2 U_C}_{>0}} \quad (4.36)$$

Here again, convexity of $A_2(I_2)$ and concavity of $U(C)$ ensures that $(A'_2)^2 U_{CC} - A''_2 U_C < 0$, we obtain from equation (4.36) that in the steady state it must hold:

$$Y_{K_2} - \frac{D_{K_2}}{U_C} = (1 + A'_2)(\rho + \delta_2) \quad (4.37)$$

The only difference to sector 1 is additional term on the LHS of equation (4.37). It is the social component of the marginal social product of capital and reflects the relative tradeoff between a higher damage and a higher utility as a consequence of a larger capital stock. Notice that the externality component $\frac{D_{K_2}}{U_C} > 0$, implying that if pollution is perceived stronger (i.e. D_{K_2} is larger) the steady-state capital stock will have to be lower (ceteris paribus) since its marginal product Y_{K_2} must rise as well in order to compensate for the externality as shown in (43). In sector 1 this term did not exist since production in sector 1 does not generate any externality. Now we consider κ_2 . Setting $\dot{\kappa}_2 = 0$ we obtain the following condition:

$$0 = \frac{\delta'_2 ((D_{K_2} - Y_{K_2} U_C) \delta'_2 K_2 - (D_{\kappa_2} - Y_{\kappa_2} U_C) (\rho + \delta_2))}{\underbrace{\delta'_2 (U_{CC} Y_{\kappa_2}^2 - D_{\kappa_2 \kappa_2} + U_C Y_{\kappa_2 \kappa_2})}_{<0} + \underbrace{\delta''_2 (D_{\kappa_2} - Y_{\kappa_2} U_C)}_{<0}} \quad (4.38)$$

which we can solve for the marginal social product of κ_2 . Doing this we get:

$$Y_{\kappa_2} - \frac{D_{\kappa_2}}{U_C} = \frac{\delta'_2 K_2}{\rho + \delta_2} (Y_{K_2} - \frac{D_{K_2}}{U_C}) \quad (4.39)$$

The LHS denotes the marginal social product of capacity utilization. The RHS constitutes the marginal social product of capital time again, a weighting factor which depends on the levels of K_2 and κ_2 .

Finally, by setting $\dot{K}_2 = 0$, we obtain the third steady-state condition in sector 2.

$$I_2 = \delta_2 K_2 \tag{4.40}$$

which is also standard and implies that the steady-state volume of investment in sector 2 has to match the depreciated volume of the existing capital stock.

4.3 Comparative statics of the steady state

In this section we study the comparative static effect of the steady state.

Simplifying (4.32), (4.34), (4.35), (4.37), (4.39), (4.40) and using (4.14) we can formulate the steady state conditions:

$$Y'_1 = (1 + A'_1) \cdot \delta'_1 \tag{4.41}$$

$$\kappa_1 \cdot \delta'_1 = \rho + \delta_1 \tag{4.42}$$

$$Y'_2 = \frac{D'}{U_C} + (1 + A'_2) \cdot \delta'_2 \tag{4.43}$$

$$\kappa_2 \cdot \delta'_2 = \rho + \delta_2 \tag{4.44}$$

$$I_1 = \delta_1 \cdot K_1 \tag{4.45}$$

$$I_2 = \delta_2 \cdot K_2 \tag{4.46}$$

$$C = Y_1 + Y_2 - I_1 - I_2 - A_1 - A_2 \tag{4.47}$$

We investigate the comparative statics effect of ρ , the discount rate. Differentiating

(4.41) - (4.47) with respect to ρ results in:

$$Y_1'' \cdot \left(\frac{\partial \kappa_1}{\partial \rho} \cdot K_1 + \kappa_1 \cdot \frac{\partial K_1}{\partial \rho} \right) = \delta_1' \cdot A_1'' \cdot \frac{\partial I_1}{\partial \rho} + (1 + A_1') \cdot \delta_1'' \cdot \frac{\partial \kappa_1}{\partial \rho} \quad (4.48)$$

$$\frac{\partial \kappa_1}{\partial \rho} \cdot \delta_1'' \cdot \kappa_1 = 1 \quad (4.49)$$

$$\begin{aligned} Y_2'' \cdot \left(\frac{\partial \kappa_2}{\partial \rho} \cdot K_2 + \kappa_2 \cdot \frac{\partial K_2}{\partial \rho} \right) &= \delta_2' \cdot A_2'' \cdot \frac{\partial I_2}{\partial \rho} + (1 + A_2') \cdot \delta_2'' \cdot \frac{\partial \kappa_2}{\partial \rho} \\ &+ \frac{D'' \cdot \left(\frac{\partial \kappa_2}{\partial \rho} \cdot K_2 + \kappa_2 \cdot \frac{\partial K_2}{\partial \rho} \right)}{U_C} \\ &- \frac{U_{CC} \cdot D' \cdot \frac{\partial C}{\partial \rho}}{(U_C)^2} \end{aligned} \quad (4.50)$$

$$\frac{\partial \kappa_2}{\partial \rho} \cdot \delta_2'' \cdot \kappa_2 = 1 \quad (4.51)$$

$$\frac{\partial I_1}{\partial \rho} = \delta_1' \cdot \frac{\partial \kappa_1}{\partial \rho} \cdot K_1 + \delta_1 \cdot \frac{\partial K_1}{\partial \rho} \quad (4.52)$$

$$\frac{\partial I_2}{\partial \rho} = \delta_2' \cdot \frac{\partial \kappa_2}{\partial \rho} \cdot K_2 + \delta_2 \cdot \frac{\partial K_2}{\partial \rho} \quad (4.53)$$

$$\begin{aligned} \frac{\partial C}{\partial \rho} &= Y_1' \cdot \left(\frac{\partial \kappa_1}{\partial \rho} \cdot K_1 + \kappa_1 \cdot \frac{\partial K_1}{\partial \rho} \right) + Y_2' \cdot \left(\frac{\partial \kappa_2}{\partial \rho} \cdot K_2 + \kappa_2 \cdot \frac{\partial K_2}{\partial \rho} \right) \\ &- \frac{\partial I_1}{\partial \rho} \cdot (1 + A_1') - \frac{\partial I_2}{\partial \rho} \cdot (1 + A_2') \end{aligned} \quad (4.54)$$

which in matrix notation reads

$$\Omega \times \begin{pmatrix} \frac{\partial \kappa_1}{\partial \rho} \\ \frac{\partial \kappa_2}{\partial \rho} \\ \frac{\partial K_1}{\partial \rho} \\ \frac{\partial K_2}{\partial \rho} \\ \frac{\partial I_1}{\partial \rho} \\ \frac{\partial I_2}{\partial \rho} \\ \frac{\partial C}{\partial \rho} \end{pmatrix} = \begin{pmatrix} 0 \\ 1 \\ 0 \\ 1 \\ 0 \\ 0 \\ 0 \end{pmatrix}$$

where

$$\Omega = \begin{pmatrix} Y_1'' K_1 - (1 + A_1') \delta_1'' & 0 & Y_1'' \kappa_1 & 0 & -\delta_1' A_1'' & 0 \\ 0 & 0 & 0 & 0 & 0 & 0 \\ 0 & Y_2'' K_2 - \frac{D''}{U_C} K_2 - (1 + A_2') \delta_2'' & 0 & Y_2'' \kappa_2 - \frac{D''}{U_C} \kappa_2 & 0 & -\delta_2' A_2'' \\ 0 & 0 & 0 & 0 & 0 & 0 \\ 0 & 0 & 0 & 0 & 0 & 0 \\ 0 & 0 & 0 & 0 & 0 & 0 \\ 0 & 0 & 0 & 0 & 0 & 0 \end{pmatrix}$$

The analysis of steady state effects on sector 2 turns out to be quite formula intensive, which is why we limit the comparative statics analysis of the steady state to sector 1. Nevertheless, Section 4.3.3 will present a numerical analysis of the model's behavior for some different parameter values.

4.4 Simulation of the model.

Next, we determine the character of the steady state and calculate the optimal paths for the endogenous variables of the model. We assume the following functional forms:

$$U(C) = u_1 \cdot \frac{C^{1-\theta}}{1-\theta} \quad (4.55)$$

$$D(K_2^e) = \frac{K_2^{e^{1+\omega}}}{(1+\omega) \cdot d_1} \quad (4.56)$$

$$Y(\kappa_1, \kappa_2, K_1, K_2) = (\kappa_1 \cdot K_1)^{\beta_1} + (\kappa_2 \cdot K_2)^{\beta_2} \quad (4.57)$$

$$\delta_1(\kappa_1) = \bar{\delta}_1 + \frac{\kappa_1^{\gamma_1}}{\epsilon_1} \quad (4.58)$$

$$\delta_2(\kappa_2) = \bar{\delta}_2 + \frac{\kappa_2^{\gamma_2}}{\epsilon_2} \quad (4.59)$$

$$A_1(I_1) = I_1^{\alpha_1} \quad (4.60)$$

$$A_2(I_2) = I_2^{\alpha_2} \quad (4.61)$$

with $u_1, \theta, \omega, d_1, \beta_1, \beta_2, \bar{\delta}_1, \bar{\delta}_2, \gamma_1, \gamma_2, \epsilon_1, \epsilon_2, \alpha_1, \alpha_2 > 0$. Using the functional forms above and setting $\dot{X} = 0$ we can solve for the steady-state values of $I_1, I_2, \kappa_1, \kappa_2, K_1, K_2$ which are denoted by $\tilde{I}_1, \tilde{I}_2, \tilde{\kappa}_1, \tilde{\kappa}_2, \tilde{K}_1, \tilde{K}_2$ respectively (see Appendix A2 for a derivation).

$$\tilde{X} = \left(\tilde{I}_1, \tilde{I}_2, \tilde{\kappa}_1, \tilde{\kappa}_2, \tilde{K}_1, \tilde{K}_2, \right)^T \quad (4.62)$$

In order to investigate the stability of the steady state we specify the model parameters. Table 4.1 depicts the parameter values that have been chosen for the simulation of the base run, i.e., the basic simulation run with the basic parameter values.

Parameter	Value	Parameter	Value
α_1	2	α_2	2
β_1	.8	β_2	.8
γ_1	2	γ_2	2
$\bar{\delta}_1$.01	$\bar{\delta}_2$.01
θ	.3	ω	.4
K_1^0	1	K_2^0	5
u_1	10	d_1	500
ϵ_1	2000	ϵ_2	2000

Table 4.1: Parameter Values Base run

with the parameter values above we use a standard root-finding routine to compute the steady-state values of the two capital stocks and the four control variables. These are: $\tilde{I}_1 = 2.16$, $\tilde{I}_2 = 0.69$, $\tilde{\kappa}_1 = 10.95$, $\tilde{\kappa}_2 = 10.95$, $\tilde{K}_1 = 30.92$, $\tilde{K}_2 = 9.86$

The Jacobian of the dynamic system is:

$$J = \begin{bmatrix} \frac{\partial \dot{I}_1}{\partial I_1} & \frac{\partial \dot{I}_1}{\partial I_2} & \frac{\partial \dot{I}_1}{\partial \kappa_1} & \frac{\partial \dot{I}_1}{\partial \kappa_2} & \frac{\partial \dot{I}_1}{\partial K_1} & \frac{\partial \dot{I}_1}{\partial K_2} \\ \frac{\partial \dot{I}_2}{\partial I_1} & \frac{\partial \dot{I}_2}{\partial I_2} & \frac{\partial \dot{I}_2}{\partial \kappa_1} & \frac{\partial \dot{I}_2}{\partial \kappa_2} & \frac{\partial \dot{I}_2}{\partial K_1} & \frac{\partial \dot{I}_2}{\partial K_2} \\ \frac{\partial \dot{\kappa}_1}{\partial I_1} & \frac{\partial \dot{\kappa}_1}{\partial I_2} & \frac{\partial \dot{\kappa}_1}{\partial \kappa_1} & \frac{\partial \dot{\kappa}_1}{\partial \kappa_2} & \frac{\partial \dot{\kappa}_1}{\partial K_1} & \frac{\partial \dot{\kappa}_1}{\partial K_2} \\ \frac{\partial \dot{\kappa}_2}{\partial I_1} & \frac{\partial \dot{\kappa}_2}{\partial I_2} & \frac{\partial \dot{\kappa}_2}{\partial \kappa_1} & \frac{\partial \dot{\kappa}_2}{\partial \kappa_2} & \frac{\partial \dot{\kappa}_2}{\partial K_1} & \frac{\partial \dot{\kappa}_2}{\partial K_2} \\ \frac{\partial \dot{K}_1}{\partial I_1} & \frac{\partial \dot{K}_1}{\partial I_2} & \frac{\partial \dot{K}_1}{\partial \kappa_1} & \frac{\partial \dot{K}_1}{\partial \kappa_2} & \frac{\partial \dot{K}_1}{\partial K_1} & \frac{\partial \dot{K}_1}{\partial K_2} \\ \frac{\partial \dot{K}_2}{\partial I_1} & \frac{\partial \dot{K}_2}{\partial I_2} & \frac{\partial \dot{K}_2}{\partial \kappa_1} & \frac{\partial \dot{K}_2}{\partial \kappa_2} & \frac{\partial \dot{K}_2}{\partial K_1} & \frac{\partial \dot{K}_2}{\partial K_2} \end{bmatrix} \quad (4.63)$$

In a next step we calculate the eigenvalues associated with the Jacobian at the steady state. They are: $r_1 = 0.28$, $r_2 = -0.24$, $r_3 = 0.13$, $r_4 = -0.09$. Thus, the system has two negative eigenvalues, and the computed steady state is saddle point stable. Given the information above, we can formulate the optimal paths for $I_1(t)$, $I_2(t)$, $\kappa_1(t)$, $\kappa_2(t)$, $K_1(t)$ and $K_2(t)$ (where we denote optimal paths by an

asterix).

$$X_t^* = \tilde{X} + e^{r_1 t} \cdot \Theta_1 \cdot \Upsilon_{r_1, X} + e^{r_2 t} \cdot \Theta_2 \cdot \Upsilon_{r_2, X} \quad (4.64)$$

for $X = I_1, I_2, \kappa_1, \kappa_2, K_1, K_2$, where r_1 and r_2 are the negative eigenvalues of the Jacobian above, $\Upsilon_{r_i, X}$ is the eigenvector of X related to the eigenvalue i and Θ_1 and Θ_2 are constants which are obtained by solving

$$K_0^* = X_0 \quad \text{for } X = (K_1, K_2) \quad (4.65)$$

The solid lines in Figure 4.1 depict the time paths for the four control variables ($I_1, I_2, \kappa_1, \kappa_2$) and two state variables (K_1, K_2) as well as the levels of effective capital in each sector (K_1^e, K_2^e), the consumption level (C), the damage (D) and the share of sector 1 in total output ($\frac{Y_1}{Y}$). We have chosen the initial levels of the capital stocks such that K_1 is initially below its steady-state level and K_2 initially above its steady-state level. We observe a monotonic behavior of the two capital stocks over time. While K_1 is increasing steadily over the simulation period, we observe the opposite for K_2 . The large initial difference in the level of K_1 from its steady-state value explains the high initial volumes of I_1 . Since for low levels of the capital stock, high utilization is relatively inexpensive (in terms of foregone consumption) we observe a strong utilization rate as compared to the steady state. Along the adjustment path towards the steady state, K_1 increases rapidly up to around $t = 40$ and slows down thereafter. The utilization of the capital stock decreases sharply due to the high maintenance cost of rising levels of the installed and operating capital stock. The direction of the essential variables in sector 2 is

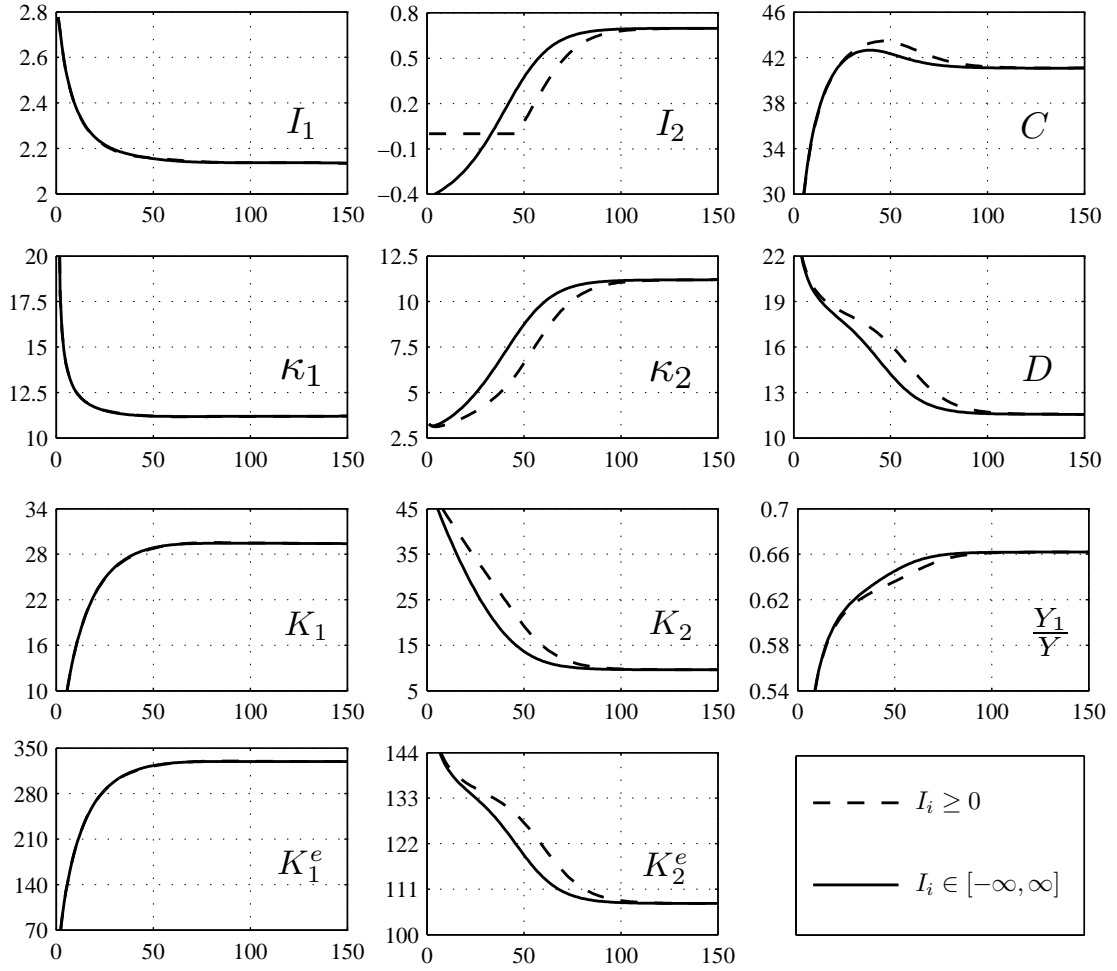


Figure 4.1: The base run

different. The capital stock is initially far above its steady-state level. As already analyzed in section 2, investment levels are negative when the related capital stock is far above its steady-state value. In this phase the economy is effectively eating up its capital stock. The capital stock in sector 2 is hardly utilized initially but the intensity grows along the transition path towards the steady state. Consider the path of consumption in the top right graph. Consumption levels are low initially.

The major reason is that the capital stock in sector 1 is very low and less output is available for consumption. However, since K_1 rises quickly, C follows this trend. From about $t = 25$ consumption overshoots its long run steady-state level. This is because (i) K_1 is getting closer to its steady state level and less investment is needed in sector 1 and (ii) the capital stock in sector 2 is eaten up ($I_2 < 0$). Notice that the overshooting vanishes at around $t = 80$ which is mainly due to the fact that investment in sector 2 has stabilized at its steady-state level. The damage from effectively using the polluting capital stock follows the decreasing trend in K_2^e , and while at the same time K_1^e is constantly increasing, the share of clean capital (output) in total output is rising.

4.4.1 Nonnegativity Constraint on Investment

We have also analyzed the model's transition towards the steady state when investment is constrained to be nonnegative (i.e. immobile capital). The results of this simulation are plotted in Figure (1) and denoted by the dashed lines. It becomes immediately visible that while disinvestment in sector 2 clearly affects sector 2 and the macro variables, its effect on sector 1 is almost nil. In sector 2 however, investment remains at the zero bound until about $t = 50$. From that onwards its level remains below the base run scenario. The reason for this is that at $t = 30$ the capital stock K_2 is much higher than in the unconstrained base run case, simply because disinvestment is not possible (even though capacity utilization has increased). The use of effective capital in sector 2 is enforced which ultimately translated in higher damage. The lower investment volumes in sector 2 combined with higher levels of effective capital strengthen the overshooting of the consumption path. Overall, a nonnegativity constraint on investment does

not alter the steady state of the economy but clearly slows down the steady state transition process of the economy.

4.4.2 Different initial values

In this section we analyze the steady-state transition paths for different initial levels. To simplify the analysis, we assume for each run $K_1^0 = 1$ but modify the K_2^0 levels. Figure 4.2 illustrated the result of these simulation runs. In particular,

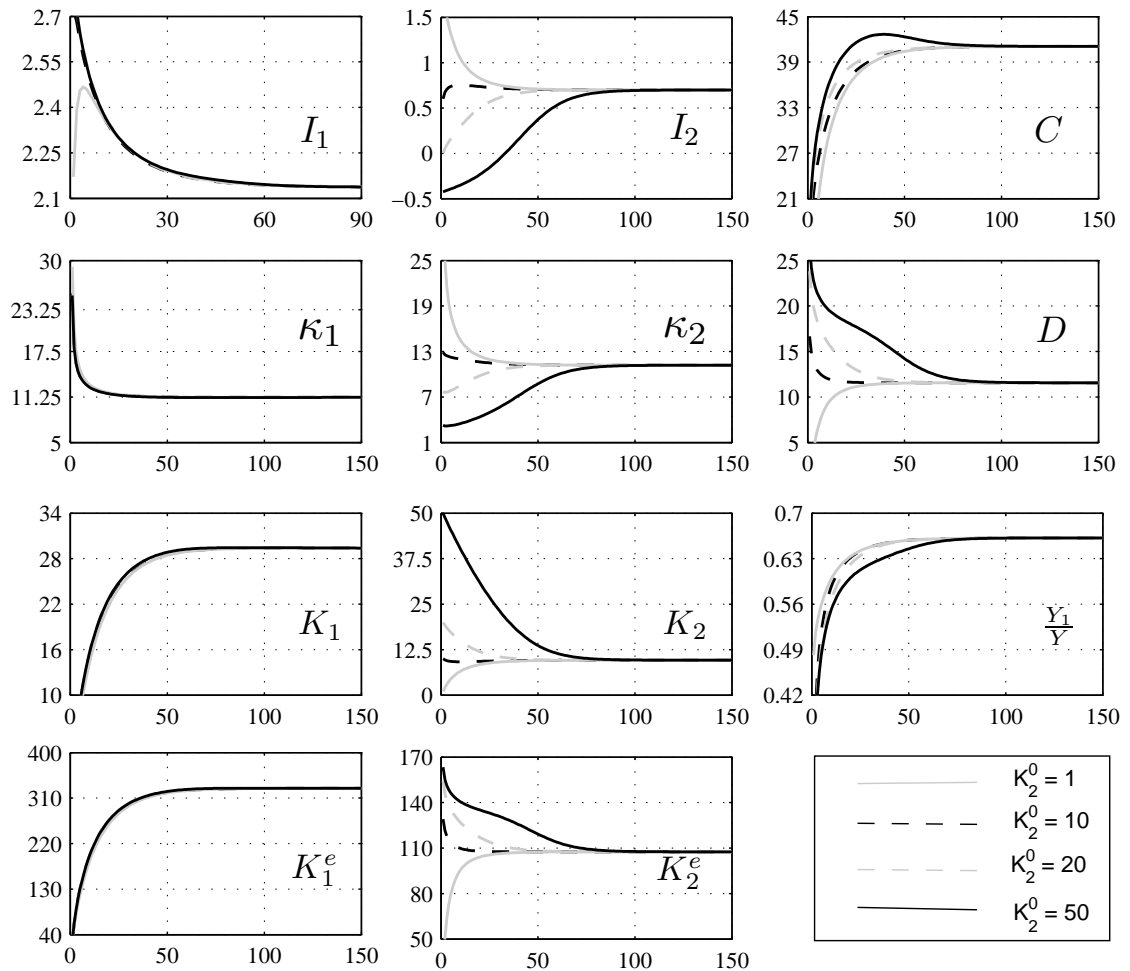


Figure 4.2: Different initial values

next to the base run case of $K_2^0 = 50$ (black solid line) we analyze the cases in which the initial level of capital in sector 2 is 1, 10 and 20. There are two major observations to be made from Figure 4.2. First, for $K_2^0 = 20$ and $K_2^0 = 10$ the main trends for the model variables remain valid except that (i) disinvestment in sector 2 does not occur since the capital stock in sector 2 in place is now much lower than in the base run case, and (ii) the overshooting of the consumption path is reduced which is due to the fact that K_2 is no longer idle. The second important observation results from the case $K_2^0 = 1$. We see that even if the initial level of the polluting capital stock is low, it is still built up. As a consequence, we observe lower investment in sector 1 and also lower consumption.

4.4.3 Sensitivity analysis for different Parameter Values

This section presents the results of a sensitivity analysis of the model with respect to some important model parameters. The parameters which we alter are (i) discount rate, (ii) damage parameter and (iii) the natural rate of depreciation in sector 2.

(i) lowering the discount rate ρ :

The solid grey lines in Figure 4.3 display the simulation results for $\rho = 0.04$. A lower discount rate implies that future welfare levels are valued more from today's point of view. As a consequence, consumption is significantly higher and damage is reduced as the system moves towards the steady state. Lower discounting has a large impact on sector 1. We observe the need for building up the clean capital stock, which results in larger investment volumes accompanied by lower capacity utilization. Overall, the flow of effective capital services increases. In sector 2 the

opposite effect occurs. The usage of effective capital is decreased, despite higher investment. The reason for this effect is the higher rate of capacity utilization. Consequently, we observe an increased share of clean output in total production.

(ii) increasing $\bar{\delta}_2$, the natural rate of depreciation in sector 2:

The dashed black lines in Figure 4.3 display the simulation results $\bar{\delta}_2 = 0.02$. We observe that this parameter change has no effect on sector 1. In sector 2 however, investment and capacity utilization are increased which results in a lower capital stock and lower flow of effective capital service. The higher investment in sector 2 seems to occur at the expense of consumption which is reduced along its optimal path. Since the total flow of services of the polluting capital stock is reduced, total damage is also lower.

(iii) increasing the damage function exponent ω :

The dashed grey lines in Figure 4.3 display the simulation results for $\omega = 1.1$. Again, this parameter seems to have no effect on the clean capital sector whereas it has a significant impact on sector 2, where we observe both, lower I_2 and κ_2 . Thus, not only the availability of the polluting stock is reduced but also its utilization. As a consequence we observe drastic reductions in the flow of effective capital services which translates in lower damage but also in lower consumption since aggregate output is reduced. The composition of aggregate output also shifts towards the clean capital sector.

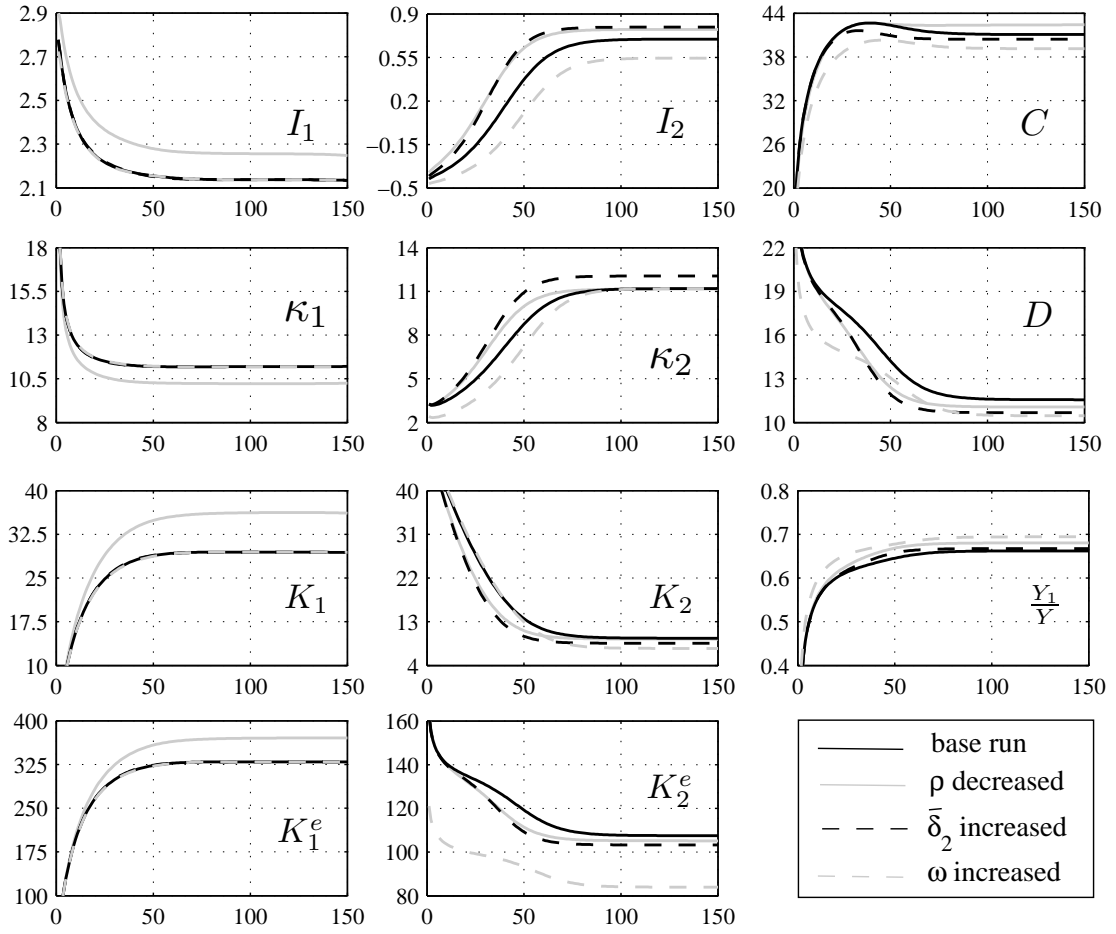


Figure 4.3: Sensitivity analysis

4.5 Stock Pollution & Uncertainty about Damage

In the previous sections we have assumed the damage to depend on the flow of emissions in each period. We have taken this simplifying approach in order to facilitate the understanding of the pure tradeoff between capacity building and capacity using of the heterogenous capital stocks, each representing a different technology.

In this section we depart from the assumption of flow pollution and introduce stock pollution, i.e. the damage depends on the size of the stock of carbon in the atmosphere. We denote the damage function by $D(S)$ with $D_S, D_{SS} > 0$. Another difference to the flow pollution case is that we no longer assume that damage is subtracted from the utility function. In the stock pollution case version, the damage reduces part of the total output, leaving less for consumption and investment. Finally, we introduce uncertainty about the level of carbon in the atmosphere. Of course, this is not a realistic assumption, since the level of carbon in the atmosphere is not uncertain at all. However, since we create a dependency of the damage function on the atmospheric carbon stock, we are de facto technically modeling stochastic damage. This simplification allows us to study the optimal capital investment and utilization decisions when a) the usage of the dirty technology accumulates pollution which results in output loss and b) the damage function is uncertain. We rewrite the optimization problem as

$$\max_{I_1, I_2, \kappa_1, \kappa_2} E \int_0^{\infty} e^{-\rho t} [U(C)] dt \quad (4.66)$$

subject to the following constraints

$$C = \frac{Y(\kappa_1, \kappa_2, K_1, K_2)}{D(S)} - I_1 - I_2 - A_1(I_1) - A_2(I_2) \quad (4.67)$$

$$dK_1 = (I_1 - \delta_1(\kappa_1) \cdot K_1) \cdot dt \quad (4.68)$$

$$dK_2 = (I_2 - \delta_2(\kappa_2) \cdot K_2) \cdot dt \quad (4.69)$$

$$dS = (\epsilon \cdot Y_2(\kappa_2, K_2) - \zeta S) \cdot dt + \sigma S dB \quad (4.70)$$

$$\kappa_1 \geq 0 \quad (4.71)$$

$$\kappa_2 \geq 0 \quad (4.72)$$

The corresponding Hamilton-Jacobi-Bellman (HJB) equation is

$$\begin{aligned}
0 = \max_{I_1, I_2, \kappa_1 > 0, \kappa_2 > 0} \{ & U\left(\frac{Y(\kappa_1, \kappa_2, K_1, K_2)}{D(S)} - I_1 - I_2 - A_1(I_1) - A_2(I_2)\right) \\
& + V_{K_1}(K_1, K_2, S)(I_1 - \delta_1(\kappa_1) \cdot K_1) \\
& + V_{K_2}(K_1, K_2, S)(I_2 - \delta_2(\kappa_2) \cdot K_2) \\
& + V_S(K_1, K_2, S)(\epsilon \cdot Y(\kappa_2, K_2) - \zeta S) \\
& + \frac{1}{2}\sigma^2 V_{SS}(K_1, K_2, S) - \rho V(K_1, K_2, S)\} \quad (4.73)
\end{aligned}$$

where $V(K_1, K_2, S)$ is the value function. A solution to (4.52)-(4.58) requires finding a value function and policy functions $I_1(K_1, K_2, S)$, $I_2(K_1, K_2, S)$, $\kappa_1(K_1, K_2, S)$ and $\kappa_2(K_1, K_2, S)$ which satisfy the Bellman equation (4.54) and the first-order conditions for I_1 , I_2 , κ_1 and κ_2 which are given by

$$U_C \cdot (1 + A'_1) = V_{K_1}(K_1, K_2, S) \quad (4.74)$$

$$U_C \cdot (1 + A'_2) = V_{K_2}(K_1, K_2, S) \quad (4.75)$$

$$U_C Y_{\kappa_1} = V_{K_1}(K_1, K_2, S) \cdot \delta'_1 \cdot K_1 \quad (4.76)$$

$$U_C Y_{\kappa_2} = V_{K_2}(K_1, K_2, S) \cdot \delta'_2 \cdot K_2 - V_S(K_1, K_2, S)\epsilon Y_{\kappa_2} \quad (4.77)$$

Equations (4.60)-(4.63) are equivalent to (4.19)-(4.22) and therefore can be interpreted in the same way.

A closed form solution to (4.59)-(4.63) should theoretically be obtained by applying specific function forms to Y, A, D, U and δ_i and using an intelligent guess for the value function $V(K_1, K_2, S)$. However, due to the dimension of the state space and the nonlinearities of the functional forms we are not able to derive a

closed form solution. Instead, we determine the value function and the policy functions numerically.

For the numerical analysis of the stochastic model with stock pollution we use the following functional forms.

$$U(C) = u_1 \cdot \frac{C^{1-\theta}}{1-\theta} \quad (4.78)$$

$$D(K_2^e) = 1 + s_1 \cdot (S - S_{PI})^2 \quad (4.79)$$

$$Y(\kappa_1, \kappa_2, K_1, K_2) = (\kappa_1 \cdot K_1)^{\beta_1} + (\kappa_2 \cdot K_2)^{\beta_2} \quad (4.80)$$

$$\delta_1(\kappa_1) = \bar{\delta}_1 + \frac{\kappa_1^{\gamma_1}}{\epsilon_1} \quad (4.81)$$

$$\delta_2(\kappa_2) = \bar{\delta}_2 + \frac{\kappa_2^{\gamma_2}}{\epsilon_2} \quad (4.82)$$

$$A_1(I_1) = I_1^{\alpha_1} \quad (4.83)$$

$$A_2(I_2) = I_2^{\alpha_2} \quad (4.84)$$

with $\alpha_1, \alpha_2, \beta_1, \beta_2, \gamma_1, \gamma_2, \bar{\delta}_1, \bar{\delta}_2, \theta, \epsilon, u_1, \zeta, \sigma, S_{PI}, s_1 > 0$. We assume the following parameter values.

Parameter	Value	Parameter	Value
α_1	2	α_2	2
β_1	.65	β_2	.7
γ_1	2	γ_2	2
$\bar{\delta}_1$.01	$\bar{\delta}_2$.01
θ	1.5	ϵ	.03
u_1	10	ζ	.003
σ	.03	S_{PI}	600
s_1	.00005		

Table 4.2: Parameter Values - Stochastic Model with Stock Pollution

Similar to the previous chapters, Equations (4.59)-(4.63) constitute a system of nonlinear second-order partial differential equations. Again, we apply the pro-

jection method to solve this system of equations. Using the Chebyshev collocation method we approximate the solution to (4.59)-(4.63) with a linear combination of basis functions whose coefficients approximately solve (4.59)-(4.63) at specific collocation nodes. The approximated value function and policy functions are given by:

$$\tilde{V}(K_1, K_2, S) = \sum_i \sum_j \sum_k c_{ijk}^V T_i(x_{K_1}) T_j(y_{K_2}) T_k(z_S) \quad (4.85)$$

$$\tilde{I}_1(K_1, K_2, S) = \sum_i \sum_j \sum_k c_{ijk}^{I_1} T_i(x_{K_1}) T_j(y_{K_2}) T_k(z_S) \quad (4.86)$$

$$\tilde{I}_2(K_1, K_2, S) = \sum_i \sum_j \sum_k c_{ijk}^{I_2} T_i(x_{K_1}) T_j(y_{K_2}) T_k(z_S) \quad (4.87)$$

$$\tilde{\kappa}_1(K_1, K_2, S) = \sum_i \sum_j \sum_k c_{ijk}^{\kappa_1} T_i(x_{K_1}) T_j(y_{K_2}) T_k(z_S) \quad (4.88)$$

$$\tilde{\kappa}_2(K_1, K_2, S) = \sum_i \sum_j \sum_k c_{ijk}^{\kappa_2} T_i(x_{K_1}) T_j(y_{K_2}) T_k(z_S) \quad (4.89)$$

$T_i(x_{K_1})$, $T_j(x_{K_2})$ and $T_k(z_S)$ are n_i, n_j, n_k -degree Chebyshev polynomials which are evaluated at the states with x_S, x_K, x_η being a mapping $[K_1^{\min}, K_1^{\max}] \times [K_2^{\min}, K_2^{\max}] \times [S^{\min}, S^{\max}] \mapsto [-1, 1] \times [-1, 1] \times [-1, 1]$. The collocation coefficients $c_{ijk}^V, c_{ijk}^{I_1}, c_{ijk}^{I_2}, c_{ijk}^{\kappa_1}, c_{ijk}^{\kappa_2}$ are then estimated in order to minimize the Bellman and Euler errors and to deliver a good approximation of (4.59)-(4.63).

Using specific functional forms and parameter values we compute numerically the deterministic steady state to obtain $\tilde{K}_1 = 118.48$, $\tilde{K}_2 = 185.1$ and $\tilde{S} = 1429$. Given these values we set up the projection grid by discretizing the state space around the steady state. We choose $K_1 \in [25, 150]$, $K_2 \in [100, 300]$ and $S \in [800, 1800]$. The Chebyshev polynomials are of degree 6 in all states i.e.: $n_i, n_j, n_k = 6$.

Figure 4.4 shows the value function in the $K_1 - K_2$ space for $S = 1300$. The value function is smooth and concave. It increases with higher levels of capital in both sectors. The curvature is due to the concavity of the production function

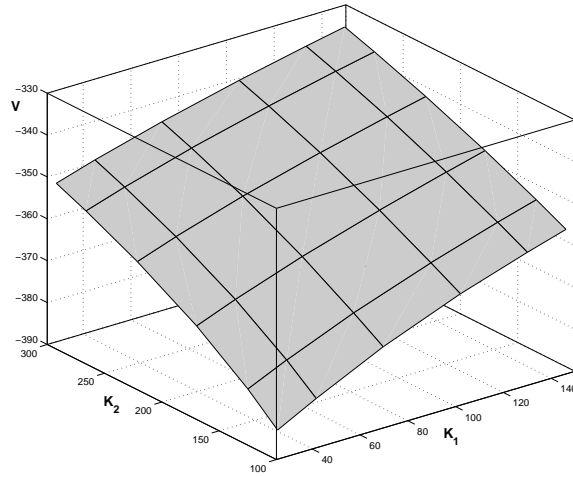


Figure 4.4: Value function for $S = 1300$

and the utility function.

Figure 4.5 displays the optimal decision rules for the four control variables I_1 , I_2 , κ_1 and κ_2 and the resulting flows of effective capital in the $K_1 - K_2$ space for $S = 1300$. In the clean technology sector (sector 1) we observe that for lower levels of capital availability, optimal investment is rather invariant to higher levels of K_2 , the capital stock associated with the polluting technology. However, for larger levels of K_1 , I_1 increases much faster with higher levels of K_2 . The optimal level of capacity utilization, κ_1 depends negatively on the the availability of K_1 . This is an intuitive result since the effective flow of capital is the product of capital availability and capital utilization. The bottom-left plot displays the optimal flow of effective capital services. It depends positively on the availability of the capital stock in sector 1, while we can observe lower values with increasing

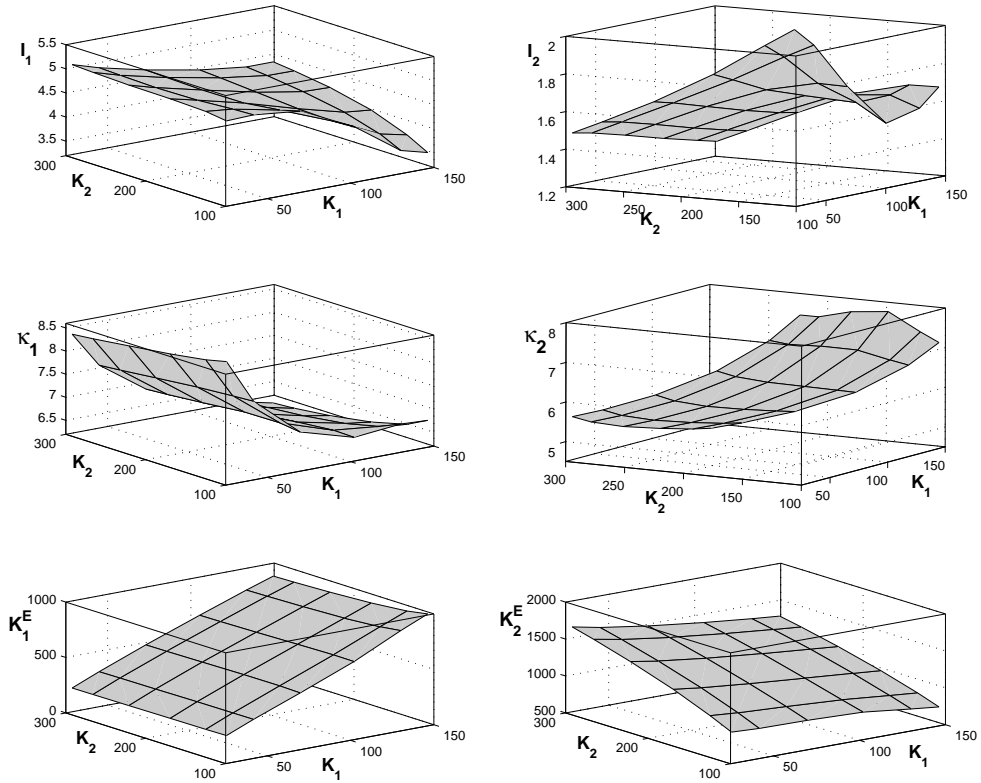


Figure 4.5: Optimal investment, capital utilization and effective capital services in the $K_1 - K_2$.

availability of K_2 for high levels of K_1 . This is mainly due to the decreasing capacity utilization, as seen in the center-left plot. For the sector associated with the polluting technology (sector 2), the flow of effective capital services depends negatively on the availability of capital. The negative dependency on the cross-sectional capital stock however is much larger for higher levels of K_2 . This result is attributed to the effect of the pollution externality which arises from utilizing K_2 . In the center-right plot we observe that at high levels of K_2 its utilization decreases with higher availability of the alternative capital stock. Note that for

a given level of K_2 , higher capital utilization implies larger emission levels (and consequently higher damage). This adverse effect is strengthened by the resulting lower marginal product of capital. This feature explains as well why I_2 also decreases with higher levels of the clean capital stock. Note that we have observed an opposite cross-sectoral pattern for I_1 . From this we can conclude that high levels of the polluting capital stock trigger an intense build-up of the clean capital stock while high levels of the clean capital stock rather lead to the allocation of aggregate output to consumption. Only at the lower bound of K_2 , higher levels of K_1 trigger larger investment into the polluting capital stock. This is the mirror image of optimal I_1 in the same region of the state space. Figure 4.6 displays

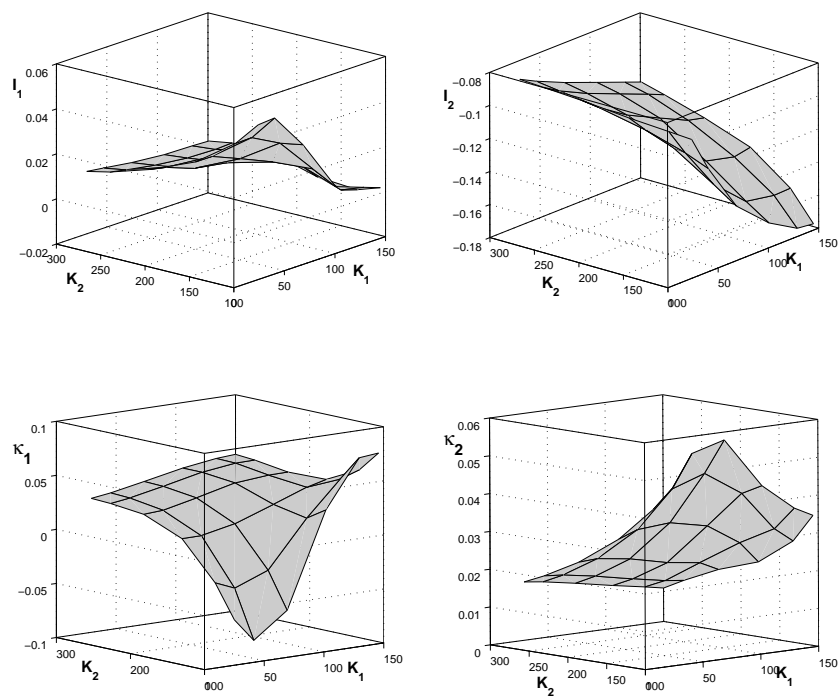


Figure 4.6: Relative change in optimal control variables when uncertainty is higher (from $\sigma = .01$ to $\sigma = .02$) for $S = 1300$

the relative change in the optimal investment and capacity utilization when uncertainty about damage resulting from the carbon stock is increased. In this case we have increased the standard deviation from $\sigma = .01$ to $\sigma = .02$. Note that in Figure 4.6, a positive value implies that a rise in uncertainty leads to higher values of the policy function under consideration. We observe that damage uncertainty triggers a reallocation of investment towards sector 1, the clean technology sector. In sector 1, the largest positive impact of higher uncertainty on investment occurs when capital availability in both sectors is limited. While for high levels of K_1 and low levels of K_2 this effect is almost zero, an obvious result since for low levels of K_2 and high levels of K_1 , emissions are low and the clean capital does not require large investment. In sector 2, increased uncertainty leads to significantly lower investment volumes over the entire state space. In general we can state that the capital stock associated with the polluting technology is reduced. This statement is further clarified by the bottom-left plot showing higher capital utilization rates (i.e. higher capital depreciation) over the entire state space. The effect of increasing damage uncertainty on capital utilization in sector 1 is mixed, depending on the state space region. While capacity utilization is increased for larger levels of either capital stock, or both, there exists a region in the state space, namely at low levels of both capital stocks in which the clean capital stock is utilized less intensively. We can therefore conclude that increasing uncertainty triggers a high need for a fast build up of the capital stock related to the clean technology. This effect is further intensified by higher investment volumes in this state space region.

Finally, Figure 4.7 shows V_S , the shadow price of the carbon stock. We show two plots for the shadow value, each for a different degree of uncertainty. In general we observe that V_S decreases with lower levels of each of the capital stocks. When

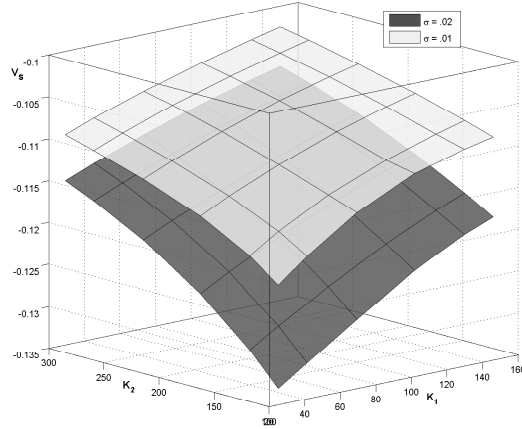


Figure 4.7: The effect of increasing damage uncertainty on the shadow value of the carbon stock for $S = 1300$.

uncertainty about the damage arising from the carbon stock is increased we observe a downwards shift of the shadow value of about ten percent. Thus, we conclude that there is a significant negative welfare effect due to uncertainty about damage.

4.6 Concluding Remarks

Within a growth setting we have analyzed the dynamics of an economy in its transition process towards the steady state. The economy operates two sector-specific capital stocks which embody different technologies. While the usage of capital in one sector has no externality, the production process in the other sector causes environmental damage. In addition, we have included a capital utilization rate. The depreciation rate of capital has been endogenized and depends positively on the capacity utilization rate. The characteristics of this model, as laid out analytically and numerically provide some useful insights that should be considered in the de-

bate about the transition towards a more intense usage of environmentally friendly energy technologies. The combination of heterogeneous capital, endogenous depreciation and capital intensity is in our view essential for extracting qualitative and quantitative implications for policy makers about the easiness of a technology switch. If the economic environment requires a sudden change in the energy mix, an economy driven by our model structure can not react without severe time lags, due to the ex post nature of investment. Installation of the desired capital stock simply takes time if one does not want to abstain from smooth consumption patterns. Next, we have modified the model by introducing a stock of carbon to account for stock pollution. This modification allows us to study the optimal interplay between capacity building and capacity utilization in a more realistic environment. We conclude that increasing uncertainty intensifies the need for a rapid build up of the clean capital stock, while it creates less demand for effective capital services using the polluting technology.

Chapter 5

General Conclusion

This thesis dealt with the interplay of economics and climate change and how it influenced by abatement activities. The analysis has been carried out for both, certain and uncertain states of the world.

In Chapter 2 we stressed the role of the oceans as a sink for atmospheric carbon by developing a dynamic global carbon cycle model with two reservoirs containing atmosphere and two ocean layers. We included the possibility of capturing carbon and sequestering it into the deep ocean reservoir. In that context, we studied the socially optimal extraction and carbon capture and storage decision rules. Our results show that carbon capture and storage accelerates the slow natural flux within the carbon cycle, and because of its temporary abatement character it dampens the overshooting of the atmospheric reservoir. Furthermore, we analyzed the optimal carbon tax. Depending on the initial sizes of the reservoirs and the speed of carbon fluxes between the reservoirs carbon taxes can be increasing, decreasing or u-shaped. Finally, we concluded that the level of the carbon tax should be positively adjusted to account for (i) damage uncertainty and (ii) the declining

ability of the deep ocean to absorb atmospheric carbon.

In Chapter 3 we investigated how the optimal mitigation of climate change evolves if intrinsic uncertainty about damage is inherent to the model. In particular, we asked the question how the effect of uncertainty on climate change mitigation changes with different levels of risk aversion. We found that the effects of uncertainty on emission control differ in sign with varying parameters: Uncertainty may increase or decrease emission control depending on parameter settings. Our analysis covered a large range of the parameter space, in particular the degree of risk aversion and the level of uncertainty. We specified regions of the state space for which higher levels of uncertainty or risk aversion result in different policy rules for emission control. Similarly, given a certain state of the world we found that the effect of uncertainty on emission control changes (in level and sign) with the degree of risk aversion. From that we concluded that uncertainty about the climate may induce people's precautionary emission reduction but also may drive away money from abatement.

In Chapter 4 of this thesis we analyzed how a capital stock which is linked to a polluting technology is maintained, accumulated and utilized optimally. We developed a model with two production sectors that generate a homogenous consumption good. The production processes in these two sectors differ with respect to the technology which is used. While in one sector the process is clean, generating output in the other sector creates environmental damage. The technologies are completely embedded in the corresponding stock of physical capital. Hence, the application of one technology can only be intensified by investing more in the associated capital stock or utilizing it more intensively. In this context, we investigated the inter- and intra-sectoral tradeoffs between capacity building and

capacity using which guide the economy's transition process towards a balanced growth equilibrium

Our findings show that the combination of heterogeneous capital, endogenous depreciation and capital intensity is essential for extracting qualitative and quantitative implications for policy makers about the easiness of a technology switch. Furthermore, we introduced a stock of carbon which is subject to uncertainty. With this modification we investigated how uncertainty about damage resulting from climate change influences the optimal interplay between capacity building and capacity utilization in a more realistic environment. We concluded that increasing uncertainty intensifies the need for a rapid build-up of the clean capital stock. It also reduces the demand for effective capital services associated with the polluting technology.

The special focus on uncertainty in this thesis has shown that accounting for it can significantly change the results in the models which were presented. In future research we should consider to include other forms of uncertainty, e.g.: costs of CO_2 abatement, availability of technologies such as carbon capture and storage or compliance of countries to meet emission targets. The models presented in this thesis have assumed at most three state and four control variables. While it is manageable to extend the dimensions of state and control variables, value function iterations, as required for a stochastic analysis pose a computational limit to the dimensionality of the models at hand. However, efficient algorithms are being developed, which can deal with several dozens of state variables. Eventually, this will allow us to formulate research questions which address the various problems of climate change more appropriately.

Bibliography

- Akimoto, K. , Toshimasa, T. , Fujii, Y. , and Yamaji, K. (2004) ‘Assessment of global warming mitigation options with integrated assessment model dne21.’ *Energy Economics* 26, 635–653
- Arrow, K.J. , and Chang, S. (1982) ‘Optimal pricing, use, and exploration of uncertain natural resource stocks.’ *Journal of Environmental Economics and Management* 9, 1–10
- Arrow, K.J. , and Fisher, A.C. (1974) ‘Environmental preservation, uncertainty, and irreversibility.’ *Quarterly Journal of Economics* 88(2), 312–319
- Azar, C. , and Lindgren, K. (1992) ‘Catastrophic events and stochastic cost-benefit analysis of climate change: An editorial comment.’ *Climatic Change* 56, 245–255
- Bovenberg, A.L. (1988) ‘The corporate income tax in an intertemporal equilibrium model with imperfectly mobil capital.’ *International Economic Review*
- Chatterjee, S. (2005) ‘Capital utilization, economic growth, and convergence.’ *Journal of Economic Dynamics and Control* 29(12), 2093–2124
- Dasgupta, P.S. , and Heal, G.M. (1979) ‘Economic theory and exhaustible resources.’ *Cambridge University Press*

- Dockner, E. (1985) 'Local stability analysis in optimal control problems with two state variables.' In *Optimal Control Theory and Economic Analysis 2*, ed. Gustav Feichtinger (Elsevier Science Publishers B.V.)
- Edmonds, J. , Clarke, J. , Dooley, J. , Kim, S.H. , and Smith, S.J. (2004) 'Stabilization of co2 in a b2 world: Insights on the roles of carbon capture and disposal, hydrogen, and transportation technologies.' *Energy Economics* 26(4), 517–537
- Epstein, L.G. (1980) 'Decision making and the temporal resolution of uncertainty.' *International Economic Review* 21(2), 269–283
- Farzin, Y.H. , and Tahvonen, O. (1996) 'Global carbon cycle and the optimal time path of a carbon tax.' *Oxford Economic Papers* 48, 515–536
- Fisher, A.C. , and Narain, U. (2003) 'Global warming, endogenous risk, and irreversibility.' *Environmental and Resource Economics* 25, 395–416
- Fisher, C. , Withagen, C. , and Toman, M. (2004) 'Optimal investment in clean production capacity.' *Environmental and Resource Economics*
- Gollier, C. , Jullien, B. , and Treich, N. (2000) 'Scientific progress and irreversibility: An economic interpretation of the precautionary principle.' *Journal of Public Economics* 75, 229–253
- Heal, G. , and Kriström, B. (2002) 'Uncertainty and climate change.' *Environmental and Resource Economics* 22, 3–39
- Henry, C (1974) 'Investment decisions under uncertainty: The irreversibility effect.' *American Economic Review* 64(6), 1006–1012

- Herzog, H. , Caldeira, K. , and Reilly, J. (2003) ‘An issue of permanence: Assessing the effectiveness of temporary carbon storage.’ *Climatic Change* 59, 293–310
- IPCC (2005) ‘Special report: Carbon dioxide capture and storage.’ Technical Report, Intergovernmental Panel on Climate Change, Cambridge UK
- Judd, K. L. (1992) ‘Projection methods for solving aggregate growth models.’ *Journal of Economic Theory* 59, 410–452
- (1998) *Numerical Methods in Economics* (The MIT Press)
- Karp, L. , and Zhang, J. (2002) ‘Controlling a stock pollutant with endogenous abatement capital and asymmetric information.’ *Department of Agricultural and Resource Economics, UC Berkeley, Working Paper Series*
- Keith, D.W. , and Minh, H.D. (2003) *CO₂ Capture from the Air: Technology Assessment and Implications for Climate Policy* (Oxford, UK: Elsevier Science)
- Keith, D.W. , Minh, H.D. , and Stolaroff, J.K. (2005) ‘Climate strategy with CO₂ capture from the air.’ *Climatic Change* 74, 17–45
- Keller, K. , Bolker, B.M. , and Bradford, D.F. (2004) ‘Uncertain climate thresholds and optimal economic growth.’ *Journal of Environmental Economics and Management* 48, 723–741
- Kolstad, C.D. (1996a) ‘Learning and stock effects in environmental regulation: The case of greenhouse gas emissions.’ *Journal of Environmental Economics and Management* 31, 1–18
- (1996b) ‘Fundamental irreversibilities in stock externalities.’ *Journal of Public Economics* 60, 221–233

- Lackner, K. (2003) ‘A guide to co2 sequestration.’ *Science* 300, 1677f
- Lempert, R.J. , Sanstad, A.H. , and Schlesinger, M.E. (2006) ‘Multiple equilibria in a stochastic implementation of dice with abrupt climate change.’ *Energy Economics* 28, 677–689
- McFarland, J.R. , and Herzog, H.J. (2006) ‘Incorporating carbon capture and storage technologies in integrated assessment models.’ *Energy Economics* 28, 632–652
- McFarland, J.R. , Herzog, H.J. , and Reilly, J.M. (2003) *Greenhouse Gas Control Technologies: Proceedings of the Sixth International Conference on Greenhouse Gas Control Technologies* (Oxford, UK: Elsevier Science)
- McInerney, D. , and Keller, K. (2008) ‘Economically optimal risk reduction strategies in the face of uncertain climate thresholds.’ *Climatic Change* 91, 29–41
- Miranda, M.J. , and Fackler, P.L. (2002) *Applied Computational Economics and Finance* (Cambridge, MA: MIT Press)
- Nordhaus, W.D. (1994a) ‘Managing the global commons.’ *Cambridge, MA: MIT Press*
- Nordhaus, W.D. (1994b) *Managing the Global Commons. The Economics of Climate Change.* (MIT Press, Cambridge, MA.)
- Nordhaus, W.D (2008) *A Question of Balance: Weighing the Options on Global Warming Policies* (Yale University Press, New Haven, CT)
- Nordhaus, W.D. , and Boyer, J. (2000) *Warming the World: Economic Models of Global Warming*, vol. 46 (MIT Press, Cambridge, Mass.)

- NRC (2002) *Abrupt Climate Change: Inevitable Surprises* (National Research Council, Washington, DC: National Academy Press)
- Peck, S.C. , and Teisberg, T.J. (1993) ‘Global warming uncertainties and value of information: An analysis using ceta.’ *Resource and Energy Economics* 15, 71–97
- Peterson, S. (2006) ‘Uncertainty and economic analysis of climate change: A survey of approaches and findings.’ *Environmental Modeling and Assessment* 11(1), 1–17
- Pezzey, J., Withagen C.A. (1998) ‘The rise, fall and sustainability of capital-resource economies.’ *Scand. journal of Economics*
- Pindyck, R.S. (2000) ‘Irreversibilities and the timing of environmental policy.’ *Resource and Energy Economics* 22, 233–259
- (2007) ‘Uncertainty in environmental economics.’ *Review of Environmental Economics and Policy* 1(1), 46–65
- Pitchford, J.D. (1977) ‘Two state variable problems.’ *in: Pitchford, J.D., Turnovsky, S.J. (Eds.): Applications of Control theory to Economic Analysis, North-Holland, Amsterdam*
- Pizer, W.A. (1999) ‘The optimal choice of climate change policy in the presence of uncertainty.’ *Resource and Energy Economics* 21, 255–287
- Rumbos, L. , and Auernheimer, B. (2001) ‘Endogenous capital utilization in a neoclassical growth model.’ *Atlantic Economic Journal*
- Stern (2006) ‘The stern review on tghе economics of climate change’

- Tahvonen, O. , and Salo, S. (2001) ‘Economic growth and transitions between renewable and non-renewable energy resources.’ *European Economic Review*
- Tahvonen, O. , and Withagen, C. (1996) ‘Optimality of irreversible pollution accumulation.’ *Journal of Economic Dynamics and Control* 20, 1775–1795
- Toman, M.A. , and Withagen, C. (2000) ‘Accumulative pollution, clean technology, and policy design.’ *Resource and Energy Economics* 22, 367–384
- Tsur, Y. , and Zemel, A. (1998) ‘Pollution control in an uncertain environment.’ *Journal of Economic Dynamics and Control* 22, 967–975
- Ulph, A. , and Ulph, D. (1994) ‘The optimal time path of a carbon tax.’ *Oxford Economic Papers* 46, 857–868
- Ulph, A. , and Ulph, D. (1997) ‘Global warming, irreversibility and learning.’ *The Economic Journal* 107(442), 636–650
- Uzawa, H. (1969) ‘Time preference and the penrose effect in a two-class model of economic growth. part 2: Symposium on the theory of economic growth.’ *The Journal of Political Economy* 77(4), 628–652
- Weitzman, M.L. (2009) ‘On modeling and interpreting the economics of catastrophic climate change.’ *Review of Economics and Statistics* 91(1), 1–19
- Zeman, F.S. , and Lackner, K.S. (2004) ‘Capturing carbon dioxide directly from the atmosphere.’ *World Resources Review* 16, 62–68

Chapter 6

Appendix

6.1 Appendix A1

We apply the following functional forms. with $A, \nu, \kappa, \tau, \epsilon, \psi, S_{PI}, \alpha > 0$

$$Y(K) = A \cdot K^\nu \quad (6.1)$$

$$D(\eta, T(S)) = 1 + \kappa \cdot (\eta \cdot T(S))^2 \quad (6.2)$$

$$T(S) = \tau \cdot (S - S_{PI}) \quad (6.3)$$

$$M(m) = \psi \cdot \epsilon \cdot Y \cdot m^2 \quad (6.4)$$

$$U(c) = \frac{c^{1-\alpha}}{1-\alpha} \quad (6.5)$$

Concerning the parameter space, we use the following specification:

Parameter	Value	Parameter	Value
ν	0.75	S_{PI}	400
κ	0.005	α	0.9
τ	0.003	ρ	0.01
ψ	40	A	1
ϵ	0.1	$\bar{\eta}$	1
θ	0.1	σ	0.05

Table 6.1: Parameter Values

6.2 Appendix A2

In this section we derive the complete dynamic system in the control-state space.

The first order conditions (4.19)-(4.24) are rewritten as follows:

$$\lambda_1 = U_C \cdot (A'_1 + 1) \quad (6.6)$$

$$\lambda_2 = U_C \cdot (A'_2 + 1) \quad (6.7)$$

$$U_C \cdot Y_{\kappa_1} = \lambda_1 \cdot \delta'_1 \cdot K_1 + \mu_1 \quad (6.8)$$

$$U_C \cdot Y_{\kappa_1} = \lambda_2 \cdot \delta'_2 \cdot K_2 - D_{\kappa_2} + \mu_2 \quad (6.9)$$

$$\dot{\lambda}_1 = \lambda_1 \cdot (\delta_1 + \rho) - U_C \cdot Y_{K_1} \quad (6.10)$$

$$\dot{\lambda}_2 = \lambda_2 \cdot (\delta_2 + \rho) - U_C \cdot Y_{K_2} + D_{K_2} \quad (6.11)$$

$$(6.12)$$

Solving (6.6) for λ_1 we obtain

$$\lambda_1 = (1 + A_{I_1})U_C \quad (6.13)$$

taking the time derivative of (6.13) we obtain

$$\dot{\lambda}_1 = A_{I_1 I_1} U_C \dot{I}_1 + (1 + A_{I_1}) U_{CC} h_1 \quad (6.14)$$

where $h_1 = Y_{K_1} \dot{K}_1 + Y_{\kappa_1} \dot{\kappa}_1 + Y_{K_2} \dot{K}_2 + Y_{\kappa_2} \dot{\kappa}_2 - A_{I_1} \dot{I}_1 - A_{I_2} \dot{I}_2$. From equation (6.14) we obtain another expression for $\dot{\lambda}_1$.

$$\dot{\lambda}_1 = \lambda_1 \cdot (\rho + \delta_1) - U_C \cdot Y_{K_1} \quad (6.15)$$

Substitution of (6.13) into (6.15) and using (6.14) we finally can eliminate the co-state variable. Solving for \dot{I}_1 we get

$$\dot{I}_1 = \frac{Y_{K_1} U_C + (1 + A_{I_1}) (U_{CC} h_2 - U_C (\rho + \delta_1))}{A_{I_1}^2 U_{CC} - A_{I_1 I_1} U_C} \quad (6.16)$$

where $h_2 = Y_{K_1} \dot{K}_1 + Y_{\kappa_1} \dot{\kappa}_1 + Y_{K_2} \dot{K}_2 + Y_{\kappa_2} \dot{\kappa}_2 - A_{I_2} \dot{I}_2$. The derivation of $\dot{\lambda}_2$ works by analogy. Solving equation(4.20) for λ_2 we obtain

$$\lambda_2 = A_{I_2} U_C \quad (6.17)$$

taking the time derivative of (6.17) we obtain

$$\dot{\lambda}_2 = A_{I_2 I_2} U_C \dot{I}_2 + A_{I_2} U_{CC} h_1 \quad (6.18)$$

From equation (6.18) we obtain another expression for $\dot{\lambda}_2$.

$$\dot{\lambda}_2 = \lambda_2 \cdot (\rho + \delta_2) - U_C \cdot Y_{K_2} + D_{K_2} \quad (6.19)$$

Substitution of (6.17) into (6.19) and using (6.18) we finally can eliminate the co-state variable. Solving for \dot{I}_2 we get

$$\dot{I}_2 = \frac{Y_{K_2}U_C + (1 + A_{I_2})(U_{CC}h_3 - U_C(\rho + \delta_2)) - D_{K_2}}{A_{I_2}^2 U_{CC} - A_{I_2 I_2} U_C} \quad (6.20)$$

where $h_3 = Y_{K_1}\dot{K}_1 + Y_{\kappa_1}\dot{\kappa}_1 + Y_{K_2}\dot{K}_2 + Y_{\kappa_2}\dot{\kappa}_2 - A_{I_1}\dot{I}_1$. Following this procedure we are able to determine the equation of motion for the remaining two control variables κ_1 and κ_2 . We start first with κ_1 . Solving equation(4.21) for λ_1 we obtain

$$\lambda_1 = \frac{Y_{\kappa_1}U_C}{\delta_{\kappa_1}K_1} \quad (6.21)$$

taking the time derivative of (XXX) we obtain

$$\begin{aligned} \dot{\lambda}_1 &= \frac{U_C\delta_{\kappa_1}K_1(Y_{K_1\kappa_1}\dot{K}_1 + Y_{\kappa_1\kappa_1}\dot{\kappa}_1) + U_{CC}Y_{\kappa_1}\delta_{\kappa_1}K_1h_1}{(\delta_{\kappa_1}K_1)^2} \\ &- \frac{Y_{\kappa_1}U_C\delta_{\kappa_1}\dot{K}_1 + Y_{\kappa_1}U_C\delta_{\kappa_1\kappa_1}K_1\dot{\kappa}_1}{(\delta_{\kappa_1}K_1)^2} \end{aligned} \quad (6.22)$$

Substitution of (6.21) into (6.15) and using (6.22) we finally can eliminate the co-state variable. Solving for $\dot{\kappa}_1$ we get

$$\begin{aligned} \dot{\kappa}_1 &= \frac{\delta_{\kappa_1}}{K_1(U_{CC}Y_{\kappa_1}^2\delta_{\kappa_1} + Y_{\kappa_1\kappa_1}U_C\delta_{\kappa_1} - Y_{\kappa_1}U_C\delta_{\kappa_1\kappa_1})} \\ &\cdot \left[U_C(Y_{\kappa_1}\dot{K}_1 - Y_{K_1}\delta_{\kappa_1}K_1^2) + K_1Y_{\kappa_1} \left(U_C(\rho + \delta_1) + U_{CC}(A_{I_1}\dot{I}_1 + A_{I_2}\dot{I}_2) \right) \right. \\ &\left. - K_1 \left(\dot{K}_1(U_{CC}Y_{K_1}Y_{K_1\kappa_1} + Y_{\kappa_1\kappa_1}U_C) - U_{CC}Y_{\kappa_1}(Y_{K_2}\dot{K}_2 + Y_{\kappa_2}\dot{\kappa}_2) \right) \right] \end{aligned} \quad (6.23)$$

We now move to κ_2 . Solving equation(4.22) for λ_2 we obtain

$$\lambda_2 = \frac{Y_{\kappa_2} U_C - D_{\kappa_2}}{\delta_{\kappa_2} K_2} \quad (6.24)$$

taking the time derivative of (6.24) we obtain

$$\begin{aligned} \dot{\lambda}_2 &= \frac{1}{(K_2 \delta_{\kappa_2})^2} \quad (6.25) \\ &\cdot \left[\dot{K}_2 \delta_{\kappa_2} (D_{\kappa_2} - Y_{\kappa_2} U_C) + K_2 \delta_{\kappa_2} \left(U_{CC} Y_{\kappa_2} h_4 + \dot{K}_2 (Y_{K_2 \kappa_2} U_C - D_{\kappa_2 K_2}) \right) \right] \\ &+ K_2 \dot{\kappa}_2 \left(\delta_{\kappa_2} (U_{CC} Y_{\kappa_2}^2 + Y_{\kappa_2 \kappa_2} U_C - D_{\kappa_2 \kappa_2}) + \delta_{\kappa_2 \kappa_2} (D_{\kappa_2} - Y_{\kappa_2} U_C) \right) \end{aligned}$$

where $h_4 = Y_{K_1} \dot{K}_1 + Y_{\kappa_1} \dot{\kappa}_1 + Y_{K_2} \dot{K}_2 - A_{I_1} \dot{I}_1 - A_{I_2} \dot{I}_2$. Substitution of (6.24) into (6.19) and using (6.25) we finally can eliminate the co-state variable. Solving for $\dot{\kappa}_1$ we get

$$\begin{aligned} \dot{\kappa}_2 &= \frac{\delta_{\kappa_2}}{K_2 (\delta_{\kappa_2} (U_{CC} Y_{\kappa_2}^2 + Y_{\kappa_2 \kappa_2} U_C - D_{\kappa_2 \kappa_2}) + \delta_{\kappa_2 \kappa_2} (D_{\kappa_2} - Y_{\kappa_2} U_C))} \quad (6.26) \\ &\cdot \left[K_2^2 \delta_{\kappa_2} (D_{K_2} - U_C Y_{K_2}) + \dot{K}_2 (Y_{\kappa_2} U_C - D_{\kappa_2}) \right] \\ &- K_2 \left((D_{\kappa_2} - Y_{\kappa_2} U_C) (\rho + \delta_2) + \dot{K}_2 (Y_{K_2 \kappa_2} - D_{\kappa_2 K_2}) + U_{CC} Y_{\kappa_2} h_4 \right) \end{aligned}$$

We are now ready to set up the complete dynamic system:

$$\begin{aligned}
\dot{I}_1 &= \dot{I}_1(I_1, I_2, \kappa_1, \kappa_2, K_1, K_2, \dot{I}_2, \dot{\kappa}_1, \dot{\kappa}_2, \dot{K}_1, \dot{K}_2) \\
\dot{I}_2 &= \dot{I}_2(I_1, I_2, \kappa_1, \kappa_2, K_1, K_2, \dot{I}_1, \dot{\kappa}_1, \dot{\kappa}_2, \dot{K}_1, \dot{K}_2) \\
\dot{\kappa}_1 &= \dot{\kappa}_1(I_1, I_2, \kappa_1, \kappa_2, K_1, K_2, \dot{I}_1, \dot{I}_2, \dot{\kappa}_2, \dot{K}_1, \dot{K}_2) \\
\dot{\kappa}_2 &= \dot{\kappa}_2(I_1, I_2, \kappa_1, \kappa_2, K_1, K_2, \dot{I}_1, \dot{I}_2, \dot{\kappa}_1, \dot{K}_1, \dot{K}_2) \\
\dot{K}_1 &= \dot{K}_1(I_1, I_2, \kappa_1, \kappa_2, K_1, K_2, \dot{I}_1, \dot{I}_2, \dot{\kappa}_1, \dot{\kappa}_2, \dot{K}_2) \\
\dot{K}_2 &= \dot{K}_2(I_1, I_2, \kappa_1, \kappa_2, K_1, K_2, \dot{I}_1, \dot{I}_2, \dot{\kappa}_1, \dot{\kappa}_2, \dot{K}_1)
\end{aligned} \tag{6.27}$$

which is in extended form:

$$\dot{I}_1 = \frac{Y_{K_1}U_C + (1 + A_{I_1})(U_{CC}h_2 - U_C(\rho + \delta_1))}{A_{I_1}^2U_{CC} - A_{I_1I_1}U_C} \quad (6.28)$$

$$\dot{I}_2 = \frac{Y_{K_2}U_C + (1 + A_{I_2})(U_{CC}h_3 - U_C(\rho + \delta_2)) - D_{K_2}}{A_{I_2}^2U_{CC} - A_{I_2I_2}U_C} \quad (6.29)$$

$$\begin{aligned} \dot{\kappa}_1 = & \frac{\delta_{\kappa_1}}{K_1(U_{CC}Y_{\kappa_1}^2\delta_{\kappa_1} + Y_{\kappa_1\kappa_1}U_C\delta_{\kappa_1} - Y_{\kappa_1}U_C\delta_{\kappa_1\kappa_1})} \quad (6.30) \\ & \cdot \left[U_C(Y_{\kappa_1}\dot{K}_1 - Y_{K_1}\delta_{\kappa_1}K_1^2) + K_1Y_{\kappa_1} \left(U_C(\rho + \delta_1) + U_{CC}(A_{I_1}\dot{I}_1 + A_{I_2}\dot{I}_2) \right) \right. \\ & \left. - K_1 \left(\dot{K}_1(U_{CC}Y_{K_1}Y_{K_1\kappa_1} + Y_{\kappa_1\kappa_1}U_C) - U_{CC}Y_{\kappa_1}(Y_{K_2}\dot{K}_2 + Y_{\kappa_2}\dot{\kappa}_2) \right) \right] \end{aligned}$$

$$\begin{aligned} \dot{\kappa}_2 = & \frac{\delta_{\kappa_2}}{K_2(\delta_{\kappa_2}(U_{CC}Y_{\kappa_2}^2 + Y_{\kappa_2\kappa_2}U_C - D_{\kappa_2\kappa_2}) + \delta_{\kappa_2\kappa_2}(D_{\kappa_2} - Y_{\kappa_2}U_C))} \quad (6.31) \\ & \cdot \left[K_2^2\delta_{\kappa_2}(D_{K_2} - U_C Y_{K_2}) + \dot{K}_2(Y_{\kappa_2}U_C - D_{\kappa_2}) \right. \\ & \left. - K_2 \left((D_{\kappa_2} - Y_{\kappa_2}U_C)(\rho + \delta_2) + \dot{K}_2(Y_{K_2\kappa_2} - D_{\kappa_2K_2}) + U_{CC}Y_{\kappa_2}h_4 \right) \right] \end{aligned}$$

$$\dot{K}_1 = I_1 - \delta_1 K_1 \quad (6.32)$$

$$\dot{K}_2 = I_2 - \delta_2 K_2 \quad (6.33)$$

with

$$\begin{aligned} h_2 &= Y_{K_1}\dot{K}_1 + Y_{\kappa_1}\dot{\kappa}_1 + Y_{K_2}\dot{K}_2 + Y_{\kappa_2}\dot{\kappa}_2 - A_{I_2}\dot{I}_2 \\ h_3 &= Y_{K_1}\dot{K}_1 + Y_{\kappa_1}\dot{\kappa}_1 + Y_{K_2}\dot{K}_2 + Y_{\kappa_2}\dot{\kappa}_2 - A_{I_1}\dot{I}_1 \\ h_4 &= Y_{K_1}\dot{K}_1 + Y_{\kappa_1}\dot{\kappa}_1 + Y_{K_2}\dot{K}_2 - A_{I_1}\dot{I}_1 - A_{I_2}\dot{I}_2 \end{aligned}$$

6.3 Appendix A3

In this section we derive the steady-state condition for sectors 1 and 2.

Sector 1

$$\tilde{I}_1 = (\gamma_1 - 1)^{\frac{\beta_1(\gamma_1-1)}{\gamma_1(\alpha_1-\beta_1)}} (\bar{\delta}_1 + \rho)^{\frac{\beta_1-\gamma_1}{\gamma_1(\alpha_1-\beta_1)}} (\bar{\delta}_1\gamma_1 + \rho)^{\frac{\beta_1-1}{\beta_1-\alpha_1}} \left(\frac{\beta_1}{\alpha_1\gamma_1} \right)^{\frac{1}{\alpha_1-\beta_1}} \quad (6.34)$$

$$\tilde{\kappa}_1 = \left(\frac{\bar{\delta}_1 + \rho}{\gamma_1 - 1} \right)^{\frac{1}{\gamma_1}} \quad (6.35)$$

$$\tilde{K}_1 = \left(\left(\frac{\alpha_1\gamma_1(\bar{\delta}_1 + \rho)}{\beta_1(\gamma_1 - 1)} \right)^{\frac{1}{1-\beta_1}} \left(\frac{\gamma_1 - 1}{\bar{\delta}_1 + \rho} \right)^{\frac{\beta_1}{\gamma_1(1-\beta_1)}} \left(\frac{\gamma_1\bar{\delta}_1 + \rho}{\gamma_1 - 1} \right)^{\frac{1-\alpha_1}{\beta_1-1}} \right)^{\frac{\beta_1-1}{\alpha_1-\beta_1}} \quad (6.36)$$

Sector 2

$$\tilde{\kappa}_2 = \left(\frac{\bar{\delta}_2 + \rho}{\gamma_2 - 1} \right)^{\frac{1}{\gamma_2}} \quad (6.37)$$

$$\tilde{I}_2 = \frac{(\gamma_2\bar{\delta}_2 + \rho)\tilde{K}_2}{\gamma_2 - 1} \quad (6.38)$$

where \tilde{K}_2 results from solving the following equation.

$$\begin{aligned}
0 &= \tilde{K}_2(\bar{\delta}_2 + \rho + \tilde{\kappa}_2^{\gamma_2})\alpha_2\tilde{I}_2^{\alpha_2-1} - \beta_2(\tilde{\kappa}_2 K_2)^{\beta_2} \\
&+ (\tilde{\kappa}_2 \tilde{K}_2)^{1+\omega} \left((\tilde{\kappa}_1 \tilde{K}_1)^{\beta_1} + (\tilde{\kappa}_2 K_2)^{\beta_2} - \tilde{I}_1^{\alpha_1} - \tilde{I}_2^{\alpha_2} \right)^\theta
\end{aligned} \tag{6.39}$$

which after dividing by K_2 on both sides ¹ and using the fact that $((\kappa_1 K_1)^{\beta_1} + (\kappa_2 K_2)^{\beta_2} - I_1^{\alpha_1} - I_2^{\alpha_2})^\theta = U_C^{-1}$ and $(\kappa_2 K_2)^{1+\omega} = K_2 D_{K_2}$ and $I_2^{\alpha_2-1} = A_{I_2}$ and $\beta_2(\kappa_2 K_2)^{\beta_2} = Y_{K_2}$ results in the following steady state condition:

$$Y_{K_2} - \frac{D_{K_2}}{U_C} = (1 + A_{I_2})(\rho + \delta_2) \tag{6.40}$$

¹and hence loosing the trivial solution $\tilde{K}_2 = 0$

Eidesstattliche Erklärung

Ich erkläre hiermit an Eides Statt, dass ich meine Doktorarbeit "Models on CO_2 abatement under uncertainty" selbständig und ohne fremde Hilfe angefertigt habe und dass ich alle von anderen Autoren wörtlich übernommenen Stellen, wie auch die sich an die Gedanken anderer Autoren eng anlehnenden Ausführungen meiner Arbeit, besonders gekennzeichnet und die Quellen nach den mir angegebenen Richtlinien zitiert habe.

Kiel, 17. Dezember 2009

(Thomas S. Lontzek)

Thomas S. Lontzek

Thomas S. Lontzek
Holtenuerstrasse 149
24118 Kiel
Germany

Tel: (+49) 431-8814-405
Lontzek@gmail.com

Date of Birth: September 29th, 1978
Nationality: German

Positions

October 2007 - Kiel Institute for the World Economy, Economist.
Research Area: The Environment and Natural Resources
2004 - 2007 University of Kiel, Economist at the chair of Prof. Dr. Till Requate

Education

2004 - present Kiel University - Ph.D. in Economics
2004 Maastricht University - M.Sc. Economics

Study & Research Stays

October 2009 University of Chicago
July 2009 Stanford University, Hoover Institution
March 2009 University of Zürich
November 2008 University of Zürich
August 2007 University of Chicago, Institute on Computational Economics 2007
August 2006 Stanford University, Hoover Institution
March - July 2003 University of California, San Diego
March - May 2001 European Parliament, Brussels (Internship)

Research Interests

Methods: Computational Economics, Constrained Optimization, Stochastic Control
Applications: Environmental and Resource Economics, Economic Growth & Endogenous Technical Change

Completed Research Projects

*The effect of uncertainty on decision making about climate change mitigation. A numerical approach of stochastic control, with Daiju Narita. Kiel Working Paper 1539, Kiel Institute for the World Economy, 2009. (submitted to *Journal of Economic Dynamics and Control*)*

*Carbon Capture and Storage & the Optimal Path of the Carbon Tax, with Wilfried Rickels. Kiel Working Paper 1475, Kiel Institute for the World Economy, 2009. (submitted to *Journal of Economic Dynamics and Control*)*

*R&D-driven Biases in Energy-Saving Technical Change: A "Putty-Practically-Clay" Approach, with Adriaan van Zon, Kiel Working Paper 1474, Kiel Institute for the World Economy, 2009. (revise and resubmit at *Resource and Energy Economics*)*

Thomas S. Lontzek

Completed Research Projects (continued)

Transition from Polluting to Clean Technology: A Differentiated Capital Approach, with Till Requate

The Optimal Transfer of Capital and Embodied Technologies to Developing Countries, with Michael Hübler, Kiel Working Paper 1478, Kiel Institute for the World Economy, 2009. (submitted to Journal of Development Economics)

Optimal Global Carbon Management with Ocean Sequestration, with Wilfried Rickels. Kiel Working Papers, 1432, Kiel Institute for the World Economy, 2008. (submitted to *Oxford Economic Papers*)

Current Research Projects

Numerical techniques for constrained optimization, with Valentina Michelangeli (Congressional Budget Office, Washington D.C.) and Kenneth, L. Judd (Stanford University, Hoover Institution)

Efficient Use of Projection Methods for Economic Analysis, with Kenneth, L. Judd (Stanford University, Hoover Institution)

Optimal Control of Carbon Capture and Storage which uncertainty about leakage, with Bob van der Zwaan (ECN, Amsterdam and Columbia University)

Introducing Stochastic Damage to the DICE Model, with Olli Tahvonen (The Finnish Forest Research Institute)

A Stochastic Model for the Economic Analysis of Climate Change, with Kenneth, L. Judd (Stanford University, Hoover Institution)

Optimal Carbon Mitigation under Stochastic Carbon Cycle Feedbacks, with Daiju Narita (Kiel Institute for the World Economy)

Teaching Interests

Dynamic Optimization, Mathematical Methods, Dynamics of Climate Change

Teaching

At Kiel University

Resource Economics (2007), - Ph.D. course with ca. 25 students

Environmental Economics (2005, 2007) - Master's degree course with ca. 30 students

Advanced Microeconomics (2004, 2005, 2006) - Ph.D. course with ca. 25 students

Competition Policy (2005,2006) - Master's degree course with ca. 30 students

New Institutional Economics (2005, 2006) - Master's degree course with ca. 30 students

Microeconomics (2005, 2006) - Bachelor's degree course with ca. 120 students

Economics of Innovation (2005) - Master's degree course with ca. 30 students

At Maastricht University

Presentation Skills (2003) - Master's degree course with ca. 20 students

International Trade (2002) - Bachelor's degree course with ca. 15 students

Microeconomics(2002) - Bachelor's degree course with ca. 15 students

Quantitative Methods (2001, 2002) - Bachelor's degree course with ca. 15 students

Operations Research (2001, 2002) - Bachelor's degree course with ca. 15 students

Analysis (2000, 2001, 2002) - Bachelor's degree course with ca. 15 students

Linear Algebra (2000, 2001, 2002) - Bachelor's degree course with ca. 15 students

Thomas S. Lontzek

Grants

- 2007 Erich Schneider Grant (Institute on Computational Economics, Chicago)
- 2006 Müller Grant (Stanford University, Hoover Institution)
- 2006 DFG grant (Stanford University, Hoover Institution)
- 2003-2004 Erich Schneider Scholarship
- 2003 Erasmus Grant (Study Semester at UC San Diego)

Conference Attendance (A) and Presentations (P)

- 2009 EEA/ESEM 2009, Barcelona. (P)
- 2009 NBER Summer Institute, Cambridge. (A)
- 2009 Climate Change Congress, Copenhagen. (A)
- 2009 German IPCC Discussion Meeting, Eisenach. (A)
- 2008 Computing in Economics and Finance, Paris. (P)
- 2008 Monte Verità Conference on Sustainable Resource Use and Economic Dynamics. (P)
- 2007 Environmental and Resource Economics Workshop, Zürich (P)
- 2006 The Third World Congress of Environmental and Resource Economists, Kyoto (P)
- 2006 Monte Verità Conference on Sustainable Resource Use and Economic Dynamics. (P)
- 2005 Annual Meeting of the Swiss Economic Society, Zürich (P)
- 2005 Environmental and Resource Economics Workshop, Rostock (P)

Referee Work

Environment and Development Economics